SERDP

FINAL REPORT

Incorporating Photoperiodism in Insect Phenology Models with Application to Biological Control of Weeds on Department of Defense Lands

Fritzi Grevstad
Leonard Coop
Oregon State University

Daniel Bean
Colorado Department of Agriculture

November 2022

SERDP Project RC-2701

REPORT DOCUMENTATION PAGE

Form Approved
OMB No. 0704-0188

1. REPORT DATE *(DD-MM-YYYY)*	**2. REPORT TYPE**	**3. DATES COVERED** *(From - To)*
01/11/2022	SERDP Final Report	9/27/2017 - 9/27/2022

4. TITLE AND SUBTITLE

Incorporating Photoperiodism in Insect Phenology Models with Application to Biological Control of Weeds on Department of Defense Lands

5a. CONTRACT NUMBER
17-C-0051

5b. GRANT NUMBER

5c. PROGRAM ELEMENT NUMBER

6. AUTHOR(S)
Fritzi Grevstad
Leonard Coop
Oregon State University

Daniel Bean
Colorado Department of Agriculture

5d. PROJECT NUMBER
RC-2701

5e. TASK NUMBER

5f. WORK UNIT NUMBER

7. PERFORMING ORGANIZATION NAME(S) AND ADDRESS(ES)
Oregon State University
Department of Botany and Plant Pathology, Cordley Hall
Corvallis, OR 97333

8. PERFORMING ORGANIZATION REPORT NUMBER
RC-2701

9. SPONSORING/MONITORING AGENCY NAME(S) AND ADDRESS(ES)
Strategic Environmental Research and Development Program
4800 Mark Center Drive, Suite 16F16
Alexandria, VA 22350-3605

10. SPONSOR/MONITOR'S ACRONYM(S)
SERDP

11. SPONSOR/MONITOR'S REPORT NUMBER(S)
RC-2701

12. DISTRIBUTION/AVAILABILITY STATEMENT
DISTRIBUTION STATEMENT A. Approved for public release: distribution unlimited.

13. SUPPLEMENTARY NOTES

14. ABSTRACT
Biological control is an important and sustainable approach for managing widespread invasive weeds. In biological control, host specific natural enemies (usually insects) are introduced with the goal of establishing a permanent population that will provide sustained, cost-effective control of the plant. The overall goal of our project was to preserve and enhance the effectiveness of biological control for weeds, including on Department of Defense installations, through an understanding of the phenological constraints that may arise with a change in climate as a result of the insects' combined responses to photoperiod and temperature. Our work applies to three important weed species that are currently (or soon to be) targets for biological control: purple loosestrife, tamarisk, and Japanese knotweed.

15. SUBJECT TERMS
Aphalara itadori, classical biological control, climate change, critical day length, degree-day model, Diorhabda carinulata, Fallopia spp., Galerucella calmariensis, insect, knotweed psyllid, Lythrum salicaria, phenology mismatch, photoperiodism, short-day diapause response, Tamarix spp., voltinism model

16. SECURITY CLASSIFICATION OF:			**17. LIMITATION OF ABSTRACT**	**18. NUMBER OF PAGES**	**19a. NAME OF RESPONSIBLE PERSON**
a. REPORT	**b. ABSTRACT**	**c. THIS PAGE**			Fritzi Grevstad
UNCLASS	UNCLASS	UNCLASS	UNCLASS	132	**19b. TELEPHONE NUMBER** *(Include area code)* 541-737-8371

Table of Contents

Abstract

Introduction and Objectives: Biological control is an important and sustainable approach for managing widespread invasive weeds. In biological control, host specific natural enemies (usually insects) are introduced with the goal of establishing a permanent population that will provide sustained, cost-effective control of the plant. The overall goal of our project was to preserve and enhance the effectiveness of biological control for weeds, including on Department of Defense installations, through an understanding of the phenological constraints that may arise with a change in climate as a result of the insects' combined responses to photoperiod and temperature. Our work applies to three important weed species that are currently (or soon to be) targets for biological control: purple loosestrife, tamarisk, and Japanese knotweed.

Technical Approach: We developed an advanced geo-climatic phenology model, which provides an innovative approach to tracking life cycle responses to both temperature and photoperiod. The model can be used to predict phenology, voltinism (number of generations per year), and the degree of asynchrony between the biocontrol agent's life cycle and the host plant's growing season under new climate conditions. Experiments carried out in controlled environment chambers were used to quantify and compare the photoperiod response among different geographic populations of all three biocontrol agents and, along with field phenology observations, to obtain parameter estimates for the model. A common garden field experiment set up in Corvallis, Oregon compared the phenology and voltinism of geographically distant source populations of biocontrol agents under a common climate, while also testing our model's ability to predict performance of agents moved into in new climates. This experiment also quantified the follow-on consequences of insect photoperiodism and climate change for impacts to the host plant.

Results: Results from the experiments and model indicate that photoperiodism plays a crucial role in determining each biocontrol agent's phenological response to a change in climate. We found that local populations of both *Galerucella calmariensis* and *Diorhabda carinulata* have evolved photoperiod responses that improve local fitness by allowing an appropriate number of generations for the season duration. For *D. carinulata* this adaptation has occurred in conjunction with a rapid range expansion to the south. With *G. calmariensis*, the local differences in photoperiodism can affect voltinism, and the resulting level of impact to the weed, when moved into new locations. For the knotweed psyllid, *A. itadori,* our model predicts one to three attempted generations throughout the range of North America where knotweeds are invasive. However, the insect is likely to attempt too many generations for the season duration in northern areas and too few generations in the south. A sweet spot with voltinism matched to the season duration is present at middle latitudes. Geographic patterns of phenological mismatch were similar for all three species and represent a generalizable pattern for other introduced insects sharing a similar multi-voltine life cycle cued by photoperiod.

Benefits: We dedicated considerable effort toward sharing the model and encouraging its application for other systems, including other biocontrol agents, invasive pests, and threatened and endangered species. The model is now publicly accessible online as part of an advanced degree-day phenology modeling system developed and managed by the Oregon IPM Center (formerly IPPC) at Oregon State University. Key results that affect management decisions were shared with DoD resource managers in customized reports. As the most comprehensive geo-climatic phenology model that incorporating photoperiodism, this project has contributed greatly to a general theoretical understanding of how photoperiodism and thermal responses interact for introduced organisms and those exposed to change in climate.

Executive Summary

Introduction and Background

Invasive non-native plants are a leading ecological threat and a major management concern in the extensive natural areas and training grounds on Department of Defense (DoD) lands and waters (Westbrook and Ramos 2005, DOD NRP 2014). Commonly referred to as "weeds" when deemed detrimental, invasive plants displace native plant communities, degrade wildlife habitat, alter hydrology and erosion dynamics, reduce navigability, impede access for recreation and training, and incur enormous costs for control. Invasive species also represent a threat to species of conservation concern (Wilcove et al. 1998), with an estimated 80% of endangered species at risk from these invaders (Pimentel et al. 2005).

Biological weed control in the classical sense involves the purposeful introduction of specialist natural enemies or "biocontrol agents" (usually insects) from the weed's native range with the goal of establishing a permanent population that will suppress the weed population. Biological control is an environmentally sound, sustainable, and cost-effective approach to managing widespread weeds. The approach has claimed many spectacular successes throughout the world, including many on U.S. military installations (Michels et al. 2013, Johnson 2007). Even at military bases where biocontrol has not been directly applied or documented, biocontrol agents spread on their own from other areas to provide the ecosystem service of maintaining lower densities and reducing the competitive ability and invasiveness of environmental weeds. However, not all biocontrol programs are successful in all locations and as many as two-thirds of introduced biocontrol agents fail to establish or do not substantially reduce the weed population (Schwarzlaender et al. 2015). Although rarely objectively confirmed, a climate mismatch between the introduced and native ranges of the biocontrol agent is a commonly implicated cause of failure. In this project, we investigated the important role of insect photoperiodism and the ways that it interacts with climate to affect the performance as biological control agents.

Photoperiodism in insects. A key feature of climatically adapted organisms is that their life cycles are precisely timed to coincide with favorable environmental conditions and resources (Danilevskii 1965; Tauber et al. 1986). Many organisms (perhaps most in temperate zones) use the annual changes in day length as a cue for optimizing timing of at least some life cycle events (Bradshaw and Holzapfel 2007). The response often takes the form of a switch between reproductive and non-reproductive states when a photoperiod-sensitive life stage is exposed to day lengths that are longer, or shorter, than a critical length. Insects, for example, often use shortening day lengths as a cue for entering diapause, a state of suspended development and reduced metabolic activity that allows them to survive through the winter or other unfavorable time periods. As a genetically encoded quantitative trait, the critical photoperiod that triggers the developmental switch is specific and adaptive to a given location but may be mal-adaptive and lead to mismatched phenology if that population is exposed to a new climate, latitude, or seasonal regime.

Although the adaptive functions and fascinating mechanisms of photoperiodism have received decades of attention, especially in plants and insects (reviewed by Danilevskii 1965, Beck 1980, Tauber et al. 1986, Danks 1987, Thomas and Vince-Prue 1996, Nelson et al. 2010), there is a notable absence of models that predict the consequences of photoperiodism when organisms are moved into a new climate or are exposed to a rapid change in climate in their home location. Progress in understanding the consequences of photoperiodism have been hampered by the lack of clear conceptual frameworks, illustrative field and lab studies, and accessible predictive tools. We developed a geo-climatic phenology model that incorporates a short-day cue for diapause (dormancy) and applied it to biocontrol insects used against 3 weed species that are widespread in North America, including on many DoD installations.

Objectives

In correspondence with the SERDP SON, our overall goal is to preserve and enhance effectiveness of biological controls used against non-native invasive plants on Department of Defense (DoD) installations in the United States (U.S.) through an understanding of the phenological constraints that arise in insects due to their responses to the abiotic factors of photoperiod and temperature. Insects that are used as biological control agents are particularly vulnerable to these effects, both because they are translocated into new regions, and exposed to climate change and climate variation due to global processes.

The specific task-oriented objectives of this project were to:

(1) Develop an advanced geo-climatic model that incorporates insect response to the abiotic factors of temperature and photoperiod and use it to predict phenology, voltinism (number of annual generations), and degree of asynchrony with the seasonal conditions and host plant growing season.

(2) Carry out a series of field and laboratory experiments to test model predictions of the ecological and evolutionary consequences of a non-stationary climate in 3 biocontrol systems important to DoD lands: Tamarisk, purple loosestrife, and Japanese knotweed.

(3) Apply the model and experimental outcomes to design strategies for improving biological control for the three target weeds.

(4) Share the model framework and encourage its application for other species of concern on DoD lands, including other biocontrol agents, invasive forest pests, and threatened and endangered species.

Technical Approach

We developed a geo-climatic phenology model that incorporates a short-day cue for diapause (dormancy) and applied it to biocontrol insects used against 3 weed species. The model was

supported with laboratory and field experiments that test the effects of climate change on insect phenology.

The main model developed in this project (Grevstad et al. 2022), expands and improved upon an earlier and simpler version (Grevstad and Coop 2015) by incorporating individual variation in development timing and photoperiod response. We apply the model to three different weed biocontrol systems and carry out related field and laboratory experiments to parameterize and test the model. These systems include a leaf beetle (*Galerucella calmariensis*) used against purple loosestrife (*Lythrum salicaria*), a wetland weed; another leaf beetle (*Diorhabda carinulata*) used against the tamarisk species complex (or salt cedar, *Tamarix* spp.) in Western desert riparian areas; and a newly approved psyllid (*Aphalara itadori*) for the Japanese knotweed species complex (*Fallopia* spp.), which is invasive in northern riverbanks and floodplains. The model combines high resolution, daily, spatialized climate data (from the PRISM group at OSU (Daly et al. 2008)) with date- and latitude-specific photoperiod calculations to predict phenology for a population of insects newly introduced across the continent's varied climate landscape. An important component of the predicted phenology is voltinism, the number of generations that occur in a year. We also developed an individual-based model, limited to tracking phenology at a single site, but capable of incorporating individual variation in parameters and of estimating the population growth resulting from different parameters.

For all three biocontrol agent species, we carried out experiments in controlled environmental chambers to quantify needed parameter estimates for the model and to compare among populations. These parameters included developmental rates, developmental thresholds, and the mean and variance of the critical photoperiod (day length) that cues diapause. The photoperiod response experiments involved rearing insects in six identical environmental chambers that were set with different light: dark cycles. We compared the photoperiod response for insects collected from different geographic locations throughout their introduced range (for tamarisk and loosestrife beetles) and two locations of origin in the native range (for the knotweed psyllid). We used our individual-based model to determine if the mean critical photoperiod was optimal for population growth in each location. A common garden experiment was set up in Corvallis, OR, for the purpose of (1) testing the model predictions in a field setting and (2) determining the consequences (for both insect and target weed) of differences in photoperiod response for insects moved into new climates. In this experiment, the loosestrife leaf beetle, collected from different locations (including DoD sites) with known differences in their photoperiod response were caged onto potted plants. Their phenology, reproductive status, and population growth was monitored throughout the growing season. At the end of the experiment, we harvested and weighed the plants to compare the impacts of difference sources of the biocontrol agent on the weed. We used time lapse field cameras to monitor the phenology of each of the three weed species at field sites throughout the U.S. and to gage the range of dates when plants were green and available for feeding by insects. Finally, we used our model tools and knowledge gained about each biocontrol agent species to develop prospectus reports for each cooperating DoD installation. These reports provided useful results and recommendations relating to managing weed biocontrol systems under variable and changing climates.

Results and Discussion

Our model results reveal geographic patterns of predicted voltinism that differ substantially from traditional phenology models that are based only on degree-days. For introduced insects, such as biological control agents, we reveal the potential for phenological mismatches between the duration of the active phase of the life cycle and the season duration. Our model also reveals the potential for abrupt (non-linear) shifts in the number of annual generations resulting from relatively small changes in climate. These results are relevant for newly introduced organisms (including insect pests and biological control agents) as well as for resident species exposed to rapid changes or variation in climate.

Populations of both the tamarisk beetle and the loosestrife beetle collected throughout their introduced range were found to have evolved geographic differences in the critical photoperiod that cues diapause. The two studied populations of the knotweed psyllid from northern and southern Japan also differed in this trait. In general, where time has allowed it to evolve, the critical photoperiod tends to be longer in more northern (cooler) locations, cuing diapause at an earlier date, and shorter in the south, allowing more generations in warmer southern locations with longer growing seasons.

Our model predicts that biological control agents moved into new regions (or new climates) may experience phenological mismatch in voltinism, attempting to have too many, or too few generations for the season duration, as quantified by our voltinism mapping model. In the case of *A. itadori*, a newly introduced biocontrol agent, the best phenological match is expected in the central regions of the United States (equivalent to the southern half of the invasive range of knotweeds) and it is in these regions where the initial released populations may have the best chance for establishing thriving populations.

Our model was useful for explaining the dramatic release of a phenological constraint in the tamarisk beetle, *D. carinulata*. With the evolution of a shorter critical photoperiod for diapause, this insect was able to increase its voltinism in southern locations from a single generation, before evolution of a shorter critical photoperiod, to seven generations afterward. In this project, we documented the evolutionary change in the critical photoperiod in recent years and the rapid southern range expansion into the Lower Colorado River Basin that became possible because of it.

Our common garden experiment demonstrated how the processes in our model play out in a real field setting. Populations of *G. calmariensis* from different geographic sources and with different quantified photoperiod responses, displayed clear differences in voltinism when moved into a common environment. Moreover, this experiment showed that the particular photoperiod response of a populations used for biocontrol can affect the level of impact that it has on a weed. At least in the near term, populations that attempted a second generation had larger impacts on the plant.

Key outputs from this project included: 1) Mapping version of our model in the DDRP online interface set up for each of the three weed biocontrol agents (at https://uspest.org/dd/dodmaps), (2) Degree-day calculator for user specified locations customized to each of the three biocontrol agent species, (3) online version of the individual-based model, (4) Corresponding software manuals for (1) and (2) above; (5) five published peer-reviewed scientific articles; (6) three manuscripts in preparation (to submit later this year); (7) Twenty presentations related to our project; (8) Seven reports provided to DoD land managers with customized results and recommendations relating to the weed biocontrol systems present at each installation; (9) a 128-page final report accompanying this executive summary.

Implications for Future Research and Benefits

In this study, we demonstrated the utility of our newly developed photoperiod phenology model to predict voltinism and phenological mismatch for insects that are exposed to changes in climate. Our results suggest that new biological control programs for weeds should carefully consider the geographic source (and corresponding photoperiod response) that will provide an appropriate number of generations for the target region. There may be situations where impacts to the weed may be increased by ensuring use of a source that will have more generations (rather than fewer) since increased generations is likely to have a larger impact on the weed, provided these generations can be completed during the favorable seasonal window. Further, we showed that future climate change and increased annual climate variation can have drastic effects on insect voltinism and the degree to which the active phase of the life cycle "fits" into the seasonal window (or gets "caught" in unfavorable weather). Our model can help predict near term booms and busts based on year-to-date and near-term future forecasted climate.

Our results demonstrate a general pattern that may arise whenever an insect or other poikilothermic organism with a short-day diapause response is moved (either purposefully or accidentally) to a new region or continent. Specifically, insects originating from a lower latitude, which typically have shorter critical photoperiods (Danilevskii 1965; Masaki 1999), will have a tendency to reproduce too late in the fall when they are moved to a higher latitude (south to north in the northern hemisphere). Conversely, those moved from higher to lower latitudes may be prone to diapausing too early, sometimes far too early, and missing part (or most) of the favorable season. We emphasize, however, that end-of-season mismatches can occur even when there has not been a change in latitude, because temperature changes alone can expose the photoperiod-sensitive stage to a different day length that may induce an inappropriately timed developmental response. Thus, the model can help us to understand the potential consequences of long-term local climate change or increased climate variation due to global processes.

Our measurement of the critical photoperiod in populations collected in different regions suggest that the critical photoperiod that cues diapause can evolve with time. Thus, these results may be most relevant for either newly introduced insects, before they have had time to adapt, or insects exposed to rapid annual changes in climate (climate variation). Insects experiencing longer term climate change may have time to adapt their critical photoperiod and alter the number of

generations to match the availability of degree days. The inclusion of individual variation in our model versions offers improved accuracy in voltinism and mismatch estimation with fractional values possible. For example, fractional increases in attempted voltinism (i.e., partial generations) with a warmer climate, rather than discrete jumps to the next whole number, would help to avoid "lost generations" as described by van Dyck et al. (2015). Including this variation also provides the groundwork from which an evolutionary model could be generated.

In customized reports provided to DoD land managers, we were able to use the model to make specific recommendations for improved biological control of weeds. For example, at wetlands near West Point, NY, where beetles normally have only one generation per year, the introduction of *G. calmariensis* from a source population with a shorter critical photoperiod (such southern Oregon), could result in two completed generations per year. The resulting higher population growth rate for the insect and longer feeding exposure time on the plant would likely result in better weed control. Other useful applications include the potential to predict near term biocontrol agent 'booms' or 'busts' based on real time climate and near term voltinism and phenology prediction.

Importantly, our work makes substantial progress toward a general understanding how climate change affects organisms that use day length as a phenological cue. The role of photoperiodism has previously been underappreciated in assessments of their predicted response of insects and other organisms to climate change due to a lack of conceptual frameworks, illustrative field and lab studies, and accessible predictive tools. All of these were provided by this project. Beyond biological control systems, the modelling tools developed in this project can readily applied to invasive pest species, insects of conservation concern, and other organisms.

List of Figures

List of Tables

List of Acronyms

ANOVA = Analysis of Variance
APHIS = Animal and Plant Health Inspection Service
AZ = Arizona
CA = California
CDL = Critical Day Length that causes a switch in development toward diapause
CDL = Critical Day Length, equivalent to critical photoperiod
CI = Confidence interval

CNWR = Cibola National Wildlife Refuge
CO = Colorado
CP = Critical photoperiod, equivalent to critical day length
DD = Degree-days
DDRP = Days Risk and Phenological Event Mapping model platform
DoD = Department of Defense
ECA&D = European Climate Assessment and Dataset
E-OBS = gridded climate data set for Europe from the EU-FP6 project UERRA (http://www.uerra.eu) and the Copernicus Climate Change Service, and the data providers in the ECA&D project (https://www.ecad.eu)
G1, G2, etc. = First generation, second generation, etc.
GHCN = NOAA National Centers for Environmental Information's Global Historical Climatology Network
INWR = Imperial National Wildlife Refuge
IPM = Integrated Pest Management
IPPC = Integrated Plant Protection Center
L : D = Light : Dark (with relative duration of each specified in hours)
LCRB = Lower Colorado River Basin
Lme4 = linear mixed effects model using 'Eigen' and S4, a statistical package in R.
LTD = Lower developmental threshold, a temperature below which development does not occur
NOAA = National Oceanographic and Atmospheric Association
NRP = Natural Resource Program
NV = Nevada
NV = Nevada
NWR = National Wildlife Refuge
NY = New York State
OR = Oregon
P = Statistical probability of outcome under the null hypothesis
PRISM = PRISM Climate Group, providing high-resolution climate data for the United States
R = programming language supported by the *R* Core Team and the *R* Foundation for Statistical Computing
SD (or sd) = standard deviation
SE = standard error
SERDP = Strategic Environmental Research and Development Program
TC = Training Center
UDT = Upper developmental threshold, a temperature above which development does not occur, or slows dramatically.
UERRA = Uncertainties in Ensembles of Regional Re-analyses; www.uerra.eu
USA = United States of America
USDA = United States Department of Agriculture
UT = Utah
WA = Washington State

Acknowledgements

This project was primarily funded by the U.S. Department of Defense Strategic Environmental Research and Development Program (US Army Corps of Engineers, Contract No. W912HQ-17-C-0051). Additional support for related work was provided by the U.S. Forest Service grants and cooperative agreements 10-CA-11420004-255, 13-CA-11420004-042, 19-DG-11420000-056, and 20-DG-11062765-733; a contract from the Washington State Department of Agriculture (K2270); a grant from the USDA-APHIS AP20PPQFO000C174; and AAFC Competitive Grant J-002201.001.03. Development of the DDRP model was funded in part by grants from USDA-NIFA (Crop Protection and Pest Management - Extension Implementation Program [CPPM-EIP] and Tactical Sciences for Agricultural Biosecurity [TSAB] programs).

We would like to acknowledge Nina Louden, Sonya Daly, Teresa Rodriquez and Meghan Cline for assistance with maintenance and rearing of *Diorhabda* cultures as well as assistance with diapause induction experiments at the Palisade Insectary. We thank Lisa Weigel at Yakima Training Center and Mike Pitcairn and Baldo Villegas at the California Department of Food and Agriculture for support with site selection and collections. We thank Brittany Barker, Katarina Lunde, Monte Mattson, and Peter McEvoy for feedback on manuscript drafts. We acknowledge the E-OBS dataset from the EU-FP6 project UERRA (http://www.uerra.eu) and the Copernicus Climate Change Service, and the data providers in the ECA&D project (https://www.ecad.eu). We thank the DoD resource managers for working with us on this project including Colin Leingang, Lisa Weigel, Chris Pray, Chris Killough, Travis Gantner, Jeff Mach, Amber Martins, Todd Zuchowski. Finally, we thank the SERDP board members and staff for making this all possible.

Keywords

Aphalara itadori, classical biological control, climate change, critical day length, degree-day model, *Diorhabda carinulata*, *Fallopia* spp., *Galerucella calmariensis*, insect, knotweed psyllid, *Lythrum salicaria*, phenology mismatch, photoperiodism, short-day diapause response, *Tamarix* spp., voltinism model.

1. Introduction and Objective

Invasive non-native plants are a leading ecological threat and a major management concern in the extensive natural areas and training grounds on Department of Defense (DoD) lands and waters (Westbrook and Ramos 2005, DOD NRP 2014). Commonly referred to as "weeds" when deemed detrimental, invasive plants displace native plant communities, degrade wildlife habitat, alter hydrology and erosion dynamics, reduce navigability, impede access for recreation and training, and incur enormous costs for control. Invasive species also represent a threat to species of conservation concern (Wilcove et al. 1998), with an estimated 80% of endangered species at risk from these invaders (Pimentel et al. 2005).

Biological weed control in the classical sense involves the purposeful introduction of specialist natural enemies or "biocontrol agents" (usually insects) from the weed's native range with the goal of establishing a permanent population that will suppress the weed population. Biological control is an environmentally sound, sustainable, and cost-effective approach to managing widespread weeds. The approach has claimed many spectacular successes throughout the world, including many on U.S. military installations (Michels et al. 2013, Johnson 2007). Even at military bases where biocontrol has not been directly applied or documented, biocontrol agents spread on their own from other areas to provide the ecosystem service of maintaining lower densities and reducing the competitive ability and invasiveness of environmental weeds. However, not all biocontrol programs are successful in all locations and as many as two-thirds of introduced biocontrol agents fail to establish or do not substantially reduce the weed population (Schwarzlaender et al. 2015). Although rarely objectively confirmed, a climate mismatch between the introduced and native ranges of the biocontrol agent is a commonly implicated cause of failure.

A key feature of climatically adapted organisms is that their life cycles are precisely timed to coincide with favorable environmental conditions and resources (Danilevskii 1965; Tauber et al. 1986). Many organisms (perhaps most in temperate zones) use the annual changes in day length as a cue for optimizing timing of at least some life cycle events (Bradshaw and Holzapfel 2007). The response often takes the form of a switch between reproductive and non-reproductive states when a photoperiod-sensitive life stage is exposed to day lengths that are longer, or shorter, than a critical length. Many insects, for example, use shortening day lengths as a cue for entering diapause, a state of suspended development and reduced metabolic activity that allows them to survive through the winter or other unfavorable time periods. As a genetically encoded quantitative trait, the critical photoperiod that triggers the developmental switch is specific and adaptive to a given location but may be mal-adaptive and lead to mismatched phenology if that population is exposed to a new climate, latitude, or seasonal regime.

Although the adaptive functions and fascinating mechanisms of photoperiodism have received decades of attention, especially in plants and insects (reviewed by Danilevskii 1965, Beck 1980, Tauber et al. 1986, Danks 1987, Thomas and Vince-Prue 1996, Nelson et al. 2010), there is a notable absence of models that predict the consequences of photoperiodism when organisms are moved into a new climate or are exposed to a rapid change in climate in their home location. Progress in understanding the consequences of photoperiodism have been hampered by the lack of clear conceptual frameworks, illustrative field and lab studies, and accessible predictive tools.

Objective

In correspondence with the SERDP Statement of Need, the overall goal of this project was to help preserve and enhance effectiveness of biological controls used against non-native invasive plants on Department of Defense (DoD) installations in the United States (U.S.) by gaining understanding of the phenological constraints that arise in insects due to their responses to the abiotic factors of photoperiod and temperature.

The specific task-oriented objectives are to:

(1) Develop an advanced geo-climatic model that incorporates insect response to the abiotic factors of temperature and photoperiod and use it to predict phenology, voltinism (number of annual generations), and degree of asynchrony with the seasonal conditions and host plant growing season.

(2) Carry out a series of field and laboratory experiments to test model predictions of the ecological and evolutionary consequences of a non-stationary climate in 3 biocontrol systems important to DoD lands: Tamarisk, purple loosestrife, and Japanese knotweed.

(3) Apply the model and experimental outcomes to design strategies for improving biological control for the three target weeds and to.

(4) Share the model framework and encourage its application for other species of concern on DoD lands, including other biocontrol agents, invasive forest pests, and threatened and endangered species.

In this final project report, we first describe two versions of our improved model (Chapter 2 and Grevstad et al. 2022), which expand upon a simpler, earlier version (Grevstad and Coop 2015) by incorporating individual variation in development timing and photoperiod response. We then describe applications of the models and associated field and laboratory experiments involving 3 different weed biocontrol systems. These systems include a newly approved psyllid (*Aphalara itadori*) for control of Japanese knotweed species complex (*Fallopia* spp.) which is invading northern riverbanks and floodplains (Chapter 3); a leaf beetle (*Galerucella calmariensis*) used against the wetland weed purple loosestrife (*Lythrum salicaria* (Chapters 4 and 5); and another leaf beetle (*Diorhabda carinulata*) used against tamarisk species complex (or salt cedar, *Tamarix* spp.) in Western desert riparian areas (Chapter 6). We use an individual-based version of the model to assess whether evolved photoperiod responses in different populations of two of these species are optimized for the local climate. Finally, we summarize our project's outreach activities in which we provided information and decision support for land managers wishing to conserve the benefits of biological control in a changing climate.

2. A geo-climatic insect phenology model incorporating photoperiod-cued diapause

Model background

Insects are poikilothermic, meaning their speed of development is determined by environmental temperature. This makes it possible to model life cycle timing (phenology) using historic or forecasted climate data. Degree-day phenology models have long been used to predict emergence timing and voltinism (number of annual generations) of pests and beneficial insects. Such models are also useful in predicting future phenological changes that might occur under predicted global climate change scenarios.

Until recently, most degree-day models that are used to predict insect responses to climate change have neglected the fact that a majority of insects in temperate zones use the seasonal changes in day length as a cue for synchronizing their life cycle with favorable seasonal conditions. In previous work (Grevstad and Coop 2015), we showed that climate change can have dramatic and unexpected effects on voltinism (number of annual generations) for insects that use photoperiod as a cue for terminating reproduction. For example, an insect that would normally have 3 generations per year might only have one generation when exposed to a warmer climate. Alternatively, in a cooler climate, they may attempt more generations than the growing season allows leading to a fall generation that is "lost" to a fall frost. Newly introduced insects, such as biological control agents, are especially vulnerable to these effects. A major objective of this SERDP project was to expand and improve this phenology model and parameterize it for our three focal biocontrol species and to make it available online for other users.

Our model applies to a common multi-voltine life cycle that alternates between diapausing and reproductive phases (Fig. 1). Day lengths shorter than a critical length serve as the cue for diapause. A change in temperature affects the date of emergence of the photoperiod-sensitive stage (newly eclosed adults for the three insects we studied) and thus the day length to which it is exposed. This interaction between temperature and photoperiod can lead to major phenological consequences from small changes in climate.

Overview of model versions and improvements

In this project we expanded our previous model creating two improved versions (see Table 1). The first is a spatialized phenology model that can be used with continent-wide climate datasets. It produces mapped output such as voltinism prediction maps (Grevstad et al. 2022) and maps of the date of predicted occurrence of phenological events. This improved mapping version also incorporates individual variation as described in our original project proposal. The second version is an individual-based model (IBM) that can be used to model populations of insects at one geographic location (or a cluster of point locations in a small region) and which fully incorporates individual variation in development timing and photoperiod response (Wepprich et

al. ms. in prep.). It also allows population growth between generations. For both of these models, we added the capacity to use future forecasted climate datasets in order to explore and understand how weed biocontrol systems may be affected by future climate change scenarios. Both models are available online. The mapping model was integrated with the Oregon IPM Center's Degree-Days Risk and Phenological Event Mapping (DDRP) model platform and can be found here: uspest.org/dd/dodmaps. The individual-based model is in its own shiny-app location: tyson-wepprich.shinyapps.io/Biocontrol_Voltinism_Simulation/. Further differences between the completed model versions are described in Table 1.

	Individual Based Model	**Mapping Model (v. 1.0)**
Scale of Application	Single site or very small region	Large regions or entire continent
Model Units	Individual-based simulation with specified random variation in emergence timing, oviposition timing, development rate, and response to photoperiod	Time distributed cohorts (see Fig. 2), each with a fixed degree-day requirement for development
Diapause	For each individual, diapause is determined by the critical photoperiod, drawn from a normal distribution with mean and variance selected to match the range of responses from chamber experiments.	The proportion of the population diapausing is a function of photoperiod at the time of adult eclosion (sensitive stage). The function represents a logistic curve fit to data from chamber experiments.
Voltinism	Tracks the mean number of generations completed each year, including partial generations accounting for the individuals in diapause	Tracks the mean number of generations completed each year, including partial generations accounting for the proportion of the population in diapause
Population Growth	Tracks population growth between generations and between years	Tracks phenology and voltinism, but not population growth

All versions share the same general input:

- Species-specific development rate and developmental thermal thresholds
- Photoperiod response derived from experiments
- Spring emergence timing estimated in degree-days
- Location-specific daily maximum and minimum temperatures (from available high resolution spatialized climate datasets), used to calculate species-specific degree-days.
- Latitude-specific day lengths calculated using method of Forsythe et al. (1995).

Table 1. A comparison of the two completed model versions.

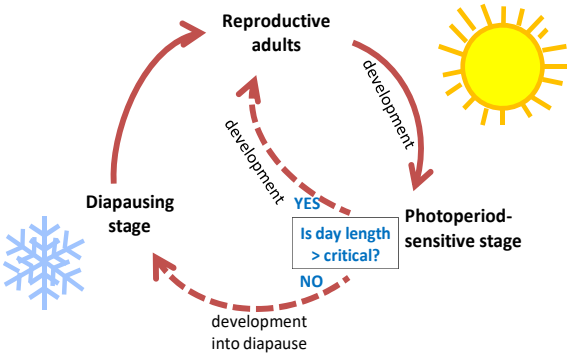

Figure 1. Multi-voltine life cycle with a short-day diapause response.

Figure 2. The new versions of the model incorporate variation in the development timing (below) and response to photoperiod (right) so that a population can have a split response to photoperiod and partial generations.

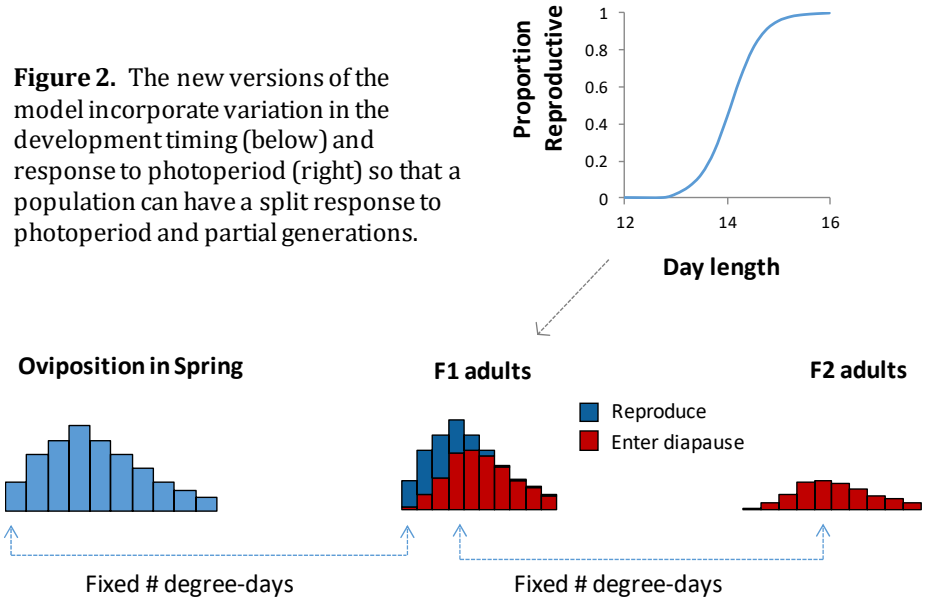

Model Details

Both versions of the model apply to a common insect life cycle that is multi-voltine with a short-day diapause response (described by Koštál 2006, Fig. 1). All three biocontrol agents studied in this project have this form of lifecycle, which includes the following characteristics: (1) The transition into diapause is triggered when the photoperiod-sensitive life stage is exposed to day lengths shorter than a critical photoperiod. (2) Diapause is maintained for a period of time during which the insect is not developmentally responsive to warm temperatures. (3) At some point during the cold season, but prior to the start of the accumulation of degree-days, diapause ends and temperature-dependent development resumes (based on accumulated degree-days). (4) During the active season, one or more generations occur until the photoperiod-sensitive life stage is again exposed to day lengths that are shorter than the critical photoperiod. We make the assumption that degree-day accumulation begins on 1 January. This is an arbitrary choice suited to locations that have moderate to cold winters, where the temperature is rarely (if at all) above the threshold for development during mid-winter.

Mapping Model

The mapping version of the model is our primary product from this project. It expands on an earlier version by Grevstad and Coop (2015) by adding variation in the timing of spring oviposition and in the day length threshold for cuing diapause. It uses a new computing platform written entirely in R, greatly simplifying model operations and parameterization for other species. The model has been integrated with, and builds on, our recently developed open-source geo-climatic phenology modeling platform, Degree-Days, Risk, and Phenological Event Mapping (DDRP) (Barker et al. 2020), by incorporating the short-day diapause response. Aside from the addition of photoperiod-cued diapause, the basic operation is similar to DDRP models that have recently been developed by our team for other species (Barker et al. 2020).

The key model parameters include spring oviposition timing, development rates, lower and upper developmental thresholds, and the mean and standard deviation of the critical photoperiod. The parameters for all three species were obtained from experiments (details in Table 1). Other parameters including the timing and standard deviation of spring oviposition (the distribution of cohorts) were approximated based on best available field and lab data. We designated the photoperiod sensitive stage of each insect species based on results of our long-to-short and short-to-long photoperiod transfer experiments.

The model is programmed in R 3.6.2 (R Core Team 2019) and uses publicly available daily spatialized climate data sets (maximum and minimum temperatures) that have been interpolated from weather station data. The source of the climate data varied by application, but included (1) Daymet version 3 which has a resolution of 1 km^2 and is updated annually with data from the NOAA National Centers for Environmental Information's Global Historical Climatology Network (GHCN)-Daily weather stations (Menne et al. 2012, Thornton et al. 2016), (2) PRISM Climate Data which is 4 km^2 near-real time and historical gridded climate data for the conterminous US (Daly et al. 2008, Daly et al. 2015), and (3) for Europe, E-OBS version 22.0e for 2010-2019 from the EU-FP6 project UERRA and the Copernicus Climate Change Service,

which is compiled from ECA&D daily station data with a resolution of 0.1 degrees (Cornes et al. 2018).

The program workflow steps through each day of a calendar year beginning with January 1 and calculates accumulated degree-days using the single triangle method (Zalom et al. 1983) and day length using the method of Forsythe et al. (1995) with 1.5° of twilight for each spatial grid cell in the geographic focal region or continent. The accumulated degree-days are used to determine the life stage present (overwintering stage, eggs, juvenile stages, and adults) and the number of generations completed.

The mapping version of the model incorporates variation in phenology through the use of six time-distributed cohorts that reflect the distribution of oviposition dates in the spring (truncated normal on a degree-day scale, Fig. 3). Thus, the daily accumulation of degree-days and accompanying life cycle transitions are carried out in six separate bins starting from each cohort's initial oviposition date. For computational simplicity, individuals within each cohort are assumed to develop in synchrony, requiring a fixed number of degree days to reach the next life stage. Oviposition in subsequent generations also occurs at one time point within each cohort (as measured in degree-days) but maintains the same variation in timing across the cohorts. The use of six cohorts was an arbitrary compromise between adding realism and keeping model run time manageable.

When a cohort reaches the photosensitive stage (e.g., first day of fifth instar nymph in the case of the knotweed psyllid, Fig. 3), the date- and latitude-specific day length determines the proportion of the cohort that switches to a diapause developmental pathway (based on probit curve fit to experimental data). Cohorts differ in the proportions entering diapause because they reach the sensitive life stage on different dates. The portion that does not enter diapause proceeds through the pre-oviposition period to the egg stage in the next generation. The above steps are repeated when the next sensitive stage is reached. Reproduction is assumed at replacement level (no population growth) and reproductive individuals are assumed to die following oviposition (i.e., they do not go on to diapause after reproducing).

After the last day of the daily time step (December 31), the program combines results across all cohorts and calculates weighted means of the output based on the relative size of each cohort. Cohorts that are in an immature stage at the end of the year count toward attempted generations, but not completed generations. Weighted means are used to estimate the overall proportion of the population in each life stage, the cumulative percent of the population in diapause, and voltinism (described below in "Predicting voltinism and phenological mismatch").

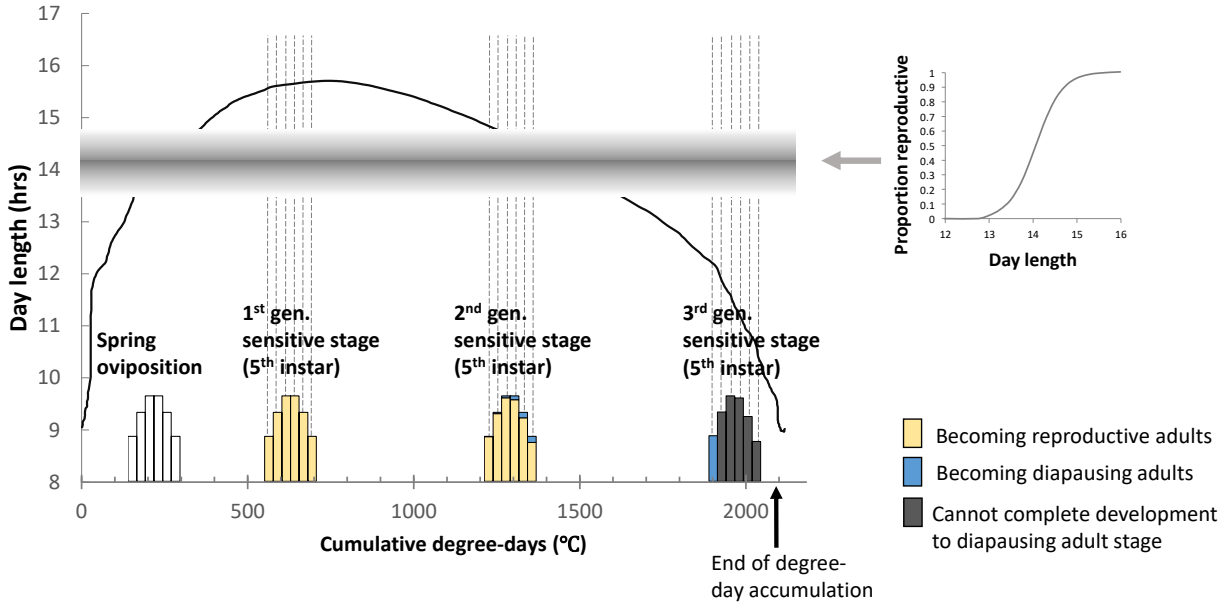

Figure 3. Phenology progression and diapause determination used in the mapping model. The curve represents site-specific day length as a function of site-specific cumulative degree-days (example for *Aphalara itadori* (knotweed psyllid) in Corvallis, Oregon, USA at 44.6 ° latitude, year 2019). The bars show time-distributed cohorts of initial spring eggs (white) and fifth instar nymphs (the photoperiod-sensitive stage, shaded bars). The proportion of nymphs in each cohort that will reproduce (light gray shading) is determined by the day length when the sensitive stage emerges in accordance with the photoperiod response curve. In this example, only the earliest of the third-generation nymphs will reach the diapausing adult stage.

Predicting voltinism and phenological mismatch

The mapping model produces three types of maps at the end of the year. The first map depicts the number of *potential* generations based on available degree-days alone (no short-day trigger for diapause induction in model). Potential generations were quantified by running the model without the diapause response to photoperiod and counting the number of generations that were completed (reaching adult reproductive or diapause stage) before the end of degree-day accumulation (or December 31). While each cohort's potential voltinism was an integer, the weighted average across cohorts could be a decimal if cohorts completed a different number of generations (made possible by the initial distributed springtime oviposition).

The second type of map shows the number of generations that would be *attempted*, given the population's diapause response (short-day trigger for diapause included in model). Attempted generations were quantified for each cohort by summing the proportion in each generation (including overwintering generation) that were reproductive at oviposition time, regardless of whether there were sufficient degree-days for their offspring to develop. Because overwintered adults are assumed to be 100% reproductive, the minimum attempted generations is always one. Attempted voltinism for the entire population was estimated as the weighted average of generations attempted across the six cohorts.

The third type of map presents the degree of phenological mismatch, quantified by subtracting the *potential* number of generations from the *attempted* number of generations for each cohort separately and then taking the average of the differences, weighted by cohort size. Negative mismatch means that, due to the diapause response to photoperiod, fewer generations were attempted than the seasonal temperatures could actually support. Positive mismatch means that diapause was not cued early enough, and its value (between zero and one) represents the proportion of the final generation that dies because there were too few degree-days to complete development to the diapause stage. We rounded the voltinism mismatch estimates to the nearest integer number (or to the nearest 0.25 in the case of positive mismatches) for mapping purposes.

Individual-Based Model

Our individual-based model is similar to the mapping model, except that it incorporates the full range of individual variation by tracking the lifecycle of each individual in a population, rather than grouping into cohorts (Fig. 4). This model was not a product originally planned as part of our proposed project, but it has proven valuable as a complement to the mapping model for certain applications. It is available online in an adaptable form for researchers with knowledge of the parameters for the organisms they work with. Individuals, assumed all females in the simulation, are assigned development rates and diapause day length threshold as random numbers drawn a specified distribution. Because tracking of individuals is computationally intensive, use of the model is restricted to single sites or small clusters of sites. The model can also incorporate demographic information to estimate the effects of phenology and voltinism on population growth from one year to the next. This makes it suitable to investigate the fitness consequences of a change in climate or latitude, as well as any evolved change in the organism's life cycle parameters such as the critical photoperiod that cues diapause.

The parameters for the model are similar to those in our mapping model, expressed as distributions estimated from field and lab studies. The initiation of oviposition by overwintered females occurs at a number of degree days assigned by random draw from a skewed normal distribution. Females in this parental generation were assumed to have one surviving offspring each. For subsequent generations, we assigned stage-specific time requirements in degree-days and day length thresholds to each simulated individual by sampling from normal distributions. We assumed that adult beetles must complete a pre-oviposition or pre-diapause stage before successfully reproducing or entering diapause, although most studies only measure pre-oviposition time requirements. We tracked the timing (day of year and accumulated degree-days) of lifecycle transitions for each simulated individual across all generations if reproduction occurred.

In our project, this version of the model was particularly useful for understanding the complicated nature of voltinism (including populations with split diapause decisions, incomplete generations, and lost generations) and for estimating the effect of climate or latitude change on not only phenology/voltinism but also its follow-on effect on population growth or fitness. We used it to determine the optimal mean critical photoperiod that would provide optimal fitness for

a population in a given location and compared these predictions to critical day lengths of field collected populations measured in controlled environment chambers (see section 7).

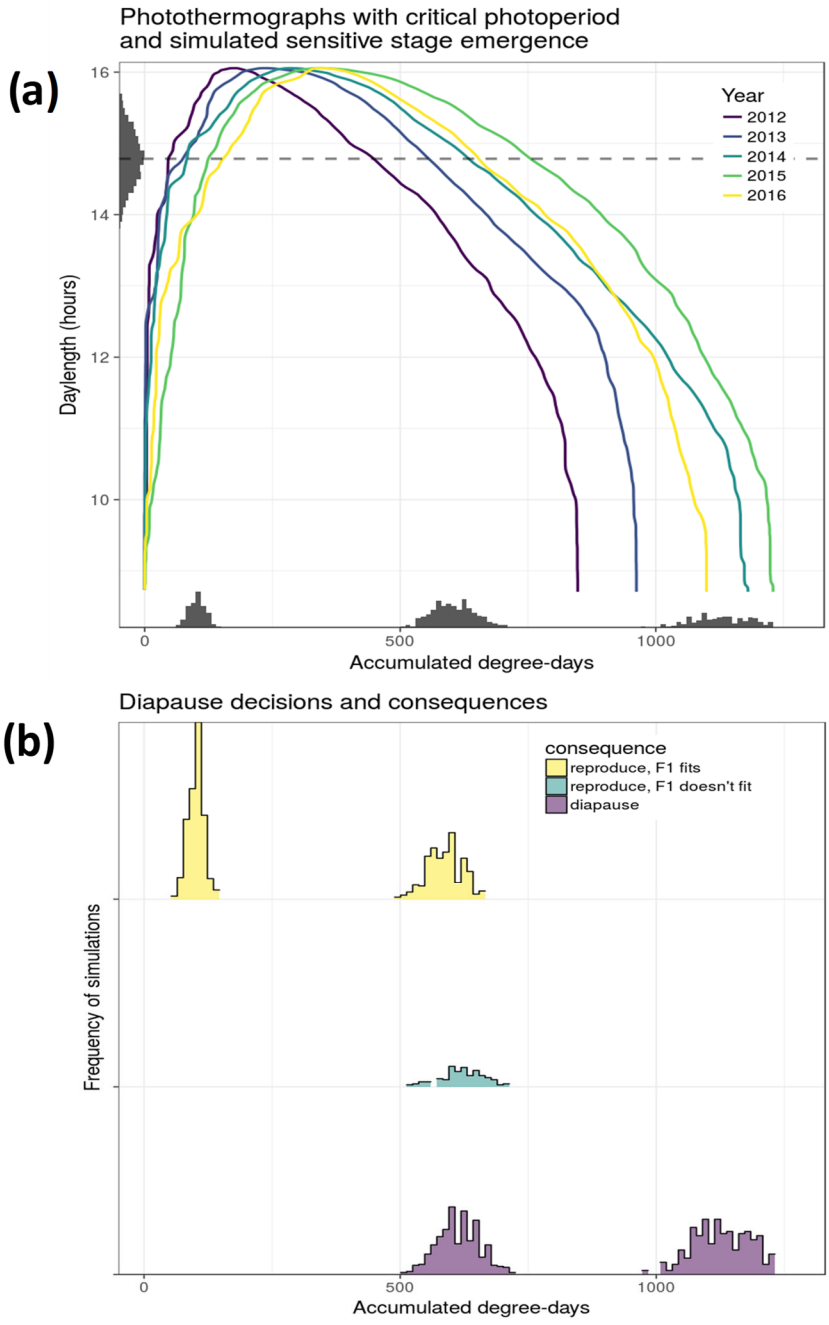

Figure 4. Example of output from the individual based model. Curves represent site-specific day lengths as a function of site-specific accumulated degree-days for each of 5 years. In (a), the histogram along the y-axis shows individual variation in the critical photoperiod that cues diapause. The histograms along the x-axis show the timing of emergence of the adult stage. In (b), the yellow histograms show adults that emerged and reproduced successfully (with sufficient time to complete development), the blue histogram shows adults that emerged and reproduced unsuccessfully (offspring did not complete development), and the purple histograms show adults that entered diapause without reproducing.

3. Predicting phenology match for a new biocontrol agent—*Aphalara itadori* introduced for Japanese knotweed

Our mapping model can be used to predict regions where biocontrol agents are likely to succeed or fail prior to their introduction. Two biotypes of the knotweed psyllid (*Aphalara itadori,* Fig. 5), one from northern Japan (Hokkaido) and one from southern Japan (Kyushu) were approved for release into the United States in 2020 as a host specific biocontrol agent for the knotweed species complex (Shaw et al. 2009; Grevstad et al, 2013). Releases of this biocontrol agent have also been made into the United Kingdom (2010), Canada (2014) and the Netherlands (2020). We use the model to map predicted voltinism, given the photoperiod response, and the degree of phenological mismatch in voltinism (or diapause timing) for the length of the local growing season throughout North America and Europe. Full details are available in our published paper (Grevstad et al. 2022).

In North America, knotweeds have become most abundant in the northern half of the United States and southern Canada (Grevstad et al. 2018). In Europe, both parental species are widespread, and the hybrid is increasingly recognized as a significant component of the invasion (Vuković et al, 2019). The plants are most problematic in riparian zones, where they crowd out native plants, alter stream nutrients and food webs, and increase erosion (Beerling and Dawah 1993; Maerz et al. 2005; Urgenson et al. 2009).

Two screened source populations of *A. itadori* were included in this study. A southern strain was originally collected from plants of Japanese knotweed [*Fallopia japonica* (Houtt.) Ronse Decraene] on the Island of Kyushu in southern Japan at 32.8° latitude, and a northern strain was collected from giant knotweed [*Fallopia sachalinensis* (F. Schmidt) Ronse Decraene] on the Island of Hokkaido in the vicinity of Lake Toya at 42.6° latitude. The southern strain was released against *F. japonica* (and hybrid genotypes) in the United Kingdom and Canada. In the United States, both strains have been released to target all three knotweed species. Despite the many years of repeated releases, establishment of permanent populations of *A. itadori* has not been confirmed in either the United Kingdom or Canada. Monitoring for establishment of the recent (2020) releases into the United States and the Netherlands has only just begun.

Aphalara itadori has a facultative multi-voltine life cycle, switching development toward diapause in response to short days in the late summer (confirmed in the photoperiod response experiment below). Eggs are laid on the surfaces of knotweed stems and leaves, especially along the leaf veins and under the leaf sheaths. Nymphs and adults feed by inserting mouthparts into leaves or stems and ingesting the sap. There are five nymphal instars. The adult stage overwinters in an apparent state of reproductive diapause and emerges to continue reproductive development in response to warming temperatures in the spring. For the two source populations, we carried out experiments to determine developmental parameters, including temperature-dependent development rates, overwintering emergence timing, and the diapause response to a range of photoperiods.

Figure 5. *Aphalara itadori* (adult with eggs) and its host plant *Fallopia japonica*

Methods for Parameterizing the Model

Determining development rates and thresholds

We carried out two experiments in controlled environment chambers to quantify the relationship between temperature and development rate and then combined these results with those previously published by Myint et al. 2012 in a linear regression (Fig. 6, details in Grevstad et al. 2022). We used the x-intercept as the estimate of the lower developmental threshold and the inverse of the slope as the degree-day requirement for development from egg to adult (Campbell et al. 1974). The upper threshold was estimated as the temperature at which a large drop in development was found.

Photoperiod response experiment

We determined the relationship between day length and the proportion of adult psyllids entering diapause in an experiment using controlled environment chambers programmed with five photoperiod treatments (light: dark cycles) as follows: 13 L:11 D, 14 L:10 D, 14.5 L: 9.5 D, 15 L: 9 D, and 16 L: 8 D. Knotweed plants were grown from seed to a height of approximately 15 cm in 13 cm square pots in a greenhouse. For each psyllid strain (northern, southern), and for each photoperiod treatment, five pairs of adult psyllids were caged onto each of eight plants for 24 hours to establish cohorts of same age eggs. We used the preferred host plant for each psyllid strain (*F. sachalinensis* for Hokkaido and *F. japonica* for Kyushu). The environmental chambers were set with a constant temperature of 22 °C and 60% relative humidity. During egg

development the chambers were set with light: dark cycle of 16 L: 8 D (for 12 days) and then the lights were programmed to the treatment photoperiod for the remainder of the experiment. The plants were watered as needed. As adults eclosed, they were removed and placed in a separate cage

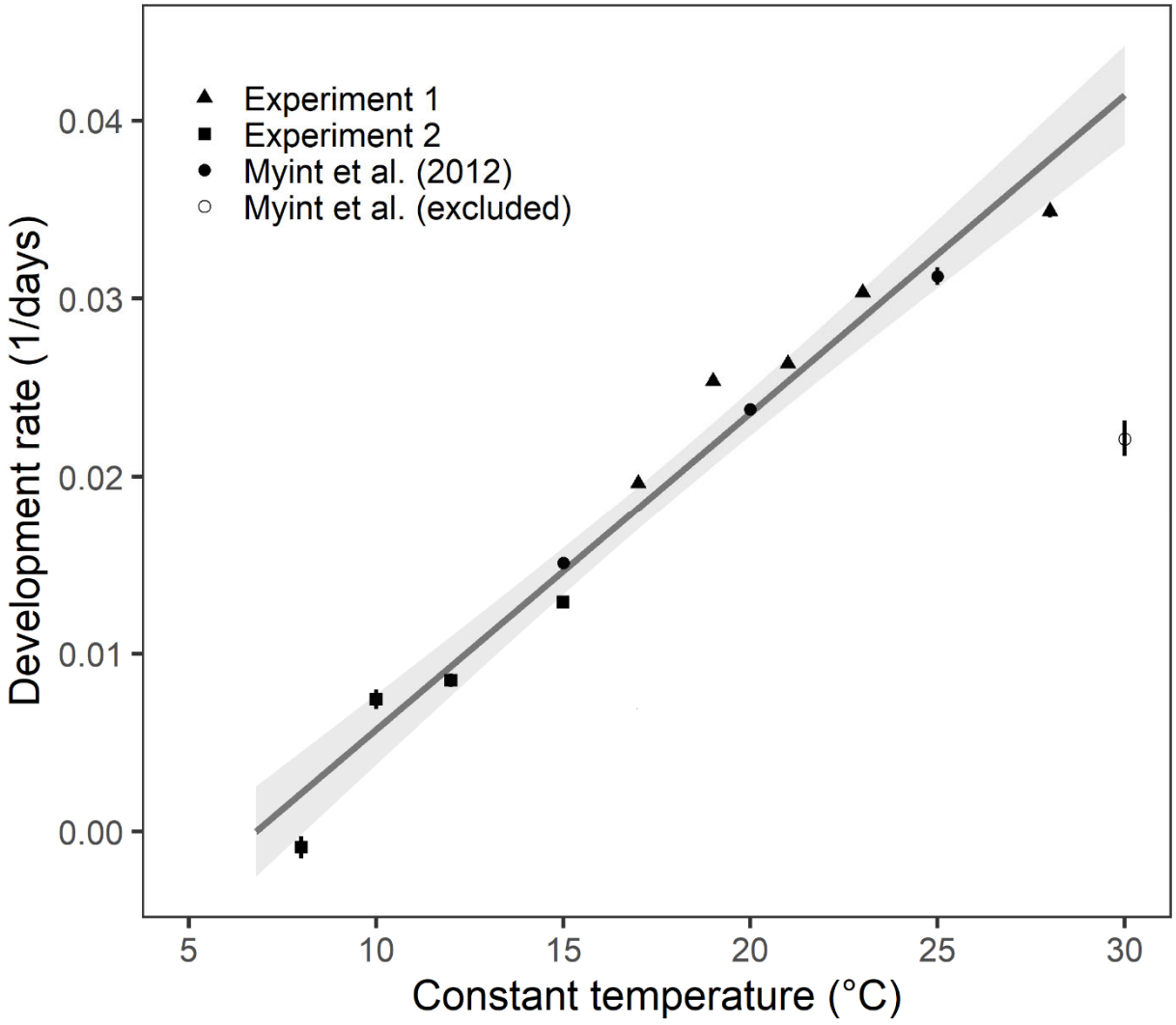

Figure 6. Relationship between development rate (egg to adult) and temperature in *Aphalara itadori* using data from three experiments (from Grevstad et al. 2022). The mean development rate (points) and spread of data for each treatment (middle 95% percentile, vertical lines) is shown. The trend line is the fitted linear regression for the linear portion of the relationship (excluding the 30 °C point): $y = 0.00183x - 0.0126$.

Table 2. Parameter values used in the phenology model for *Aphalara itadori.* Degree-days are in Celsius units.

Parameter	**Estimate**	**Source**
Lower developmental threshold (LDT)	6.9 °C	X-intercept of linear regression of development rates on constant temperatures from three separate chamber experiments (Fig. 6).
Upper developmental threshold (UDT)	30 °C	Approximated based on observed decrease in development rate at 30 °C (data from Myint et al. 2012, Fig. 6)
Degree-days required to develop (egg to new adult)	546	Inverse of the slope in linear regression (Fig. 6)
Degree-days required for each life stage (important for cohort model and to know when sensitive stage happens)	Egg: 143 Nymph stages 1-4: 270 Nymph stage 5: 133	From Myint et al. (2012), the mean proportion of development time spent in each stage multiplied by 546 degree-days.
Pre-oviposition/pre-diapause degree-days	70	From Myint et al. (2012): pre-oviposition period was ~4.5 days at optimal temperatures 20 or 25 °C or an average of 70 required $DD_{6.9}$. Pre-diapause assumed to be similar.
Photoperiod Response (Critical photoperiod (CP) and standard deviation (sd)	Hokkaido: 14.7 h Kyushu: 14.1 h sd =0.284	Probit regression fit to data from photoperiod experiment (Fig. 7).
Sensitive stage	Early 5^{th} instar	Based on test of nymph vs. adult exposure to 12 vs. 16 hours day length (Appendix S1)
Delay for peak oviposition timing	50	Approximated based on oviposition schedule and assumed greater contribution of earlier eggs to future generations.
Start of post-overwintering oviposition in the spring, in degree-days	Normal (μ = 220, sd = 50), truncated between 150 and 300 to avoid unrealistic outliers	Estimated from spring emergence experiment, mostly from Kyushu strain that had more reliable data (Fig. 8). Also corresponds with observed emergence timing in Japan.

on a fresh plant in the same chamber. After one week, adult females were placed individually into a small petri dish with moist filter paper and a piece of knotweed leaf to determine if they were reproductive, as evidenced by the presence of eggs on the leaf after 48 hours. The relationship between photoperiod and reproductive status was quantified using probit regression and assumed similar slopes for each psyllid strain. The southern biotype was found to have a shorter critical photoperiod (14.1 h) (where 50% entered diapause) than the northern psyllid (14.9 h). This relationship was then used in our phenology model to determine the timing of diapause.

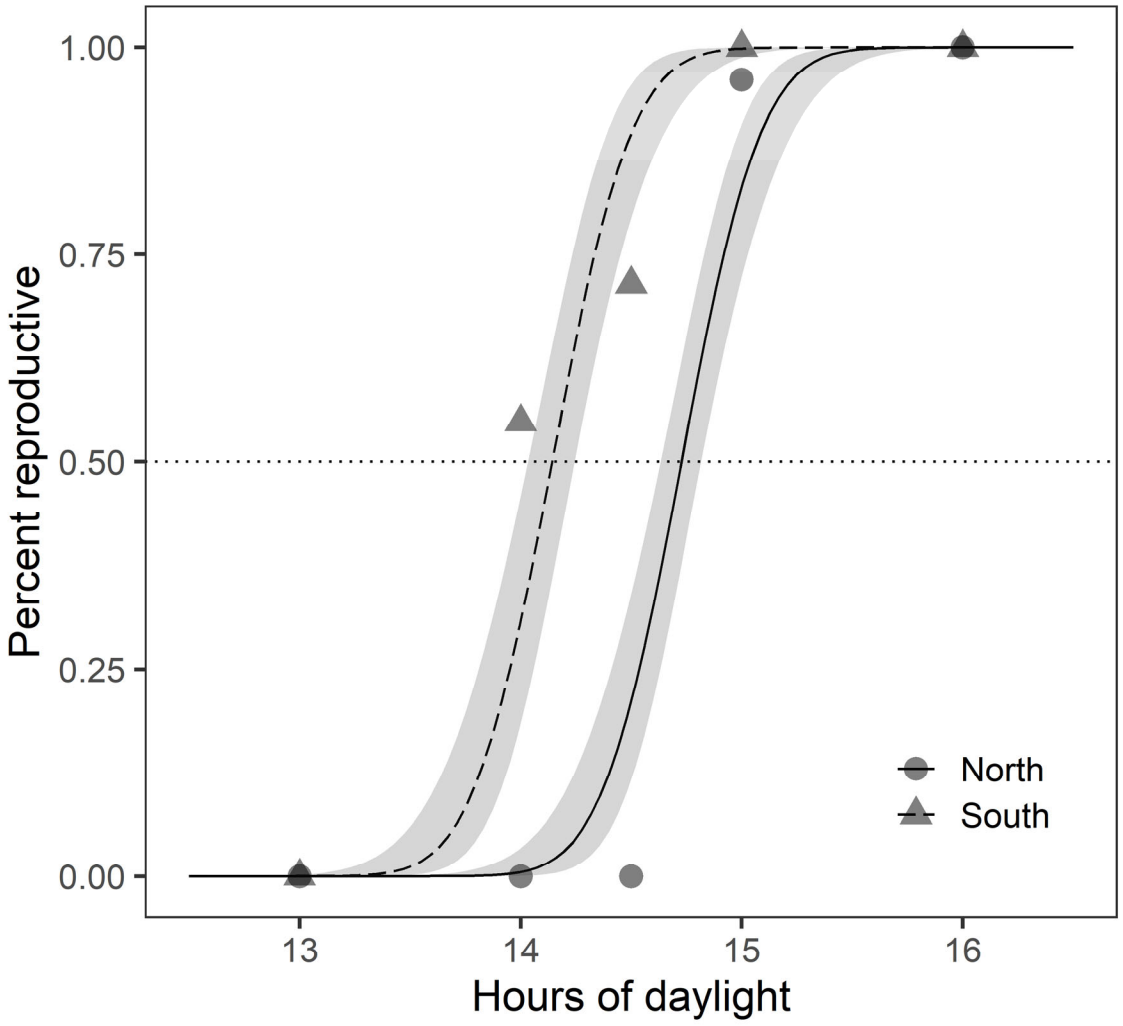

Figure 7. Proportion of adults of both northern (from Hokkaido, Japan) and southern (from Kyushu, Japan) strains of the knotweed psyllid (*Aphalara itadori*) that remained reproductive (as opposed to diapausing) when reared at different photoperiods. Fitted probit models assume similar slopes (or individual variation) for the two populations (from Grevstad et al. 2022).

Spring emergence timing

We experimentally determined the degree days required to bring psyllids out of diapause. Both populations were reared on caged potted knotweed plants under conditions that induced diapause in the adult stage (gradually decreasing photoperiod and temperature). The caged plants with dormant psyllids were kept in a refrigerator at 4 °C for 4 months. We then transferred psyllids into each of 24 15-cm diameter petri dishes lined with damp filter paper and a fresh piece of leaf. Each dish (containing approximately 30 psyllids) was then exposed to one of 12 treatments. The treatments consisted of 6 photoperiods (ranging from 10 to 16 hours of light) crossed with two constant temperatures (14 °C and 26 °C). The leaves were replaced as needed and the number of eggs on the leaves were counted every two days. We also tracked adult mortality in the petri dishes allowing us to estimate oviposition rates per live adult.

For both psyllids and both temperature treatments, oviposition appeared to reach full capacity at around 220 or 230 degree-days (Fig. 8). There was a very slight delay in emergence timing for the two shortest photoperiods. However, this effect is omitted from our model since photoperiods this short would only occur before the spring equinox and well before sufficient degree days are reached in the regions of interest. For the model, we represented the start of oviposition after springtime diapause termination with a normal distribution with mean 220 degree-days and standard deviation of 50 degree-days.

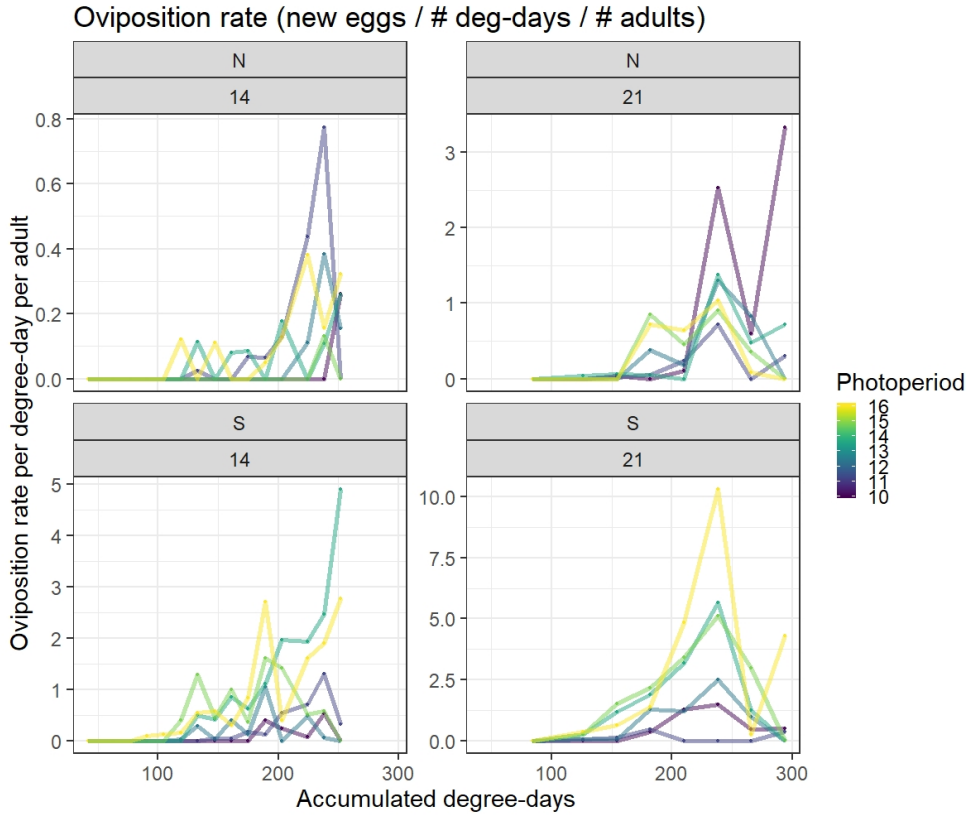

Figure 8. Timing of oviposition of artificially overwintered adults of northern (top) and southern (bottom) biotypes of the knotweed psyllid when moved into two temperature treatments (14 °C left, 21 °C right) and six photoperiod treatments.

Results

Knotweed psyllid predicted voltinism and phenology match

Using the developmental parameters obtained from the above experiments, we used our model to map the number of *potential* generations (based on degree days alone, Fig. 9b. We then compared this with the number of expected *attempted* generations (given the photoperiod response, Fig. 10), and create a third map of the degree of mismatch (= *attempted* minus *potential* generations, Fig. 11).

Estimates of potential voltinism, based on a model without photoperiod-cued diapause, closely align with the geography of climate. For both North America and Europe, a greater number of generations are possible in warmer regions with longer growing seasons (Fig. 9). Potential voltinism generally increases to the south, but climate influences of coast and mountain ranges break up the pattern on both continents (in western North America and south-central Europe). In the regions where knotweed is most prevalent (for example, north of the 36th parallel in North America), the number of potential generations ranges from one to four.

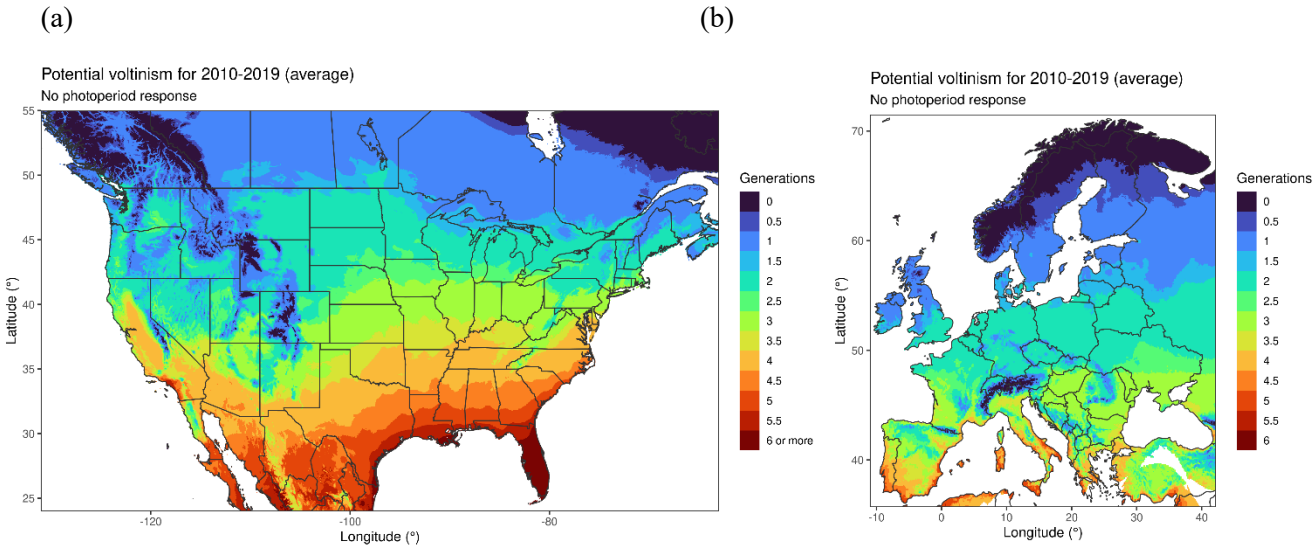

Figure 9. Potential number of annual generations (voltinism) of *Aphalara itadori* based on the availability of degree-days alone (without photoperiod cued diapause response) and using daily degree-days averaged across years 2010-2019 for (a) North America and (b) Europe.

Incorporating *A. itadori*'s experimentally determined photoperiod response in the model results in a very different map for *attempted* voltinism (Fig. 10). For both the northern and southern psyllid strains, the number of generations ranged from one to three for most of North America and Europe, with 3.5 attempted generations in very limited locations. The highest attempted generations are expected in the middle latitudes. Attempted voltinism decreases to the north and with increasing elevation in mountainous zones because of a combination of low degree-days and shortening photoperiods in the fall. Perhaps surprisingly, voltinism also decreases moving toward the south. For some locations, fewer generations in the south may occur because shorter southern day lengths induce earlier diapause in late summer, but usually earlier diapause is made up for by faster development. Instead, the major cause for the gradual decline in voltinism

toward the south, as we have quantified it, is that there is an increasing proportion of the population that enters diapause in earlier generations during spring or early summer. In the far south (e.g., the Southwest and Gulf Coast states), the entire population (all individuals in all cohorts) is expected to diapause after only a single spring generation that is completed before the summer solstice.

The model results show that the northern (Hokkaido) strain would attempt one fewer generation than the southern (Kyushu) strain in many regions because of its longer mean critical photoperiod, which cues the insects into diapause at an earlier date (compare Figs. 10a, b with Figs. 10c,d). While these results represent the average of model runs using temperature data from 10 recent consecutive years (2010-2019), results from individual years vary from this average. For example, compared to the presented averages for the southern strain (Fig. 10c, d), the warmest years within this span (e.g., 2012 in North America and 2018 in Europe) result in much larger regions where three generations would be attempted (see Grevstad et al. 2022).

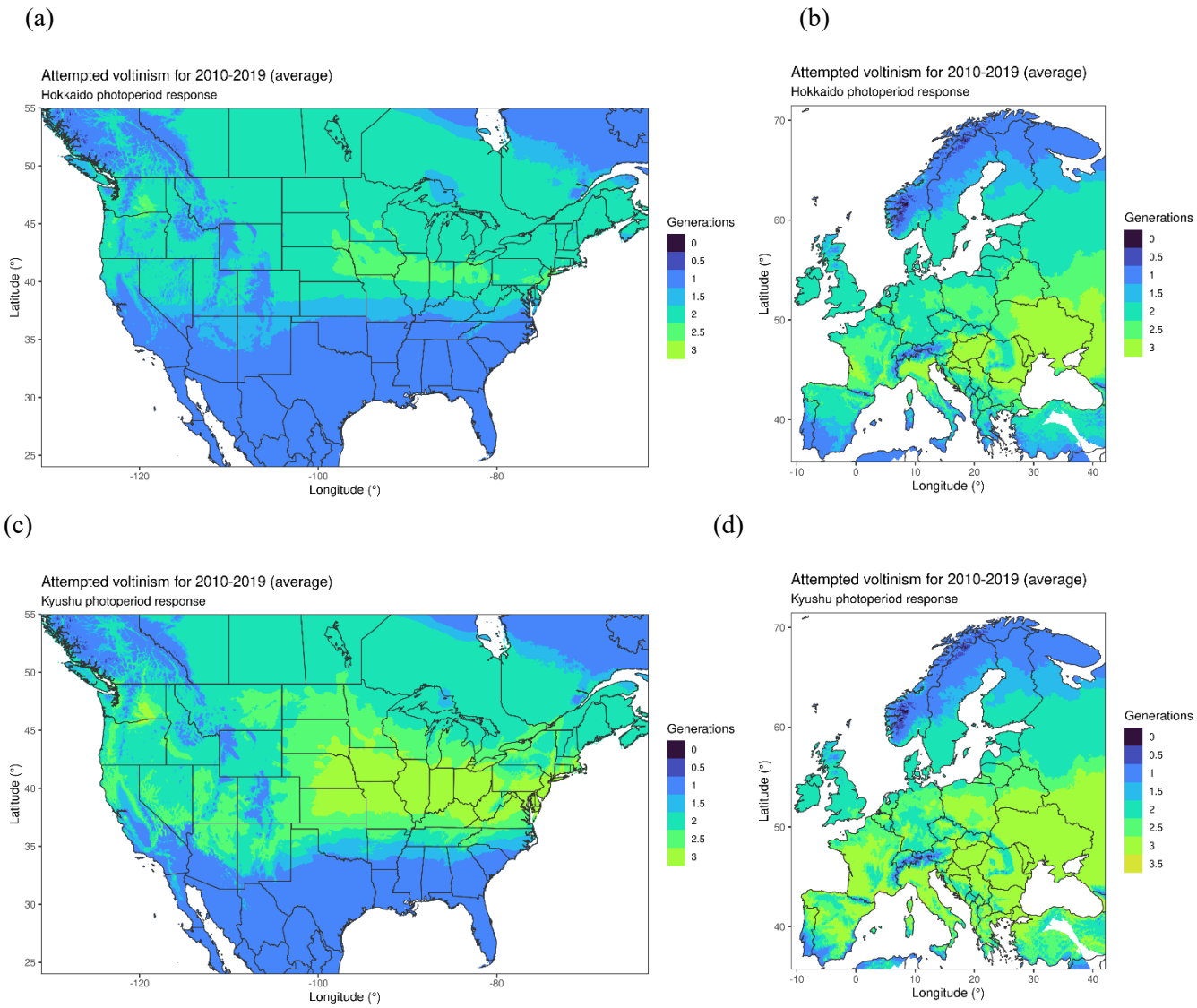

Figure 10. Expected number of generations that would be attempted by the introduced knotweed psyllid *Aphalara itadori,* based on degree-day accumulation and incorporating its diapause response to photoperiod (averages for years 2010-2019). (a) Northern strain (from Hokkaido, Japan) in North America. (b) Northern strain in Europe. (c) Southern strain (from Kyushu, Japan) in North America. (d) Southern strain in Europe.

(a) (b)

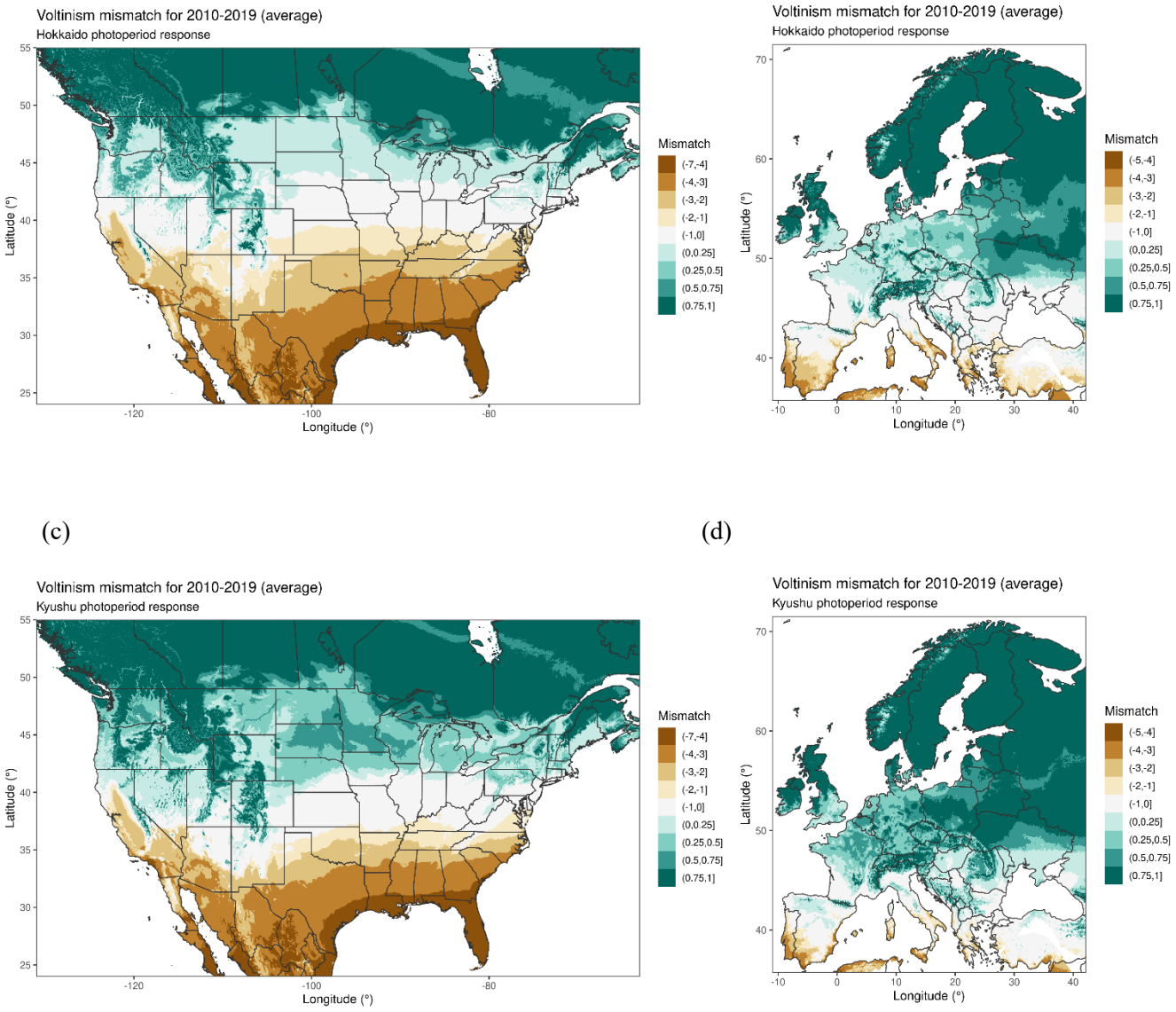

Figure 11. Degree of phenological mismatch expected for introduced populations of *Aphalara itadori.* Mismatch values are quantified as the weighted average of the difference between the expected number of attempted generations (given the photoperiod response) and the potential generations (based on degree-days) among the time-distributed cohorts. Shown are regions where the insect is expected to attempt an appropriate number of generations for the available degree-days (white), too few generations (negative mismatch, light to dark brown), or up to one generation too many (positive mismatch, light to dark green). For mapping purposes, negative values were rounded to the nearest integer and positive values were rounded to the nearest 0.25. (a) Northern strain (from Hokkaido, Japan) in North America. (b) Northern strain in Europe. (c) Southern strain (from Kyushu, Japan) in North America. (d) Southern strain in Europe.

The phenological mismatch maps (Fig. 11), which depict the difference of the number of potential generations and the number of attempted generations, reveal regions where *A. itadori* populations may experience mismatched diapause timing at the end of the season. For both psyllid strains, populations introduced into northern regions of both North America and Europe are predicted to attempt up to one more generation than can fit based on degree-days, whereas those introduced into the south are predicted to have too few generations. For both strains, there is a central region within the range of approximately 36 to 43° where diapause is expected to occur with good timing, shortly before degree-day accumulation slows (white areas in Fig. 11 maps). The region with a good match is shifted slightly more northward for the northern psyllid strain due to its longer mean critical photoperiod.

The maps reveal how the degree of mismatch fluctuates across the latitudinal gradients. This is particularly evident for the southern strain across the north central United States and Canada, where mismatch displays as alternating horizontal bands of near zero and positive one mismatch (Fig. 11c). This pattern arises because the geographic shifts in attempted voltinism are out of phase with the change in season duration across the same gradient. Similar changes in the degree of mismatch can also occur at the same location from one year to the next with annual climate variation. For example, positive mismatch values in parts of the north central United States dropped substantially from 2012 to 2013, which were the hottest and coolest year that were modeled, respectively.

Discussion

In this study, we demonstrated the utility of our newly developed photoperiod phenology model to predict voltinism and phenological mismatch in the knotweed psyllid (*Aphalara itadori*) which has been recently introduced into new climates as a biocontrol agent in North America and Europe. Experimentally determined photoperiod thresholds for diapause induction were found to differ between the two studied strains of *A. itadori*. While these genetic-based responses are likely well-suited for their respective locations of origin in Japan, we show how they could cause the insects to attempt too many generations in cooler northern regions (diapausing too late) and limit them to only one generation in warmer southern locations (diapausing too early). Not unexpectedly, the region with a good phenology match is shifted northward for the more northern source population.

These results illustrate an emerging general pattern that may arise whenever an insect or other poikilothermic organism with a short-day diapause response is moved (either purposefully or accidentally) to a new region or continent. Specifically, insects originating from a lower latitude, which typically have shorter critical photoperiods (Danilevskii 1965; Masaki 1999), will have a tendency to reproduce too late in the fall when they are moved to a higher latitude (south to north in the northern hemisphere). Conversely, those moved from higher to lower latitudes may be prone to diapausing too early, sometimes far too early, and missing part (or most) of the favorable season. These findings are in line with predictions generated for the loosestrife leaf beetle *Galerucella calmariensis* (Grevstad and Coop 2015), and with observed field phenology

in the tamarisk leaf beetle *Diorhabda carinulata* (Bean et al. 2007, Bean et al. 2012, and section 6 in this report). We emphasize, however, that end-of-season mismatches can occur even when there has not been a change in latitude, because temperature changes alone can expose the photoperiod-sensitive stage to a different day length that may induce an inappropriately timed developmental response.

The addition of time-distributed development and variation in the photoperiod response (versus Grevstad and Coop 2015) offers improved accuracy in voltinism and mismatch estimation with fractional values possible. While not specifically explored in this study, within-generation dimorphism in the diapause response resulting from this variation likely provides populations with increased resilience and adaptability in the face climate change. For example, fractional increases in attempted voltinism (i.e., partial generations) with a warmer climate, rather than discrete jumps to the next whole number, would help to avoid "lost generations" as described by van Dyck et al. (2015). Including this variation also provides the groundwork from which an evolutionary model might be generated.

Our results suggest that a tendency to diapause too late in the season may be a factor hindering establishment and/or population growth of *A. itadori* in the northern countries of Canada and the United Kingdom, where releases have been ongoing for many years without confirmation of establishment. Other contributing factors such as predation and foliage quality could also be involved (Jones et al. 2020). More recent releases of *A. itadori* made in the southern part of knotweed's range (e.g., in North Carolina, U.S.A.) could face the opposite problem of an ill-timed spring diapause after a single generation. Our model suggests that *A. itadori* is likely to initially perform best in the central parts of the United States and in southern Europe, where up to three generations are likely to be attempted and where there are sufficient degree-days to complete all three. Although the northern (Hokkaido) strain of *A. itadori*, which has the longer critical photoperiod, is a better match for more northern regions, this strain is only considered effective against giant knotweed, *F. sachalinensis*, and not the more common *F. japonica* or *F.* x *bohemica*. Field monitoring of the phenology of released populations of *A. itadori* is ongoing and will serve as a test of the model predictions.

4. Divergence in the photoperiod response of the loosestrife leaf beetle (*Galerucella calmariensis*) across a climatic and latitudinal gradient

A key concern in classical biological control is whether, and by what means, insect agents adapt to novel environmental conditions following their introduction into new regions (McEvoy et al. 2012, Roderick et al. 2012). The loosestrife leaf beetle (*Galerucella calmariensis*) was introduced from Germany to North America in 1992 for the biological control of purple loosestrife, an aggressive weed of wetlands. This agent (along with 3 others introduced against this weed) has provided successful control in some areas but not others, with success more likely in regions where more than one generation occurs. The number of generations occurring at a location is largely determined by the diapause response to photoperiod (i.e., the critical photoperiod). As part of this project, we completed two experiments to gain understanding of this biocontrol system: (1) a chamber experiment to determine and compare the photoperiod response curve among beetle populations from different climates and latitudes; and (2) a common garden field experiment to test how these differences affect phenology, voltinism, and phenological mismatch when these populations when exposed to a new climate in a common environment. The latter experiment also serves as a test of the predictions of our phenology and voltinism model (section 2).

Study System

G. calmariensis (Fig. 12) has a facultative multivoltine lifecycle. Adults overwinter and emerge as reproductive regardless of photoperiod exposure in spring (Blossey 1995, Bartelt et al. 2008). Based on degree-day (base 10°C) requirements, oviposition from overwintered adults occurs around 100 accumulated degree-days and subsequent development from egg to adult to oviposition requires around 523 degree-days (McAvoy and Kok 2004, Grevstad and Coop 2015). Newly eclosed (teneral) adults from subsequent generations are photoperiod sensitive and will enter diapause in response to short days (Velarde et al. 2002). The baseline critical photoperiod (=critical day length) in beetles introduced from Germany was not measured experimentally. However, soon after release, it was estimated as < 15.2 day-hours by Bartelt et al. (2008) and between 15 and 15.5 day-hours by Grevstad (1999) based on conditions inducing oviposition during rearing. In North America, the insect has between one and three generations depending on location.

Figure 12. *Galerucella calmariensis* adult (left) and its target weed, *Lythrum salicaria* (right, purple loosestrife).

Methods

In 2018, beetles were collected from ten geographic locations that span a range of climates and latitudes and in both the West and the Northeastern U.S. For publication purposes (Wepprich and Grevstad 2020), and most of the results presented here, we decided to focus on 7 populations spanning the western U.S. due to a greater reliability of the data and because we were able to combine and compare results with the 2014 experiment that used the same populations and similar methods. The environmental conditions, model-predicted phenology, and known release history for these sites is summarized in Table 3.

The insects were reared for one generation under similar conditions to eliminate maternal effects and the F1 adults were overwintered outdoors from November 2018 through April 2019 in Corvallis, Oregon. We obtained same-age cohorts of eggs by placing 3 adult pairs on each of 12 caged potted *L. salicaria* plants (15-20 cm tall) for each beetle population for a 48-hour period. This resulted in roughly 90 eggs per plant. When larvae started to hatch, they were carefully transferred using a moist paintbrush onto sprigs of fresh foliage in 150mm-diameter petri dishes (approximately 30 individuals per dish). The chambers were set to 23°C and had built in lights. We assigned rearing dishes from each population to photoperiod treatments at 14.5/9.5, 15.0/9.0, 15.5/8.5, 16.0/8.0, 16.5/7.5, and 17.0/7.0 L/D hours (2 dishes x 6 populations x 6 photoperiod treatments). As they emerged each day, we removed teneral adults and re-pooled them (within treatments) into new petri dishes with fresh leaves for the pre-oviposition or pre-diapause development period of ten to 14 days. To assay their reproductive status, adults were then isolated into 50mm-diameter petri dishes with a leafy shoot tip and moist filter paper for 48 hours. They were scored as reproductive if observed to be feeding, ovipositing (if female), and active. They were scored as diapausing if they were inactive, hiding, and not feeding. In ambiguous cases (which were rare), we replaced the shoot tip with a fresh one and repeated the assessment after another 48 hours. A total 1,782 beetles were scored. The proportion reproductive for each treatment combination (pooled across rearing dishes) served as the dependent variable for our analysis.

Table 3. Description of sites in the western USA with introduced *Galerucella calmariensis* populations.

Site	Elevation (meters above sea level)	Max day length (hours)[a]	Avg annual degree-days (SD)[b]	Average F1 adult emergence prediction[c]	Population history (year introduced)[d]	Voltinism in the field[e]
Bellingham, Washington (48.76°, -122.48°)	17	16.3	1067 (122)	July 20	Introduced from Ephrata, WA (unknown year in 1990s)	1 generation
Ephrata, Washington (47.16°, -119.66°)	350	16.1	1677 (127)	June 24	Original release from north and south German sources (1992-93)	3 generations
Yakima Training Center, Washington (46.76°, -119.99°)	204	16.0	1809 (131)	June 19	Introduced from Ephrata, WA (unknown year in 1990s).	Not observed, assumed similar to nearby Ephrata, WA
Rickreall, Oregon (44.98°, -123.27°)	64	15.8	1366 (114)	July 9	Original release from south German source (1992)	1 generation
Sutherlin, Oregon (43.39°, -123.32°)	153	15.6	1601 (143)	June 27	Original release from south German source (1992)	2 generations
McArthur, California (41.10°, -121.41°)	1006	15.3	1559 (122)	July 1	Introduced from Rickreall, OR and vicinity (1998, 2000) & Ephrata, WA (2002)	2 generations
Palermo, California (39.41°, -121.58°)	35	15.1	2769 (175)	May 13	Introduced from Rickreall, OR and vicinity (1998-2001) & McArthur, CA (2006). Release from Ephrata, WA 10km northwest of this site (2004-05) could have dispersed here.	3 generations

[a]Maximum day length includes twilight until the sun is 1.5° below the horizon (using method of Forsythe et al. 1995).
[b]Degree-days are calculated with the triangle method with 10°C/30°C thresholds over 25 years (1994-2018) from Daymet daily gridded interpolations of weather station observations.
[c]Predicted sensitive stage emergence is based on 25 years (1994-2018) of results from a degree-day lifecycle model (Grevstad and Coop 2015).
[d]History is from Hight et al. (1995) for original releases in Washington and Oregon and from M. Pitcairn (personal communication) for transfers to California
[e]F. Grevstad and M. Pitcairn surveyed sites in 2014 to coincide with the expected timing of larval emergence in later generations.

Statistical analysis. We combined results for the 2019 experiment with results from a 2014 experiment that used the same populations and similar methods (details in Wepprich and Grevstad 2020). We performed all analysis and visualization with R 3.6.2 (R Core Team 2019). First, each year's diapause data (2014 and 2019) were analyzed separately for beetle reproductive rates with generalized linear mixed effects models with a binomial error distribution and logit link using the *lme4* package (Bates et al. 2015). The fixed effects of population and photoperiod treatment (scaled continuous covariate) and their interaction predicted the proportion reproductive in each treatment combination, accounting for the total number of beetles in each group. As these groups contained beetles from the same population reared in the same growth chamber, they were assigned random intercepts to account for non-independence and allow for overdispersion in the residual variance (Bolker 2015). We removed the interaction term if non-significant ($p > 0.05$) by a Chi-square test. Population differences in responses (estimated marginal means) were compared using the *emmeans* package with post-hoc pairwise comparisons while adjusting for multiple comparisons using Tukey's method (Lenth 2020). Populations' critical photoperiods (=critical day lengths), the hours of light exposure at which half of the beetles are predicted to diapause, were derived with 95% confidence intervals using inverse prediction from the generalized linear mixed models (Venables and Ripley 2002).

Second, we tested for a latitudinal gradient in the diapause response by analyzing the 2014 and 2019 experiments in the same model. We changed the predictor variables in the generalized linear mixed models to shift the focus from populations' critical photoperiods to the latitudinal cline in the trait. The fixed effects were photoperiod treatment, latitude (scaled), year of experiment, and all interactions. We removed interaction terms if non-significant ($p > 0.05$) by a Chi-square test. The two experiments differed in methods such that the results from their separate models (see above) had substantial differences in the slope of the diapause response to photoperiod treatments. By including year and its interactions with other variables in this model, we account for the potential different responses to photoperiod treatment across the latitudinal gradient that might be artifacts from the experiments' methods. In addition to the random intercept for treatment combination to control for the non-independence of beetles reared in the same chamber, we included a random intercept for population because we are attempting to make inferences about the larger, unsampled set of beetle populations along the latitudinal gradient rather than just these seven populations (Bolker 2015). The predicted change in critical photoperiods across the latitudinal gradient was derived from this model with 95% confidence intervals using simulations from the model parameters and their uncertainty (Population Prediction Intervals in Bolker (2008)).

Third, we tested if development time was affected by population and photoperiod exposure with a generalized linear mixed effects model with a gamma error distribution and log link using the *lme4* package (Bates et al. 2015). The fixed effects of population and photoperiod treatment (scaled continuous covariate) and their interaction predicted the duration from oviposition to adult eclosion in days for each beetle. Rearing dishes, the experimental unit, with beetles from the same population and oviposition day, were assigned random intercepts to account for their non-independence. We removed the interaction term if non-significant ($p > 0.05$) by a Chi-square test. Population differences in responses (estimated marginal means) were compared

using the *emmeans* package with post-hoc pairwise comparisons while adjusting for multiple comparisons using Tukey's method (Lenth 2020).

Results

All populations tested in the 2019 experiment exhibited a short-day diapause response where shorter photoperiod treatments induced diapause and longer photoperiod treatments resulted in reproduction (Table 4, Fig. 13). Populations differed in their critical photoperiods by up to 2.3 hours in the 2019 experiment. There was no interaction between population and photoperiod response in either experiment, meaning that the slopes of the photoperiod response curves do not significantly differ across populations.

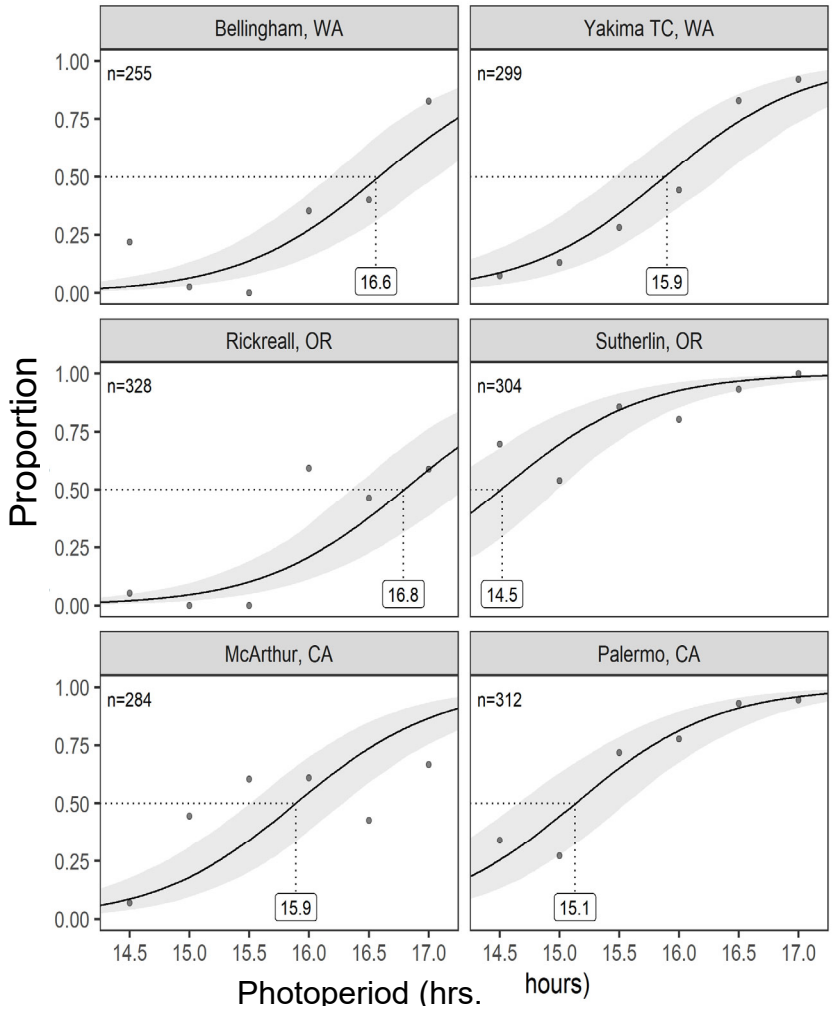

Figure 13. Photoperiod responses diverged between populations in 2019. Each data point shows the proportion of male and female beetles that were reproductive for each treatment combination, with size scaled by number of beetles, for six populations (panels) and six photoperiod treatments (*x*-axis). Solid lines and 95% confidence intervals show generalized linear mixed model predictions. The critical photoperiods, at which 50% choose to diapause, are labeled below the dotted lines.

Populations had a lower proportion reproductive, regardless of photoperiod, at higher latitudes (β = -0.918, SE = 0.393, P = 0.0196, Table 4). The 2019 experiment had marginally higher proportions reproductive (β = 0.747, SE = 0.414, P = 0.0709, Table 4) and a significant interaction with the photoperiod response (β = -2.97, SE = 0.643, P = <0.0001, Table 4). From this model, critical photoperiods increased by 15.7 (CI 13.9-17.4) minutes per 5° latitude in the 2014 experiment and 51.0 (CI 45.0-56.9) minutes per 5° latitude in the 2019 experiment (Fig. 14).

However, the six populations tested in 2019 do not have a monotonic increase in critical photoperiod with latitude (Fig. 14). For example, the two central populations (Rickreall and Sutherlin, Oregon) have the longest (16.8, CI 16.3-17.3) and shortest (14.5, CI 14.0-15.1) critical photoperiods, respectively (3.87 difference, SE = 0.551, P < 0.001 on logit scale). Populations from McArthur, California and Yakima Training Center, Washington have similar critical photoperiods in spite of their separation of 5.7° latitude (0.00679 difference, SE = 0.502, P > 0.999).

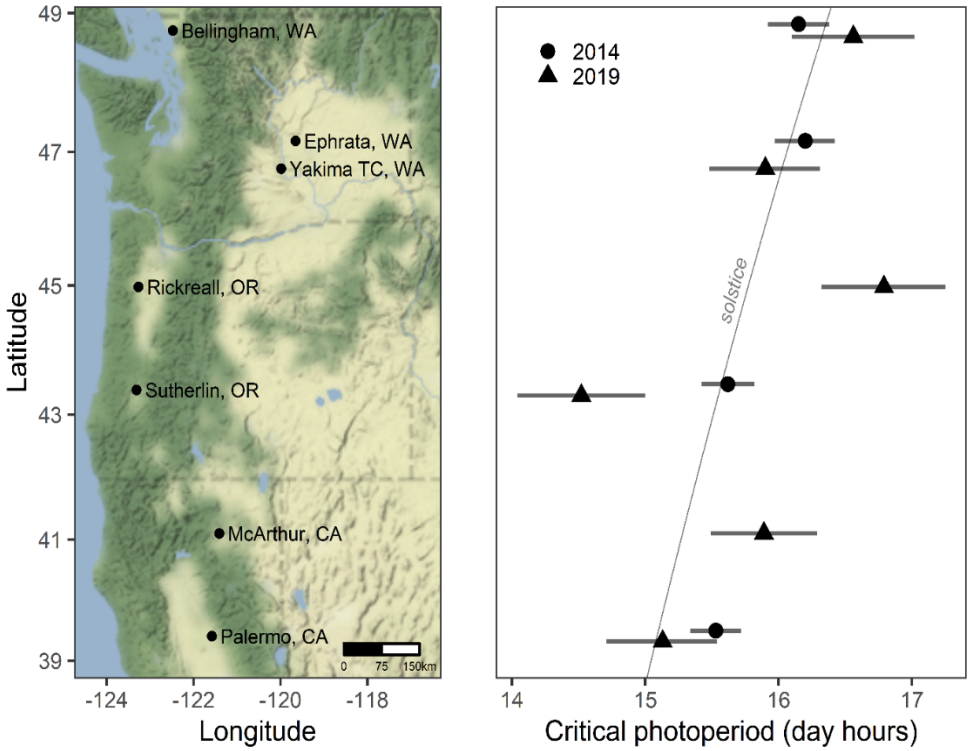

Figure 14. (A) Map of collection locations of *Galerucella calmariensis* in the western United States. (B) Experimentally determined mean critical photoperiod (x-axis) as it related to latitude (y-axis to correspond with the map).

Table 4. Photoperiod responses of *Galerucella calmariensis* populations in two experiments at constant 23°C temperatures.

	2014 Photoperiod response					2019 Photoperiod response				
Predictors	Beta	Std. error	*P*	CP[a] (95% CI)	Population differences[b]	Beta	Std. error	*P*	CP (95% CI)	Population differences
Photoperiod: light hours	4.05	0.67	<0.001	-	-	1.29	0.16	<0.001	-	-
Bellingham, Washington	-2.20	0.58	<0.001	16.1 (15.9-16.4)	A	-1.36	0.40	<0.001	16.6 (16.0-17.1)	A
Ephrata, Washington	-2.43	0.59	<0.001	16.2 (16.0-16.4)	A	-	-	-	-	-
Yakima TC, Washington	-	-	-	-	-	-0.29	0.41	0.488	15.9 (15.5-16.4)	AB
Rickreall, Oregon	-	-	-	-	-	-1.76	0.41	<0.001	16.8 (16.3-17.3)	A
Sutherlin, Oregon	0.40	0.52	0.443	15.6 (15.4-15.8)	B	1.84	0.40	<0.001	14.5 (14.0-15.1)	C
McArthur, California	-	-	-	-	-	-0.34	0.37	0.365	15.9 (15.5-16.4)	AB
Palermo, California	0.86	0.49	0.080	15.5 (15.3-15.7)	B	0.95	0.38	0.013	15.1 (14.6-15.6)	BC

[a]Critical photoperiod (CP), or the light hours at which 50% would enter diapause, was estimated for each population and year with 95% confidence intervals by inverse predictions from the models.

[b]Populations with significant differences have different letters, which come from pairwise comparison tests with Tukey's method to adjust *P* values.

Table 5. ANOVA for tests of photoperiod and population effects on diapause proportion and development time.

	2014 Diapause			2019 Diapause			2018 Development time		
Fixed effects	Chi square	df	P	Chi square	df	P	Chi square	df	P
Photoperiod (light hours)[a]	36.6	1	<0.001	82.7	1	<0.001	0.0396	1	0.842
Population	25.8	3	<0.001	68.7	5	<0.001	14.8	5	0.0113
Photoperiod x Population	1.41	3	0.703	6.53	5	0.258	9.62	5	0.0869
Random effects	Groups	SD		Groups	SD		Groups	SD	
Intercept[b]	16	0.602		36	0.708		71	0.0135	

[a]Photoperiod is modeled as a continuous variable and had different growth chamber treatments in different experiments.
[b]Random intercepts were based on treatment group for diapause models and rearing dish for development time model. Standard deviation (SD) shows between-group variation.

Table 6. Test of latitudinal gradient in photoperiod effects on diapause proportion over two experiments.

	Type II ANOVA			Coefficients (reduced model)		
Fixed effects	Chi square	df	*P*	Beta	Std. error	*P*
Intercept	-	-	-	-1.06	0.482	0.0282
Photoperiod (light hours)[a]	78.9	1	<0.001	4.28	0.629	<0.001
Latitude	5.70	1	0.017	-0.918	0.393	0.0196
Year indicator (2019)	4.09	1	0.043	0.747	0.414	0.0709
Photoperiod x Latitude	0.710	1	0.400	-	-	-
Photoperiod x Year	21.8	1	<0.001	-2.97	0.643	<0.001
Latitude x Year	1.40	1	0.326	-	-	-
Photoperiod x Latitude x Year	0.113	1	0.737	-	-	-
Random effects	Groups	SD		Groups	SD	
Population (intercept)	7	0.907		7	0.875	
Treatment group (intercept)	52	0.845		52	0.930	

Development time averaged 33.5 days and did not change with photoperiod treatments (Fig. 15). Populations had similar development times with the exception that the Rickreall, Oregon population required an additional day of development compared to the Sutherlin, Oregon population (0.0419 difference on log scale, SE = 0.0127, $P = 0.0122$) and the Yakima Training Center, Washington population (0.0364 difference on log scale, SE = 0.0127, $P = 0.0471$). There was no interaction between population and photoperiod for development time (Table 5).

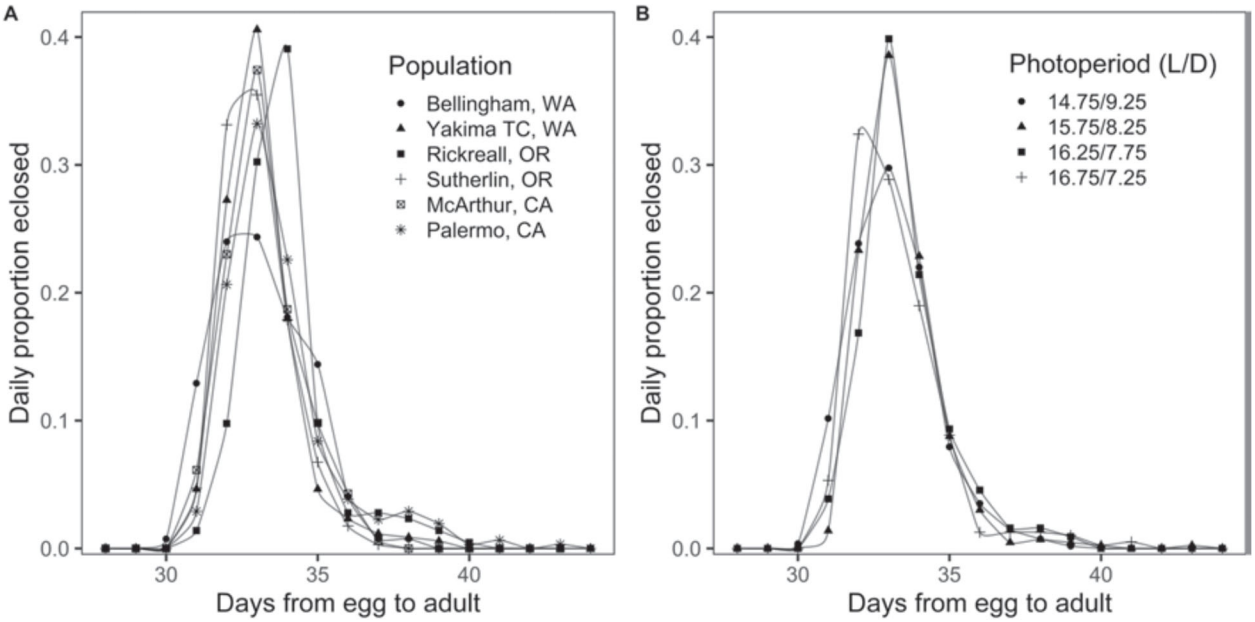

Figure 15. Main effects of (A) population and (B) photoperiod on development time at constant 21°C. Points represent daily observations of the proportion of the total number of beetles that eclosed in each group. Development time is similar for most populations, but the populations in Rickreall, OR took longer than the populations in Sutherlin, OR, and Yakima, WA (A). Photoperiod treatments had no effect on development time in the four growth chambers (B).

Discussion

Nearly three decades after their introduction, populations of the introduced leaf beetle *Galerucella calmariensis* have genetically diverged in their diapause response to photoperiod across 9.4° of latitude in the western USA. Despite a genetic bottleneck at the time of their introduction from Germany in the 1990's, the measured critical photoperiods, where 50% of the population enters diapause, range from 14.5 to 16.8 hours of daylight, greatly extending the estimated 15 to 15.5 hour critical photoperiod in the original population. The measured critical photoperiods roughly correlate with latitude, with longer critical photoperiods found in the north where summer days are longer and where conditions favorable for reproduction tend to end earlier in the year. Critical photoperiods were shorter in the south where summer day lengths are shorter, and conditions usually remain favorable later into the autumn.

The evolved geographic variation resembles the photoperiod response clines commonly seen in native or long-established insects. Typical latitudinal gradients for critical photoperiods in locally adapted insects in temperate zones range from 60-90 minutes per 5° latitude in classic experiments (Danilevskii 1961) or 48 minutes per 5° latitude in a recent meta-analysis (Joschinski and Bonte 2020). For the studied *G. calmariensis* populations, we estimated critical photoperiod clines of 15.7 minutes and 51.0 minutes per 5° latitude in 2014 and 2019 experiments, respectively (Fig. 14). The lower rates of change with latitude found in this study may reflect incomplete adaptation in this introduced insect or may be a result of the particular locations sampled (see below). If we assume that the latitudinal clines in native insects represent adaptations to the local seasonal environment, then we can say that *G. calmariensis* has evolved in an adaptive direction. However, reciprocal transplant experiments would be needed to confirm that these changes in photoperiod responses are local adaptations that increase fitness (Kawecki and Ebert 2004, Merilä and Hendry 2014, Tsai et al. 2020).

We found that development rates remain similar among populations with the exception of a slower development rate, by one day, in the Rickreall, Oregon population (Fig. 15). The small difference, in comparison to the wider variation found in critical photoperiods, suggests that photoperiod response plays a relatively larger role in adapting to local seasonal regimes (Bradshaw and Holzapfel 2007). It is intriguing that this population with slower development also has a longer critical photoperiod than its neighboring populations. Field observations from recent years confirm a single generation at this site, whereas the Sutherlin, Oregon population just 1.6° latitude to the south and unsampled populations within 0.5° latitude to the north have 2 generations (Table 3, F. Grevstad personal observations). It is unclear why this population should be limited to one generation given sufficient degree days for two generations and plants that remain green until early fall. Relaxation of selection for faster development may be a result of the predominantly univoltine lifecycle at this site. Other insects have evolved nonlinear "stepped" or "sawtooth" clines in developmental traits across latitudes in tandem with locally adapted photoperiod responses, which has the added effect of limiting attempted generations in places where season length is only marginally supportive of increased voltinism (Roff 1980, Tauber and Tauber 1981, Levy et al. 2015).

Estimations of critical photoperiods may be used in combination with developmental degree-day requirements to predict voltinism at a given location over time (Beck and Apple 1961, Tobin et al. 2008, Kerr et al. 2020). The relationship of a population's mean critical photoperiod to modeled voltinism for a given climate and latitude has been covered in detail in Grevstad and Coop (2015). In brief, a degree-day phenology model predicts when the photoperiod-sensitive stage emerges, and if the day length on that date for the latitude is longer than the critical photoperiod then the population is reproductive and attempts another generation. Voltinism can shift (sometimes dramatically) when an insect is moved to a new climate or latitude, or as a result of annual variation in phenology of the photoperiod-sensitive stage (Grevstad and Coop 2015, Kerr et al. 2020).

How well laboratory-measured critical photoperiods align with those expressed in the field, where other environmental cues may also come into play, is a topic in need of more research.

The temperature that insects are exposed to during development, which varies in the field across time and space, has been shown to modify the critical photoperiod in some insects. Our 2018 experiment anecdotally had much lower reproductive rates (and presumably higher critical photoperiods) which may be a result of using a chamber temperature 2°C cooler than the other experiments. Day to night fluctuations (thermoperiods) could also be involved in cuing diapause, with the amplitude of the difference affecting the response (Beck 1983). In another chrysomelid beetle species (*Diorhabda carinulata*), the critical photoperiod was found to be 15 minutes longer when reared at constant temperatures compared to that in a fluctuating day and night temperature regime with the same mean (Bean et al. 2007). Finally, we note that laboratory measured critical photoperiods based on abrupt light:dark transitions can be difficult to translate to field day lengths, which have gradual transitions through dawn and dusk. We do not know what proportion of the twilight period *G. calmariensis* perceives as part of the day length for comparison against its internal critical photoperiod. Where this has been studied in other insects, the portion of twilight included appears be quite variable among insect species (Menzel 1979) and may even vary asymmetrically between dawn and dusk (Takeda and Masaki 1979). Now that our study has demonstrated genetic differences in a simplified experimental setting, field validation would help gauge how diapause initiation changes with environmental conditions and cues interacting to influence these traits (Abarca 2019).

The estimated critical photoperiods vary substantially between experiments and about the latitudinal trend. We cannot rule out that the photoperiod response evolved over a few years (Bean et al. 2012, Urbanski et al. 2012) or even changes annually with strong fluctuating selection (Bell 2010). However, methodological differences likely caused variation between years, such as the higher precision of critical photoperiods estimated in 2014. The use of whole potted plants for rearing in the 2014 experiment could have provided beetles with additional cues from the host plant to induce a stronger diapause response (Izzo et al. 2014). The inclusion of males in the sample in 2019, but not 2014, may have led to increased standard deviation in the critical photoperiod (Table 2) and the marginally significant higher proportion of reproduction beetles (Table 4). There are also climatic and phenological reasons why populations' critical photoperiods vary from the latitudinal trend. In the western United States, local climates are influenced by complex topography relative to the eastern United States. The sawtooth pattern in critical photoperiods estimated in 2019 (Fig. 14) correspond to differences in average degree-days and sensitive stage phenology at the sampled sites. Local climate determines the number of generations that are possible in a location and the evolved critical photoperiod may vary over short distances at similar latitudes (Lindestad et al. 2019). Insect phenology models that incorporate demography along with photoperiod-based diapause can estimate annual fitness for a particular critical photoperiod (Kerr et al. 2020) and extending these models across years could answer whether a critical photoperiod has reached an optimum for a population's environment (similar to trait models in Kivelä et al. (2013)).

The photoperiod response in *G. calmariensis* appears to be quite variable among individuals, with a mix of reproductive and diapausing beetles in the same treatment groups (Fig. 13). While less individual variation, and a steeper slope in the photoperiod response curve, may show stronger selection on the critical photoperiod (Tauber et al. 1986), some insect species show

substantial individual variation with flatter slopes (Joschinski and Bonte 2020). In the field, this variability can translate into partial generations toward the end of the season, where a portion of adults within the same generation enters diapause while the rest go on to reproduce. Two years of observations suggest that this commonly occurs in colonies reared outdoors in Corvallis, OR (T. Wepprich personal observation). The extent to which this occurs in natural populations of *G. calmariensis* would be worth further study. Higher individual variation, or a weaker diapause response to photoperiod cues, may facilitate insect invasions to new locations (Reznik et al. 2015) and may be a trait to screen in potential biological control agents.

Based on this study, there was sufficient genetic variation from two source populations to evolve divergent photoperiod responses across a range of environmental conditions within 27 years. The evolution of *G. calmariensis*, as well as other biological control agents (Bean et al. 2012, McEvoy et al. 2012, Szűcs et al. 2012), suggests the importance of season length as a selective force over ecological timescales. Screening for developmental traits or environmental factors that predict successful establishment and population growth of biological control agents would advance our ability to manage planned introductions (Zalucki and van Klinken 2006, Abram and Moffat 2018). More targeted matching of observed photoperiod responses in the native range combined with lifecycle simulations of growing season lengths in the introduced range may reduce the length of time or number of introductions needed to establish robust populations (Grevstad and Coop 2015, Pitcairn 2018). Beyond the field of biological control, evolution to changing seasonality is the predominant genetic response to rapid climate change in natural populations (Bradshaw and Holzapfel 2006) and photoperiodism will likely determine range shifts across diverse taxa (Saikkonen et al. 2012). Quantifying changing photoperiod responses in introduced populations provides examples of how quickly and to what extent evolution can track anthropogenic warming, with the changes in both season length and timing of environmental cues it brings.

5. Comparing voltinism and weed impact among different geographic populations of *Galerucella calmariensis* when moved to a common environment

Having shown that populations of the loosestrife leaf beetle (*Galerucella calmariensis*) from different regions in the United States have evolved since their introduction to have different critical day lengths for inducing diapause (section 4), we next tested whether these differences would have significant effects on phenology, voltinism, and impact to the target weed when populations are moved into a new location. This study is valuable for demonstrating the importance of selecting an effective source population in biocontrol programs and also serves as a test of the assertion of our model that the measured critical photoperiod of a population can predict voltinism and biocontrol effectiveness. This study is currently being written up for publication.

Methods

We set up a common garden experiment in a mowed grass field at the Oak Creek Center for Urban Horticulture in Corvallis, Oregon, to compare the voltinism and diapause response of six populations of *G. calmariensis* collected from throughout the western United States. The experiment was initially carried out in 2018, but it was repeated in 2019 to correct several issues with the methodology (including preventing an aphid infestation and controlling for maternal effects). Here we report only the 2019 experiment because it has the more reliable results.

Adult *G. calmariensis* were collected from 6 locations throughout the western United States between May 13 and 18 of 2018. The sites included Palermo, CA, McArthur, CA, Sutherlin, OR, Rickreall, OR, Yakima Training Center, WA, and Bellingham, WA. The beetles were reared for a generation in the greenhouse followed by a generation in an environmental chamber under conditions that induced them into diapause for storage out of doors through the winter. When these insects became reproductive in the spring of 2019 (April 26), four pairs of adults were placed onto each experimental plant. The plants were grown in 3-gallon pots from small uniform overwintered root stocks that were grown from seed the previous summer. The plants were fit with a sleeve cage and arranged into blocks set in plastic pools (Fig. 16), with each block containing plants assigned to each of the 6 beetle populations and one control plant that had no beetles. After the three-day exposure period, the adults were removed leaving a cohort of similar age eggs on the plants. The sleeves cages were rolled down to the level of the pots, exposing the plants and developing eggs and larvae to natural conditions until they reached the 3rd instar. At that time, the sleeves were put back up in order contain pupae and emerging adults.

When adults began to emerge during both the first and second generations, we carried out timed searches to estimate the rate of emergence. When the number of newly emerging adults peaked, we carried out a thorough count of adults on each plant by using an aspirator to collect all of

Figure 16. Common garden setup. Insects were caged in sleeves over potted loosestrife plants that were placed in pools maintained with standing water.

them into vials. We sampled 20% of the beetles from each plant for assaying reproductive status. The other 80% were pooled within each population and returned evenly among the plants that they were collected from. The sampled beetles were brought into the laboratory and placed into petri dishes with fresh loosestrife shoot tips. The dishes were placed near a window where they continued to be exposed to natural day lengths. The shoot tips

were replaced every two to three days as needed. The reproductive status of the beetles was assessed after 7 to 10 days. Beetles that were active, feeding, and ovipositing were scored as reproductive, while those that were hiding and not feeding were scored as diapausing.

We compared the proportion of beetles that remained reproductive among populations using analysis of variance. We also compared the proportion reproductive to the proportion that our phenology model (section 2) would predict using photoperiod response parameters (mean and variance of the critical photoperiod) and development rates previously determined in chamber experiments (section 4, Wepprich and Grevstad 2021). This served as a field validation test for the model.

To compare the level of impact that each beetle population had on the plants in the field experiment, we clipped the inflorescences weekly and dried and weighed them. When the plants senesced in the fall, we cleaned, dried, and weighed the roots.

Results

The six populations differed in their tendency to enter diapause, with a high proportion of beetles from Bellingham, WA (the northernmost population) entering diapause after one generation and nearly all beetles from Palermo, CA and Sutherlin, OR going on for a second generation (Fig. 17). Beetles from McArthur, CA, Rickreall, OR, and Yakima Training Center, WA showed

intermediate responses where the first generation of adults included a sizable portion of both reproductive and diapausing individuals. In the second generation, nearly all individuals went into diapause with slightly more reproductive individuals in the Sutherlin population.

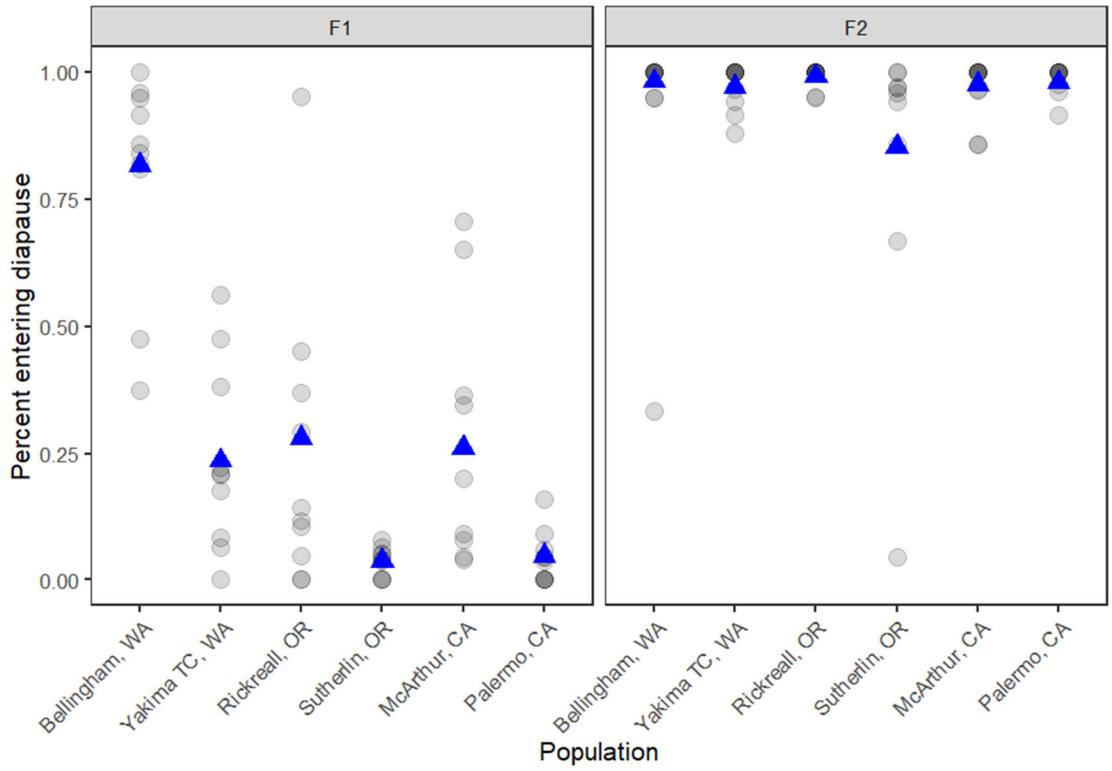

Figure 17. Percentage of beetles sampled from (a) the F1 generation and (b) the F2 generation in our common garden experiment that entered diapause (as opposed to reproducing). Circles represent the diapause proportion from each replicate plant. Blue triangles are the weighted means.

The proportion of sampled beetles in each population that remained reproductive was found to correlate with the proportion predicted from the model (Fig. 18). The model uses the photoperiod on the sampling date for Corvallis, OR latitude of 44.5 ° N (using Forsythe et al. 1995) and the mean and variance of the critical day length that was previously measured in chamber experiments. However, comparable values of the proportions were achieved only by including a larger portion of the twilight period into calculated day lengths, including the period of time when the sun is up to 6° below the horizon, rather than the 1.5° previously estimated for this insect (Grevstad and Coop 2015). That is, *G. calmariensis* appears to be sensitive to lower light levels than previously estimated.

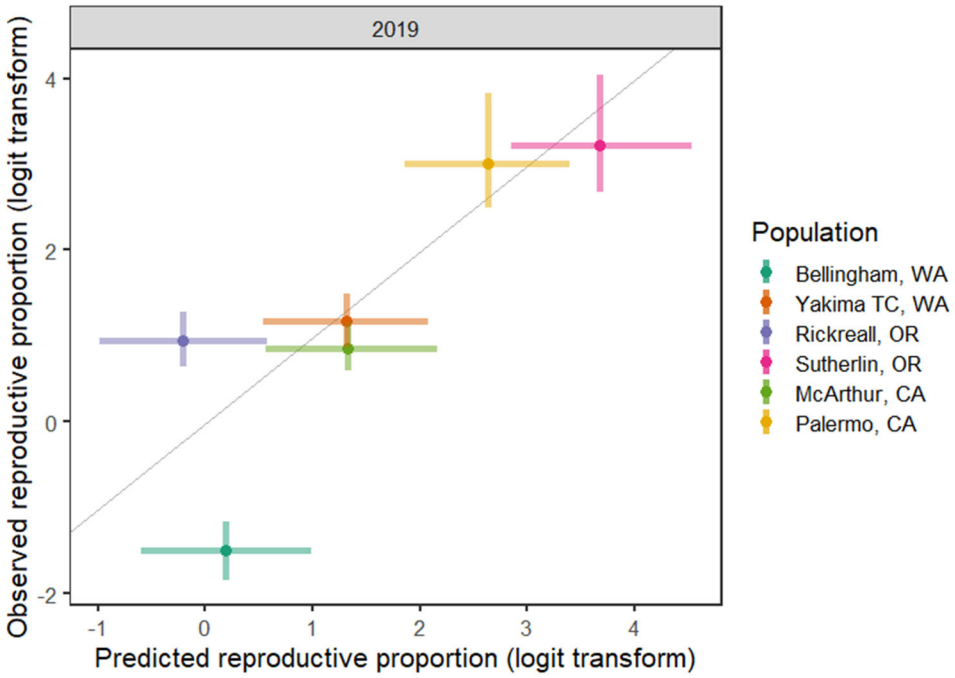

Figure 18. Observed vs. model-predicted proportion (logit transformed) of the first generation of *G. calmariensis* adults that remained reproductive. For the model predictions, we used the mean and variance of the critical photoperiod measured by Wepprich and Grevstad 2021 in chamber experiments and day length calculated using Forsythe et al. 1995 for the date the garden beetles were sampled. The amount of twilight included in the day length in the model was adjusted to align the data points with the y = x line.

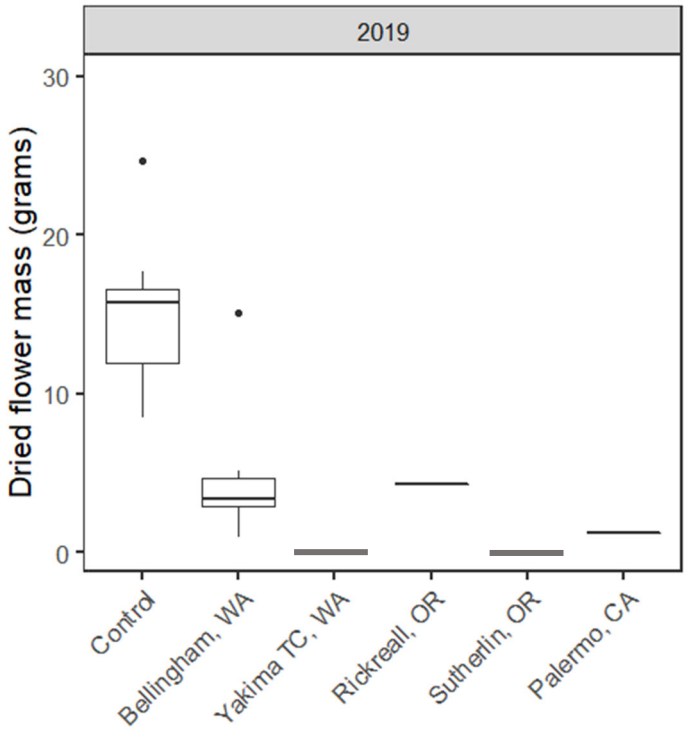

Figure 19. Mass of dried inflorescences collected from potted field plants exposed to different populations *Galerucella calmariensis* when grown in a common environment in Corvallis, OR.

Populations that went on for a full second generation had a greater level of impact on the plants as measured by total inflorescence mass (Fig. 19) and root mass (Fig. 20). More total beetles on the plant over the course of the summer (F1 + F2) was also associated with a decrease in mass of flowers and roots.

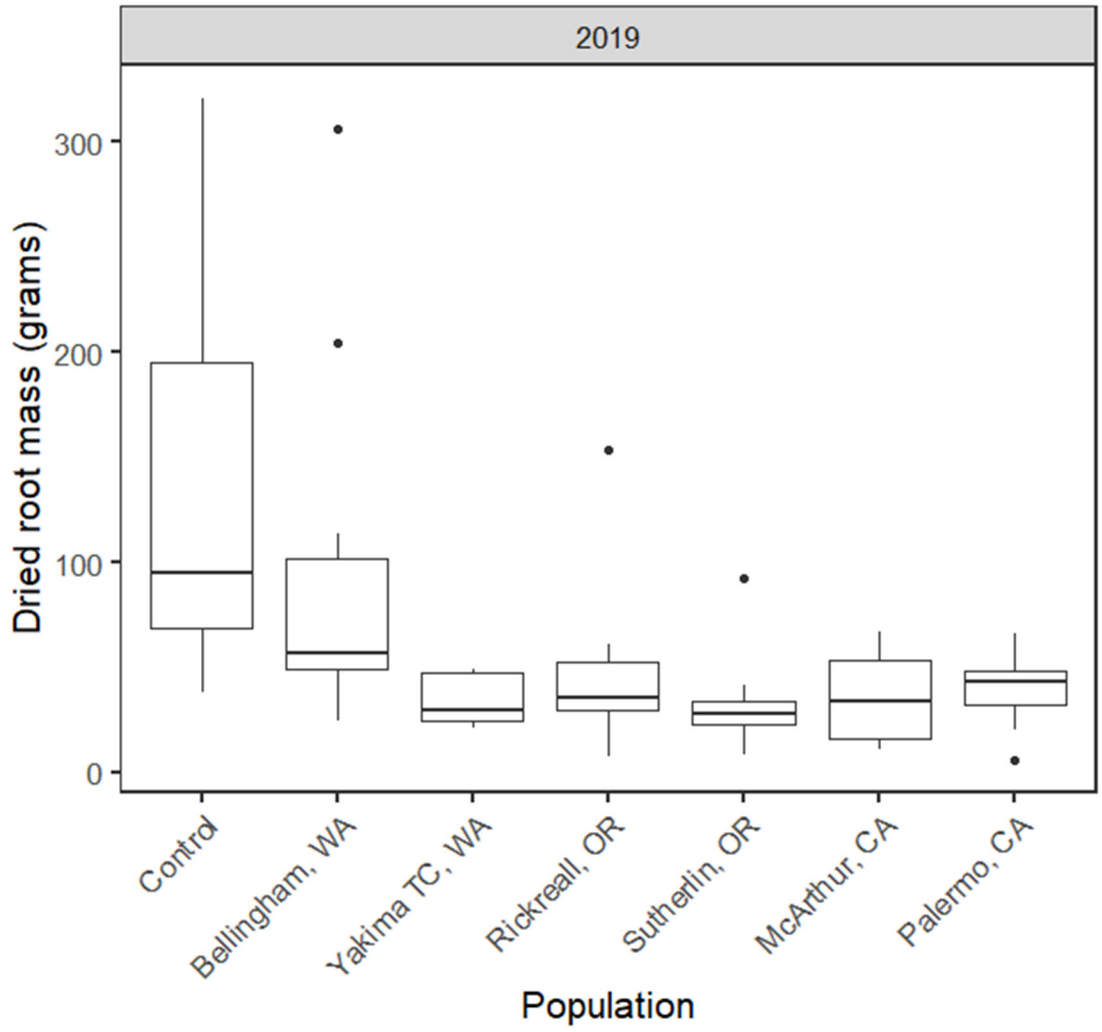

Figure 20. Dried root mass of purple loosestrife plants exposed to different populations of *Galerucella calmariensis* when grown in a common environment in Corvallis, OR.

Conclusions

By bringing together populations of *Galerucella calmariensis* from different geographic locations that are known to have different mean critical day lengths that cue diapause, we demonstrate how voltinism and the resulting impacts on plants are affected by this important trait. The results were largely predicted by our model, validating the utility of the model to predict voltinism and relative impact of different sources of biocontrol agents prior to their introduction. We show how populations that have a shorter critical day length, giving rise to two generations (in Corvallis) tended to have larger impacts on the plants. Our results suggest that biocontrol programs may have greater success by seeking sources of agents that have photoperiod responses that will allow more generations, provided that the number of degree days (or other season defining conditions) will allow it. The possibility for strategic redistribution of

biocontrol populations with specific photoperiod-response profiles within the introduced range may be warranted to improve biocontrol effectiveness.

6. Evolution of the critical day length cue allows range expansion in the tamarisk leaf beetle

Introduction

The practice of classical biological control (biocontrol) of invasive plants (targets) begins with the collection of host specific natural enemies (agents) from one or a few locations within the native range of the target, safety testing to ensure host specificity (Pemberton 2000; Schaffner et al 2018), and release for suppression of the target in the invaded range (Schwarzländer et al 2018). Agents are expected to encounter novel ecological challenges while colonizing the invaded range, providing settings conducive to rapid evolution (Roderick and Hufbauer 2005; Hufbauer 2012) as seen in other types of colonization events (Reznick and Galambor 2001). The desired outcome, following evolution, is increased biocontrol efficacy in novel ecological settings, which makes consideration of evolutionary principles essential to the modern practice of biocontrol (Hufbauer 2012, Szücs et al 2019). It is also likely that biocontrol will offer instructive examples of rapid evolution of agents, and perhaps targets, within settings where key information is available, such as origin, dates and locations of releases and numbers of agents released (Marisco 2012). Recent theory seeks to link rapid evolution and ecology into a process termed eco-evolutionary dynamics (Hairston et al 2005; Schoener 2011) which is an instructive way to view biocontrol, since success hinges on ecological and evolutionary processes and their interplay (McEvoy 2018; Szücs et al 2019). The high economic and ecological value of invasive species suppression (Pimentel et al 2005) combined with the need to improve biocontrol success (Schwarzländer et al 2018; Müller-Schärer et al 2020) underscores the practical value of defining the ecological and evolutionary bases of biocontrol success (McEvoy 2018; Szücs et al 2019), which remains understudied.

When introduced in 2001, the tamarisk leaf beetle (*Diorhabda carinulata*), Fig. 21) was unable to persist south of 38° N latitude due to an ill-timed diapause (after a single spring generation, Lewis et al. 2003, Bean et al. 2007). Within a few years, the critical day length (CDL) that cued diapause had evolved to be shorter at more southern latitudes (Bean et al. 2012). Selection and evolution continue as beetles spread southward. This has resulted in ever-decreasing CDL. In our SERDP-sponsored project, we measured CDL at the advancing southern front of range expansion of *D. carinulata* in North America over a five-year period in which beetles moved southward from 35.27° N to 33.04° N along the Colorado River, into some of the warmest regions of North America. We used our phenology model (Grevstad and Coop 2015; Grevstad et al. 2022) to compare CDL and the timing of diapause induction with predicted optimal CDL based on seasonal temperature patterns encountered at locations in the new range of this species. The model accurately predicts/explains the dramatic shift in voltinism observed in southward moving field populations from one generation (with an ill-timed diapause in the spring) to seven generations corresponding with full use of the growing season and a high level of impact to the target weed.

Study System

Diorhabda carinulata collected from two sites in Central Asia provided the starting populations for the first releases in 2001, initiating tamarisk biological control in North America (DeLoach et al. 2003). Beetles used in the current studies were descendants of beetles that originated from collections of fewer than 1000 beetles each made in northwestern China, near the city of Fukang (44.17° N; 87.98° E) in 1997 and 1998 and similar collections of beetles made near the city of Chilik (Shelek), Kazakhstan, (43.67° N; 78.50° E) (DeLoach et al. 2003, 2004; Tracy and Robbins 2009). These are hereafter referred to as the Fukang and Chilik populations, which have not been distinguished by traits indicative of distinct ecotypes. They readily interbreed (Bean et al 2013), with no known morphological differences, but can be distinguished using molecular markers (Stahlke et al 2022). Three related *Diorhabda* species were also introduced, primarily within the Rio Grande Basin, and the Mississippi River Basin, and have since expanded along river drainages in those areas (Tracy and Robbins 2009; Knutson et al 2019). To our knowledge, the other three species have not been purposely introduced into the Colorado River Basin or other areas in the intermountain west of North America, where *D. carinulata* were initially introduced.

Figure 21. The tamarisk leaf beetle (*Diorhabda carinulata*) and invasive tamarisk (*Tamarix* spp.)

Facultative diapause occurs during the adult stage of *D. carinulata* and is characterized by accumulation of metabolic reserves in the fat body, undeveloped reproductive systems in females (ovaries and ovarioles) and males (accessory glands) behavioral changes including descent into the leaf litter beneath the host plants, and cessation of aggregation pheromone release by males (Bean et al 2007b). Photoperiod is the primary cue used to signal diapause, with long days

promoting continuous development and short days cueing diapause (Bean et al 2007a, b). Adult *D. carinulata* are sensitive to photoperiod, with insects able to switch from a reproductive state to diapause, even following oviposition (Bean et al 2007b). Beetles remain in the leaf litter until spring and emerge in response to increasing temperatures. Like many insect species that are adapted to temperate climates, they lose sensitivity to photoperiod in the early winter and reproductive development may resume under permissive temperatures, even in the absence of long days (Koštál 2006). Beetles have three larval instars, which feed exclusively on *Tamarix* foliage. Mature third instar larvae cease feeding and descend into the leaf litter to pupate. Newly emerged adults climb from the leaf litter to green tamarisk foliage and feed, then either enter diapause or become reproductive.

Methods

Mapping range expansion

The presence and density of *D. carinulata* in the Colorado River Basin has been monitored by an array of resource managers and stakeholders interested in invasive species control, riparian restoration, wildlife habitat, water salvage and other topics involving tamarisk. A protocol was used that employed sweep net sampling of tamarisk, recording presence, number of *Diorhabda* captured and geocoordinates, and these data were submitted to a nonprofit organization, RiversEdge West (formerly the Tamarisk Coalition), for curation and use in mapping. Maps of *D. carinulata* occurrence have been published annually since 2007 (https://riversedgewest.org/services/tamariskbeetle). We used data from the beetle mapping project to estimate the range expansion front as it moved southward. The Lower Colorado River Basin (LCRB) has been an area of high interest to resource managers, so in addition to sweep net data there have been a number of publications documenting southward movement of *D. carinulata* (e.g., Bateman et al 2010; Dudley and Bean 2012; Nagler et al 2014; Hultine et al 2015).

The monitoring data document the rapid expansion of the range southward between 2006 and 2019 (Fig. 22). High population densities of D. carinulata and mass defoliation of tamarisk have frequently been observed in areas near the front (with lower densities of colonizers beyond the front). Between 2012 and 2015, the rate of expansion slowed somewhat near the southern point of Nevada (Princess Wash and Big Bend State Park, NV), but then accelerated again starting in 2016 reaching the Arizona border with Mexico at the end of 2019.

Beetle collection and diapause experiments

Populations of *D. carinulata* were collected from locations throughout the southwestern U.S. (Fig 22) across the years from 2007 through 2019 (Table 7) with the 2017-2019 collections made as part of this SERDP project (see also Bean et al. 2012). Collections consisted of 60 to 200 individuals which were brought to the laboratory facilities in Palisade, CO. There they were

reared on fresh foliage through a generation under standard conditions of temperature and photoperiod in which all individuals are reproductive (16L:8D, 25°). Rearing a generation under identical conditions was done to minimize the possibility that field conditions could impact the first laboratory generation through parental effects (Bean et al 2012). The subsequent generation of eggs or newly hatched larvae were either used in experiments or were reared under diapause inducing conditions for use in experiments the following spring. Initially the conditions used to induce diapause prior to storage were a photoperiod of 12L:12D and temperature of 25°C but due to CDL evolution the southernmost populations were found to require an even shorter day of 11L:13D, 25°C to reliably induce diapause. To hold beetles in diapause, temperatures were dropped incrementally to 5°C. Diapausing adult beetles held at 5°C survive for six months or longer without green foliage.

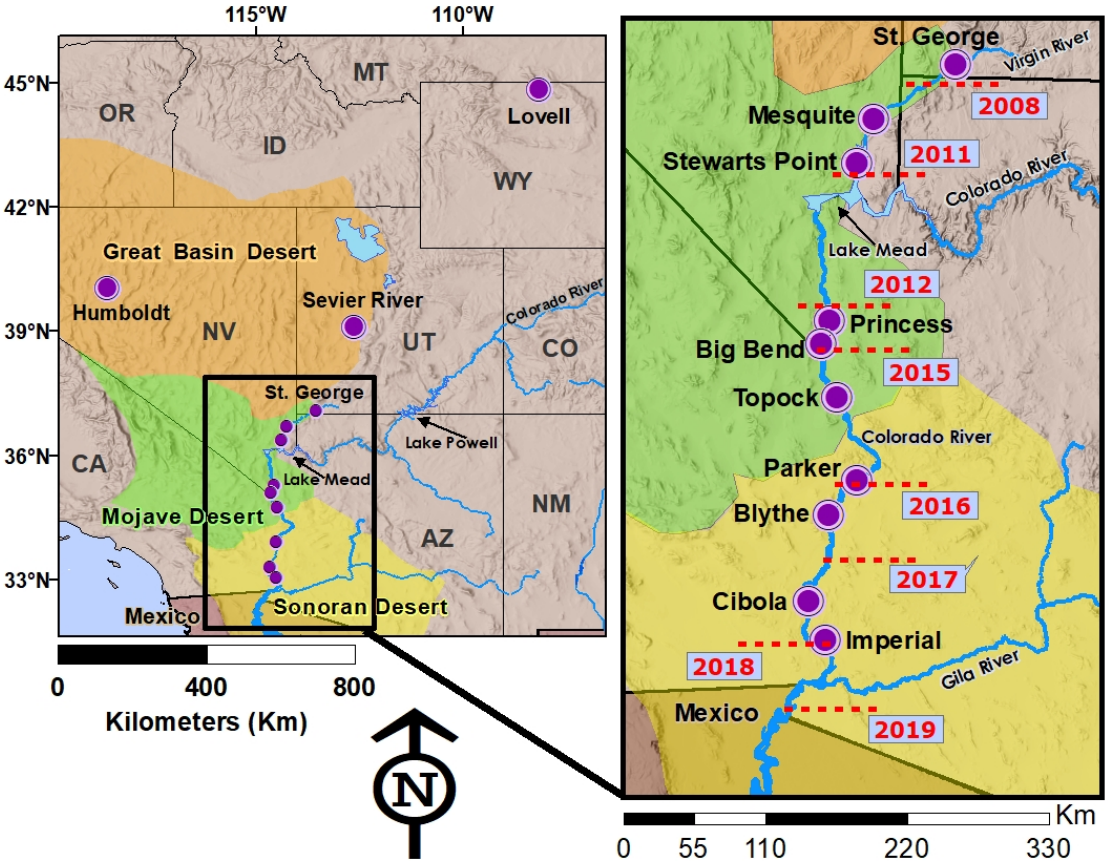

Figure 22. Southward range expansion of *D. carinulata* along the Colorado River corridor. Following initial releases in 2001 beetles became established in western Nevada at the Humboldt site, in Utah at the Sevier River (Sevier site) and in Wyoming at the Lovell site. Following the 2006 introduction of beetles from the Sevier River site into the St. George site beetles moved southward along the Virgin River expanding beyond the St. George area in 2008. They moved through the Virgin River Valley past the Mesquite site and reached Lake Mead (the Stewarts Point site) in 2011 then were found as far south as Princess/Big Bend in 2012. By the autumn of 2016 they had become established in Topock Marsh (Topock site) and were detected as far south as Parker (Parker site). In the years 2017-2018 they moved south to Imperial NWR. By the autumn of 2019 they had defoliated tamarisk within Imperial NWR and had moved south to the US/Mexico border.

Insects taken from stock cultures were transferred as eggs or first instar larvae into programmable incubators (Model I30BLL or Model I36VL, Percival, Perry, IA) where they were reared under test conditions on freshly cut tamarisk foliage comprising admixtures of *T. ramosissima* and *T. chinensis*, commonly found in the western US (Gaskin and Schaal 2003; Gaskin and Kazmer 2009; Williams et al 2014). Larvae were reared in groups of 100-150 in well-ventilated clear plastic containers ranging in volume from 4-10 liters. Late third instar larvae were transferred to well-ventilated plastic containers with sand 5-7 cm deep at the bottom, as pupation substrate. Larvae typically burrow into the sand where they pupate within a hibernaculum constructed of sand grains. Newly emerged adults were removed daily from the pupae containers, paired in well ventilated plastic deli cups (177 ml), and fed ad libitum with fresh *Tamarix* foliage (Bean et al 2007b). The number of pairs tested at each photoperiod ranged from 25-90 depending on the population, treatment, and the year in which the experiment was performed. Paired adults were held under experimental conditions for 20 d after emergence and if no oviposition was recorded the insects were scored as being in diapause. Diapausing insects were occasionally dissected after 20 d to verify developmental status (Bean et al. 2007b).

All photoperiod experiments were conducted in the presence of a thermoperiod as previously described (Bean et al 2012). The thermoperiod amplitude was 20°C with an average of 25°C and was superimposed on test photoperiods. The thermoperiod was structured with a 9-hour thermophase (35°C) occurring during the photophase and the 9-hour cryophase (15°C) occurring during the scotophase. The thermoperiod had a 3-hour transition between 15° C and 35°C starting at lights-on, followed by 9 hours at 35°C then a 3-hour transition down to 15° C which was held for 9 hours. The three-hour transitions between cryophase and thermophase were programmed in 2°C increments, occurring every 20 minutes, and initiated at lights-on. Thermoperiods with a 20° C amplitude are typical of summer temperature patterns in the arid interior western US and were used in a previous study (Bean et al. 2012). In addition, use of photoperiods combined with thermoperiods under laboratory conditions have been shown to more accurately reflect the developmental response of *D. carinulata* to photoperiod cues in the field than use of photoperiods under constant temperatures (Bean et al 2007a).

Results

The short-day diapause response of *D. carinulata* has evolved through both time and space, with the most recent and southernmost populations now having mean critical day lengths that are 3.25 hours shorter than the original imported populations (Table 7, Fig. 23). In contrast, the northern populations of Lovelock, NV, Delta, UT, and Lovell, WY maintained CDL's that were very close to those of the original imported populations.

Site	Lat	Year	CDL	SE
Lovell, WY	44.85	2007	14.71	0.03
Lovell, WY	44.85	2019	14.72	0.05
Lovelock, NV	40.03	2007	14.16	0.04
Lovelock, NV	40.03	2017	14.24	0.05
Delta, UT	39.13	2014	14.43	0.04
Delta, UT	39.13	2017	14.31	0.06
Delta, UT	39.13	2019	14.44	0.06
St. George, UT	37.09	2014	14.24	0.05
St. George, UT	37.09	2019	13.46	0.05
Mesquite, NV	36.77	2014	14.28	0.05
Gold Butte, NV	36.77	2017	13.91	63.10
Stewart's Point, NV	36.38	2014	14.19	0.04
Princess, NV	35.27	2014	13.86	0.06
Princess, NV	35.27	2019	13.48	0.06
Big Bend, NV	35.08	2017	13.67	0.06
Big Bend, NV	35.08	2019	11.94	0.13
Topock Marsh, AZ	34.76	2017	12.75	0.09
Blythe, CA	33.91	2019	12.44	0.08
Cibola, CA	33.30	2019	12.29	0.07
Imperial, AZ	33.04	2019	11.19	0.09

Table 7. Critical Day Length and standard error, measured in populations of *D. carinulata* collected in North America between 2007 and 2019. Latitude is also shown for each collection site. Tests carried out on beetles collected in 2017 and 2018 were supported by this project.

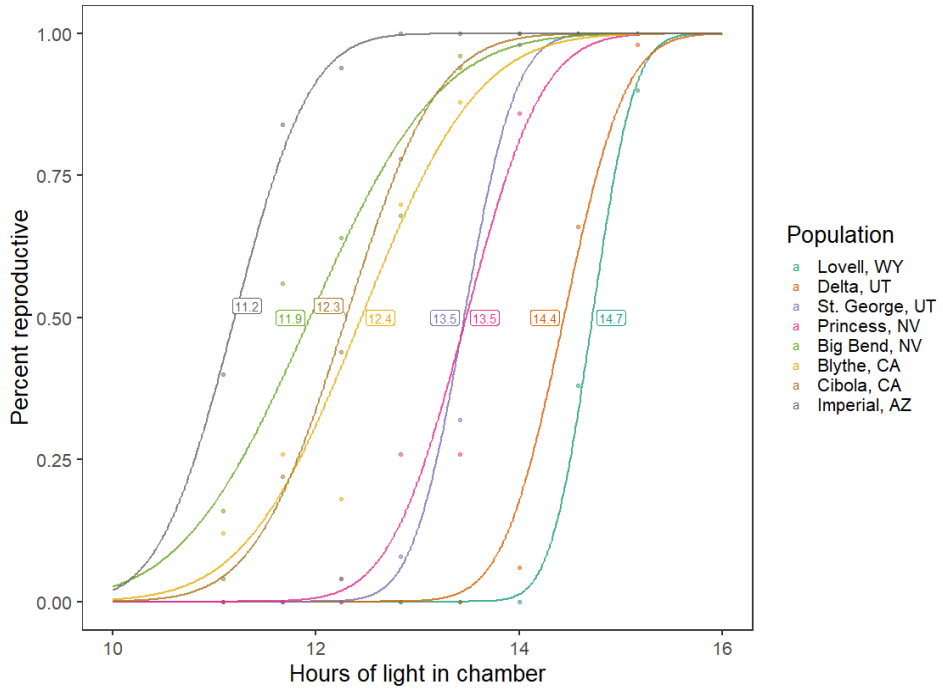

Figure 23. Proportion of *Diorhabda carinulata* that were reproductive (as opposed to diapausing) from populations collected along a N/S gradient from Lovell, WY to Imperial AZ and reared in chambers at different photoperiods (x-axis) and a thermoperiod of 35° day/ 15° night. The mean critical photoperiod is indicated for each population. All populations were collected in 2018-2019, except Lovell, WY which was collected in the fall of 2017.

Critical Day Length during range expansion

We measured CDL at the range expansion front in 2014 after *D. carinulata* had moved southward to the area around Big Bend State Park, NV (Fig 22). The southernmost populations were represented by a collection made at Princess Wash with a CDL of 13.86 hrs. and the northernmost, measured in beetles from the Sevier River, was 14.43 hrs. Beetles collected from three sites at intermediate locations had CDLs measured between 14.28 and 14.19. Measurements were made again in 2017 using beetles collected in late 2016 or 2017. The southernmost population used for CDL measurement was collected from Topock Marsh within the Havasu National Wildlife Refuge. Northern tamarisk beetles had arrived at Topock in 2016 where they reached defoliating numbers by the autumn. The CDL for beetles from this site was 12.75 hrs., the first time CDL measured in *D. carinulata* had been shorter than 13 hours. The CDL from beetles from Big Bend, NV was 13.67 while the CDL from the Sevier River site was 14.31 hrs. and from the Humboldt, NV site was 14.24 hr. The CDL from Humboldt had been measured at 14.16 in beetles collected during the fall of 2007, indicating stability of CDL at that location over the past decade.

The final experiment, conducted in 2019, showed that the population at the leading front, 33.04°N, in the INWR, had a CDL of 11.19 hr. The four populations collected from 35.08°N and southward all had CDLs less than 12.5 hrs (Table 7). There was a notable break in CDLs between the population collected from Big Bend (35.08°N, 11.94 hrs) and that from nearby Princess Wash (35.27°N, 13.48 hrs) which may indicate mixing between the Big Bend population and more southern populations with shortened CDLs, while Princess Wash remained isolated. The CDLs measured in beetles from two of the original release sites, Lovell, WY and Sevier River, UT, were nearly identical to those measured from those sites in past years (Table 7, Fig 24). The difference between CDL at the Sevier River original release site and at INWR was 3.25 hrs. over a range of 6.09 degrees latitude. Over the course of the study southward moving populations experienced evolution while beetles at the original release sites retained stable CDLs (Fig 24).

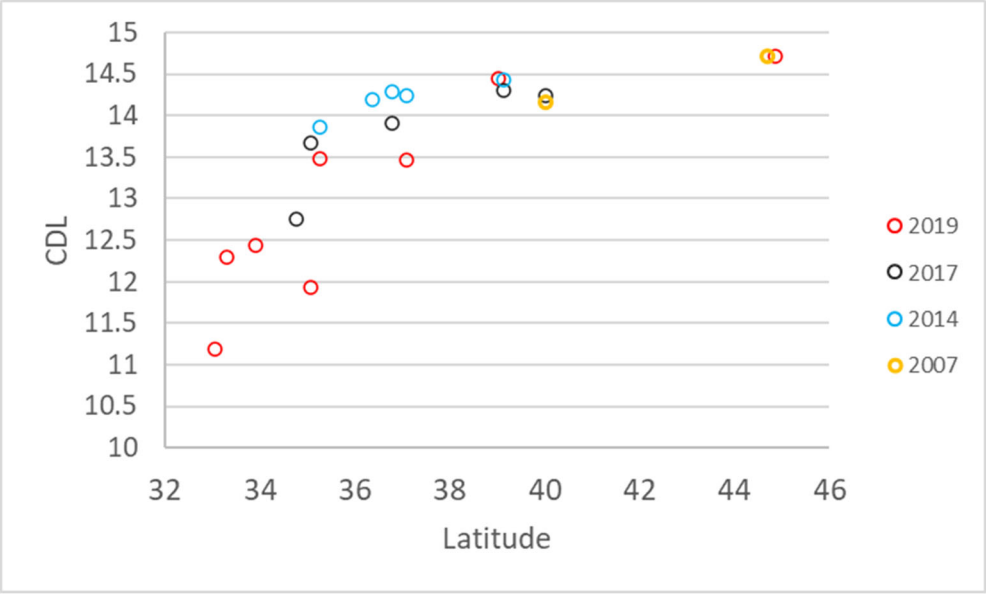

Figure 24. CDL measurements, over a 12-year period from 2007-2019, made under a thermoperiod of 35° day/ 15° night. Field collections were made at or near the leading front of range expansion in the intermountain west on each of the dates listed. The three sites north of 38° N were original release sites (releases made in 2001).

Temperature patterns at *Diorhabda* field sites

Annual developmental degree-days for *D. carinulata* were calculated for field sites used in this study (Fig 24). The three northern sites, located in the Great Basin Desert (Humboldt and Sevier) and the Wyoming Basin (Lovell), have long winters and short hot growing seasons. Annual degree-days are well under 2,000 for all three sites. There is a transition between Great Basin Desert and the upper Mojave Desert where winters are shorter and summers hotter. The St. George site has over 3,000 annual degree days while lower in the Virgin River drainage at the Mesquite and Stewarts Point sites have about 3,700 degree-days. Below Lake Mead all sites have well over 4,000 annual developmental degree days. The Sonoran Desert, which includes the Blythe, CNWR and INWR sites, is subtropical with milder winters than the Mojave.

Average degree days accumulated during the spring before summer solstice increases at lower latitudes which enables beetles to complete one or more generations in the spring. This pattern is key to *D. carinulata* voltinism since beetles reach the photosensitive G1 early enough in the season to encounter short days of spring which may induce diapause and limit populations to a univoltine life history.

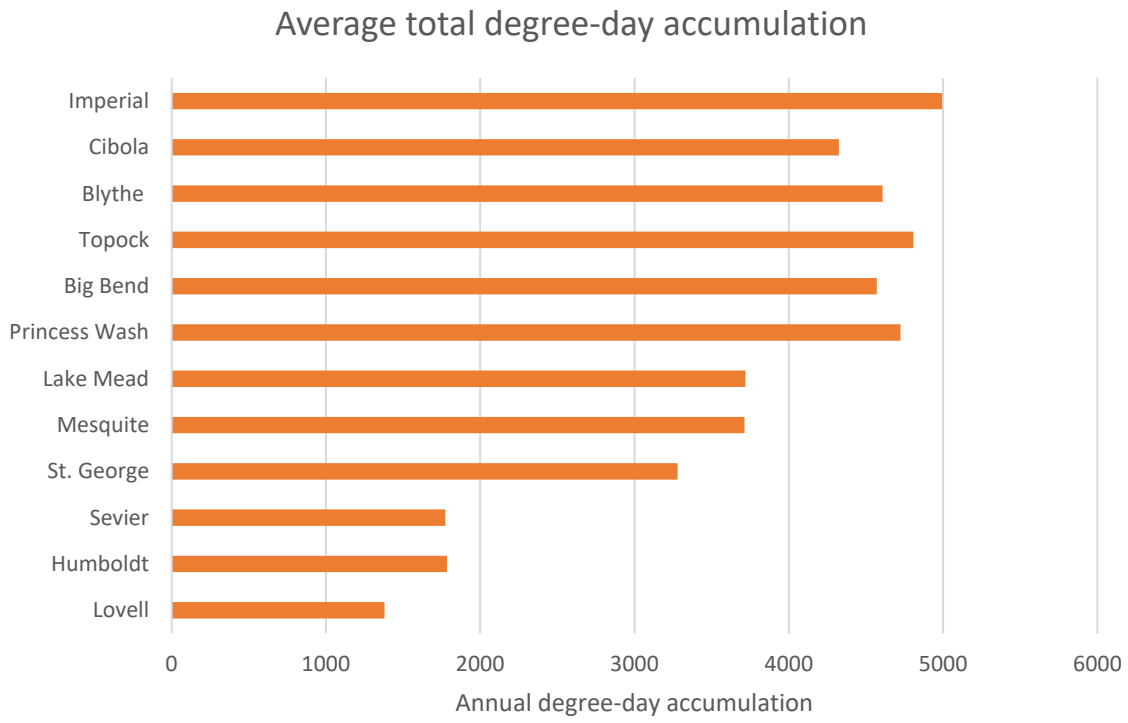

Figure 25. Annual degree-day accumulation averaged over ten years (2010-2019) at three initial release sites (Sevier, Humboldt, and Lovell) and field sites on the southern range-expansion front of *D. carinulata*. Following spring emergence at 128 degree-days each generation requires a minimum of 551 degree-days.

Photothermographs predict multivoltinism at *Diorhabda* field sites

Our photoperiod phenology model is illustrated here using photothermographs from the Big Bend site (Fig. 26). The photothermograph shows that as many as seven generations would be possible at the site, given the average accumulated degree-days (Figs 25, 26). With a CDL of 13.67 hrs, measured in 2017, the first summer generation, represented by the first vertical bar, would appear when day lengths were shorter than the CDL (indicted by the photothermal line passing beneath the horizontal CDL line). At that point there would be selection for insects with shorter CDLs that would be reproductive and able to produce a second generation in the spring. This is indicated on the graph as strong selection for a shorter CDL. The photothermal line crosses the next four vertical bars at points above the CDL line, indicating that generations 2-5 would be exposed to days long enough to cue reproductive development. Generation 6 would emerge as days are getting shorter in the summer and at a time when day lengths are shorter than the CDL measured in 2017 and generation 6 would then enter diapause even though sufficient degree days remain for a seventh generation. During the 2019 season beetles in the Big Bend area had a substantially shorter CDL, most likely the result of movement of beetles from the south, up to the Big Bend site. The shorter CDL would then enable a high percentage of G1 beetles to avoid spring diapause and G6 beetles to remain reproductive and produce a G7 (Fig 26).

Photothermographs illustrate that two generations per year are likely for three sites, Lovell, Humboldt, and Sevier, north of 39°N (Fig 27). The model also predicts that the first summer generation, G1, at these sites will emerge after summer solstice but early enough that the days are still longer than the CDL cuing reproduction into the next generation, corresponding with observations made for these populations in the field (Bean et al. 2007a). When the second generation (G2) emerges, day lengths are shorter than critical and most individuals enter diapause, but this can vary based on annual thermal patterns. By considering accumulated degree days for individual years, it is seen that during some years a third generation would be possible, while during others the degree days accumulated would fall short of enabling a third generation (Fig 27).

At the St. George site, which lies within the northern reaches of the Mojave Desert (Fig 22), there are on average over 3,000 degree-days accumulated annually (Fig 25). This is sufficient to enable five generations per season (Fig 27 representing a substantial shift from the two to three generations at the Sevier site where the population originated in 2006 (Bateman et al 2010). However, this number of generations is only possible if the CDL is shorter than 13.5 hours, which was not the case during the first measurement in 2014, while it was the case in 2019.

The Mesquite and Stewart's Point sites have similar thermal and photoperiod profiles with six full generations predicted (Fig 27) and the G1 emerging in early May prior to when day lengths exceed the CDL, on average, at those sites. However, during some seasons (2010 and 2011) within the 10-year span, day lengths at the G1 exceeds the CDL measured at those sites (Fig 27)).

As discussed above, the Big Bend site average annual degree-day accumulation would enable seven generations (Figs 26, 27)) and in warm years, comprising five out of the ten between 2010 and 2019, eight generations could complete development (Figs 26. 27)). Severe limitations on voltinism are imposed by the CDL of 13.67 hrs., measured in 2017. First, the spring emergence of G1 occurs on April 15, when day lengths are 13.15 hours, not long enough to cue reproductive development in most of the population (Fig 26). In contrast beetles collected from Big Bend in 2019 had a CDL of 11.94 hrs. which would enable the majority of G1 beetles to bypass spring diapause (Fig 26).

Beetles collected from the INWR site in 2019 had the shortest CDL yet measured in *D. carinulata*, 11.19 hrs. Even though spring emergence of G1 is predicted to occur on March 31 the CDL is short enough to prevent spring diapause in most insects (Fig 27). The INWR site is in one of the warmest areas of North America, with 5,000 degree-days annually (Fig 25) supporting development of eight generations of *D. carinulata* (Fig 27). Interestingly, during at least half of the years G8 beetles would emerge when days are long enough to initiate a ninth generation, because of the short CDL. There are insufficient degree days to allow completion of a ninth generation, which would impose a fitness cost if beetles could neither complete development nor enter diapause.

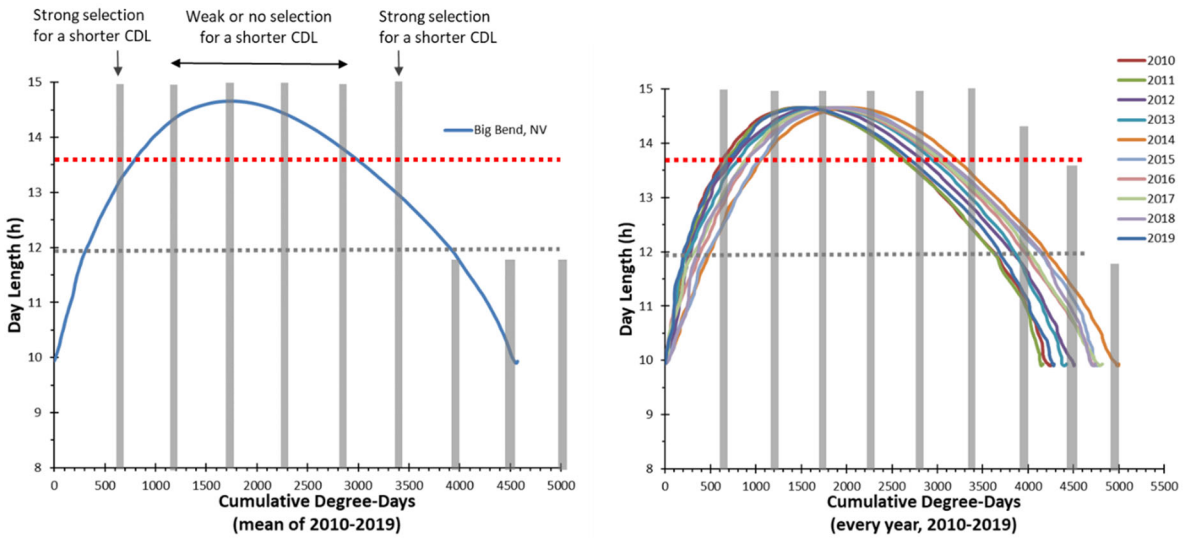

Figure 26. Photothermographs drawn from temperature data at the Big Bend, NV site illustrating selection pressure for a shorter critical photoperiod. (A) Average 2010-2019. (B) Each year's data drawn separately. Dotted lines represent the CDL measured in *D. carinulata* populations collected from that site in 2016 (13.67 hr., red dashed line) vs 2019 (11.94 hr., grey dashed line). Vertical lines show emergence of the photoperiod-sensitive stage. Selection for a shorter CDL is indicated in both early spring and mid-summer, when the longer (2016) CDL would result in an ill-timed diapause.

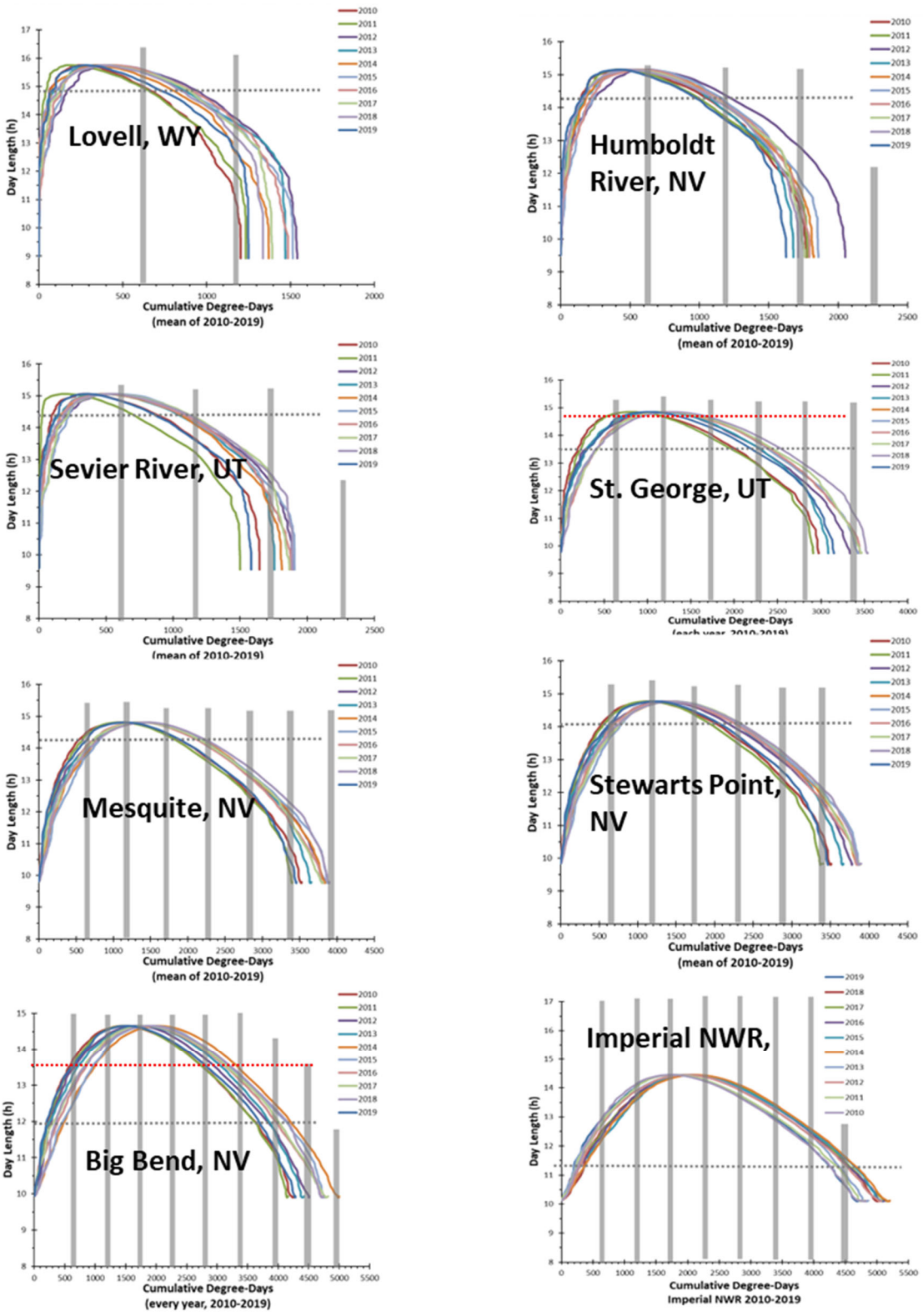

Figure 27. Photothermographs plotting day length as a function of site-specific degree days (years 2010-2019) at Diorhabda collection locations throughout the western U.S. The horizontal gray dotted lines represent recent mean critical day lengths (CDL) measured in *Diorhabda* populations from that site. The red dotted lines represent mean CDL's measured in 2014 (for St. George, UT) and 2016 (for Big Bend, NV).

Using the mapping model to predict voltinism with original and evolved photoperiod response

We applied the mapping versions of our phenology model (section 2) using developmental parameters obtained from Herrera et al. (2005) and photoperiod response curves obtained from the above experiments (Table 7, Fig. 23). Geospatial display from our model reveals a univoltine life cycle throughout most of the Lower Colorado River riparian corridor if beetles had retained their ancestral CDL of 14.44 hours.

However, with the evolved CDL of 11.19 hours (as measured in this region in 2019), *D. carinulata* populations are modelled to have eight generations along the Lower Colorado River (Fig. 27). While no direct measurements of field voltinism have been made, the appearance of first-generation adults on 3/29/2019 at the INWR (D. Bean personal observation and collection data) and late season (November) occurrence of larvae at the INWR site, suggests that at least 7 generations could have been experienced by beetles in 2019.

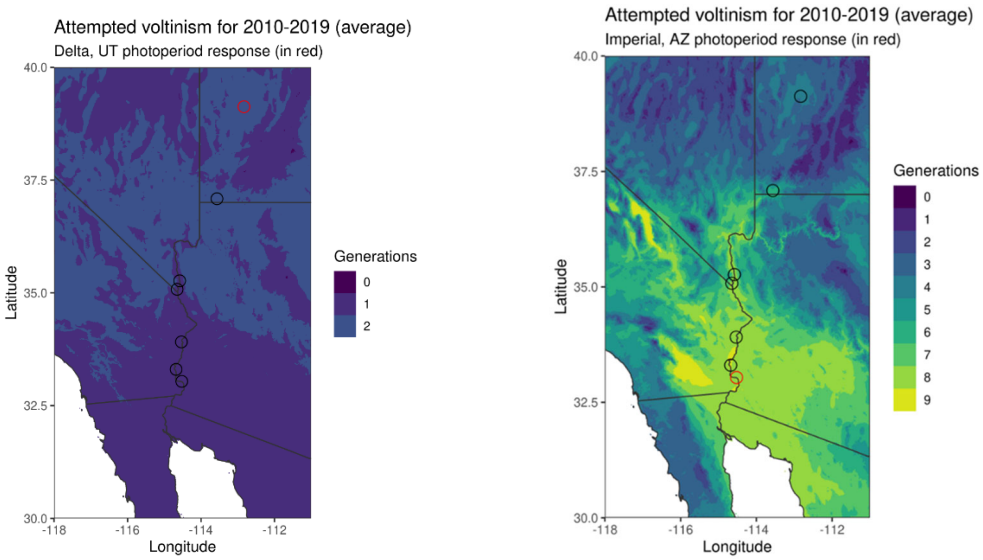

Figure 28. Modeled predicted attempted generations for *Diorhabda carinulata* before and after evolution of the photoperiod response. (A) Given the CDL measured for beetles collected from Sevier River, UT, in 2019 (14.44 hr) this map displays the expected number of generations attempted by *D. carinulata* in the southwestern US. The Sevier River site is shown in red while the other sites where beetles were collected for CDL measurement in 2019 are shown as black circles. (B) Given the CDL measured for beetles collected from Imperial NWR (11.19 hr) this map displays the expected number of generations attempted by D. carinulata in the southwestern US. The Imperial NWR site is shown in red while the other sites where beetles were collected for CDL measurement in 2019 are shown as black circles.

Range expansion and rapid CDL evolution

The range of the northern tamarisk beetle *D. carinulata* expanded southward from release sites in North America, including the Great Basin Desert (Fig 22), to the southern subtropical Sonoran Desert where they encounter shorter day lengths, longer growing seasons and milder winters.

During this study CDL remained stable in northern *D. carinulata* populations, including at the initial Sevier release site (core population, 39.13° N). Beetles at the southern front of range expansion showed rapid CDL evolution with the rate increasing as beetles moved southward. The rate of evolution averaged 0.067hr/ year during the first eight years (2006-2014) 0.33hr/year during the next three years (2014-2017) and 0.845hr/ year during the last two years (2017-2019). Beetles at the leading edge of range expansion (33.04° N) in 2019 had a CDL of 11.19 hours, 3.25 hours shorter than that measured at the Sevier site (Table 7, Fig 24).

Southward range expansion and CDL evolution were correlated (Fig 24) and during the years 2014-2019 there were two southward dispersal events that coincided with rapid shifts in CDL. The first occurred in 2016 when beetles moved from tamarisk stands in and around Big Bend State Park (35.12° N) to Topock Marsh (34.76° N) about 40 km south, then as far south as Parker, NV (34.16° N) (Fig 22). CDL measured in the Topock Marsh population was 12.75 hrs., nearly an hour shorter than measured in a population from nearby Big Bend that same year (Table 7). Range expansion continued with beetles reaching Cibola NWR in the late summer of 2018. In November of 2018 beetles were found in the Imperial Nation Wildlife Refuge (INWR), approximately 50 km south of the Cibola population. In the spring of 2019 beetles collected from the INWR population had the shortest CDL thus far recorded in *D. carinulata*, at 11.19 hrs. (Table 7) while the Cibola population had a CDL of 12.29 hrs. (Table 7). In 2017 and again in 2019 beetles at the leading edge of range expansion had a CDL which was about one hour shorter than the CDL from the closest population to the north, presumed to be the population of origin.

Selection for optimal CDL

The optimal CDL for an insect population at a specific location is one that is short enough to enable continuous growth and reproduction while resources are available, yet long enough to induce diapause before the onset of potentially lethal conditions including biotic (e.g., host plant senescence) and abiotic (e.g., subfreezing temperatures) (Saunders et al 2002; Tauber et al 1986). In the case of the northern tamarisk beetle, the optimal CDL varied during range expansion as beetles move into regions with shorter spring and summer day lengths and warmer temperatures. We used a voltinism model to estimate optimal CDL at sites along the expansion front of *D. carinulata* and compared those to CDLs measured during range expansion (Grevstad and Coop 2015).

CDL was stable at three of the original release sites, including the presumed origin site at the Sevier River where beetles that colonized the Lower Colorado River Basin (LCRB) were collected (Bateman et al 2010). Photothermographs created for the three original release sites illustrate the relationship between photoperiod, degree-day accumulation and CDL when CDL is optimal for timing of diapause induction. At the three original sites the first photosensitive stage, G1 adults, emerge after summer solstice, when day lengths are near the annual maximum and starting to decline . Previous field observations showed emergence of G1 adults from late June to mid-July at the Humboldt and Lovell sites, a time when day lengths exceed 14.5 hours and cue

reproductive development (Bean 2007a; Bean 2012; Table 7). These relationships are illustrated in Fig 27 in which the photothermal line passes above the CDL (indicating days are longer than the CDL) at the point where both lines intersect the first seasonal appearance of photosensitive adults at the three northern sites, depicted as the G1 vertical bar. The first summer generation is reproductive, emerging when days are longer than the CDL, and produces a second summer generation. The second generation reaches the photosensitive adult stage in August to early September, when days are shorter than the CDL, indicated by the photothermal line passing beneath the CDL where they both intersect the G2 bar. Cued by short days, second generation adults feed, enter diapause and descend into the leaf litter to overwinter, a pattern which has been observed at the Lovell site (Bean et al 2007a, b).

Beetles in the LCRB are exposed to higher temperatures, shorter spring and summer day lengths and longer growing seasons for tamarisk than those found at the original release sites (Hultine et al 2015), conditions which permit more than two generations per season. At St. George, the first known site of establishment in the LCRB (Bateman et al 2010), spring and summer day lengths are shorter than those at the Sevier site, but the most notable difference is the greater accumulation of developmental degree days, which could enable as many as five generations per season (Figs 25, 27)). The G1 adults are predicted to emerge and become reproductive in late spring, since they would be exposed to days longer than the 2014 CDL of 14.24 hr (Table 7 Fig 27) while the G2 and G3 would be cued for reproductive activity by longer day lengths as the season progressed (Fig 27). With declining day lengths of mid-summer, G4 beetles are predicted to enter diapause while the photothermograph shows that there are on average sufficient degree-days to allow a fifth generation, indicating a possible late season mismatch (Fig 27). The 2019 CDL was 13.46 hrs, which would allow a fifth generation at the St. George site (Fig 27). Five generations are the maximum possible given the average degree-day accumulation at the St. George site, so the CDL of 13.46 hours would be near the optimal value at that location. Future measurements are needed to determine if the CDL remains stable in the St. George area.

In the years following establishment at St. George beetles moved downstream along the Virgin River, following tamarisk stands that extend into the Virgin River Valley and then to the shores of Lake Mead (Fig 22). The Mesquite site in the Virgin River Valley and Stewarts Point on the shores of Lake Mead are warmer than St. George, measured both as greater average developmental degree days and earlier emergence of the photosensitive G1 (Fig 24). During some years, the majority of the newly emerged G1 adults are expected to appear when spring days are short enough to cue diapause, resulting in suboptimal population growth, diminished fitness, and strong selection for shorter CDLs (Figs 12 and 13). These are the most northern locations in the LCRB where spring diapause is expected to be a major factor defining fitness.

By 2012 beetles were established as far south as Princess Wash, after which they stalled southward expansion and did not move beyond the Big Bend area until 2016 (Fig 22). The Big Bend photothermograph indicates that during most years the G1 emerges when day lengths are shorter than the 2017 CDL of 13.67 hrs. (Table 7, Fig 26). Although a portion of the population has a shorter CDL and would be reproductive, most would enter diapause in the spring and perish in the leaf litter over the summer months. Selective pressure for shorter CDLs would

occur twice during the season, in the spring and again in the late season (Fig 26). Having two points in the season where shorter CDLs are selected may have contributed to the rapid evolution of CDL in populations from the Big Bend area.

Following southward range expansion in 2017 and 2018, beetles were discovered as far south as the INWR in what appeared to be a geographically isolated population. A population collected in the spring of 2019 at the INWR had a CDL of 11.19 hours, short enough to enable nearly 100% of the G1 generation to be reproductive at that site (Fig 27). The photothermograph for the INWR shows that a CDL of 11.19 hours will allow up to eight generations and that the eighth generation will remain mostly reproductive (Fig 27) even though there are not enough degree days to complete a ninth generation. This indicates a potential mismatch in which the newly evolved CDL could be shorter than optimal, an observation that deserves further study.

Factors Affecting CDL Evolution

The evolution of CDL in *D. carinulata*, resulting in a 3.25 hour decline, occurred over thirteen years during a period of range expansion (Table 7) making it exceptional in terms of rate and magnitude. Latitudinal clines in CDL are a common feature of insect ecophysiology (Danilevskii 1965; Beck 1980; Tauber et al 1986; Danks 1987; Ragland et al 2019) and while existing CDL clines of three hours or more have been identified in a number of species (Tauber et al 1986; Danks 1987; Bradshaw and Holzapfel 2001a) and rapid CDL cline formation has been observed in several species (Urbanski et al 2012, Gomi 2007) to our knowledge clines of over three hours have not been tracked during the process of formation. Phenology mismatches are critical in defining species range (Chuine 2010) so it is likely that a persistent CDL mismatch would have prevented *D. carinulata* range expansion and excluded the beetles from the LCRB (Bean et al 2007a). Instead, the *Diorhabda-Tamarix* system provided a setting in which CDL could rapidly evolve, allowing beetles to reset a mismatched phenology and move into areas initially considered out of their range, with implications for control of tamarisk and conservation of wildlife habitat (Dudley and Bean 2012). A steep gradient of CDL selection pressure along with behavioral biology and introduction of populations from two widely separated areas in Eurasia may have contributed to rapid evolution, as discussed below.

Selection pressure for shorter CDLs increases along three gradients that coincide with the direction of range expansion (Hultine et al 2015) so beetles at or near the leading edge of expansion encounter the strongest selection pressures. The gradients include decreasing spring and summer day lengths moving into lower latitudes, as well as increasing temperatures, reflected in increased developmental degree-day accumulation at more southern locations (Fig 25). In addition, the seasonal window of host plant availability widens moving southward (Dalin et al 2010). While the selection gradient is steep, incremental southward range expansion would allow beetles at the leading edge to undergo evolution, making them better adapted for further southward expansion. For example, beetles in the Princess Wash/Big Bend area had a CDL less than 14 hours, measured in 2014, which most likely enabled them to persist at that location. If they had been translocated directly from the Sevier River site, bringing with them a CDL of

14.44 hours, the population would have likely been extirpated with nearly all insects entering spring diapause, as previously seen early in the program with introductions of beetles south of the 38th parallel (Bean et al 2007a).

The occurrence of spring diapause in regions with spring temperatures permissive for development in *D. carinulata* brings about a dramatic shift in predicted voltinism (Grevstad and Coop 2015; Figure 28). Early season accumulation of developmental degree-days (Fig 25) drives early emergence of G1, exposing photosensitive insects to days shorter than the CDL (Fig 26). Induction of spring diapause may limit a population to a univoltine life history, even in regions where five or more generations would have been possible (Grevstad and Coop 2015). In the case of *D. carinulata*, G1 may emerge early in southern locations when day lengths are nearly two hours shorter than the ancestral CDL of 14.44 hr (Table 2) making seasonal thermal patterns even more significant than latitudinal photoperiod patterns in causing diapause cue mismatches.

It is interesting to compare the CDL latitudinal gradient formed in *D. carinulata* with CDL gradients in other species. A pattern was noted early in photoperiod studies that CDL shifted by about 1 hour for every 5° latitude (Danilevskii 1965) and in the mosquito *Wyeomyia smithii* the value was fine-tuned through extensive studies to 1 hour for every 5.4° latitude (Bradshaw 1976), while additional studies showed values ranging from one hour per 3° latitude to one hour per 7° latitude (Danks 1987). For *D. carinulata* the value is 1 hour for every 1.85° latitude between the core site (Sevier) and the edge of expansion (INWR). This value reflects the magnitude of impact that seasonal temperature patterns may have on CDL and selective pressure for shorter CDLs. Using *W. smithii* Bradshaw calculated an elevation effect on CDL in which 142 m of elevation was equivalent to a 1° shift northward (Bradshaw 1976). Using Bradshaw's formula, inclusive of elevation, the predicted CDL gradient between Sevier, Utah (1,410 m, 39.13° N) and INWR (59 m, 33.04° N) would be about 2.9 hours, whereas without elevation difference factored in it would be 1.1 hours. In the *Diorhabda*/*Tamarix* system warm spring temperatures (Fig 25) advance the emergence of the photosensitive G1 (Fig 26, 27) exposing the G1 to substantially shorter day lengths than they would be at cooler more northern sites. It isn't then simply a matter of day length differences between northern and southern sites but also temperature effects which had previously (Bradshaw 1976) been represented in elevational differences.

The potential for a short-day induced premature diapause has been recognized in other species (Denlinger et al 2017). Spring diapause may be averted through physiological mechanisms, transmitted maternally, that prevent diapause in the offspring of insects that had experienced diapause (Heinrich and Denlinger 1982). This is not the case in *D. carinulata* where there are no known maternal effects and adults may enter spring diapause at southern latitudes (Bean et al 2007a). The fitness consequences of spring diapause have not been measured, but we assume that ecological processes (e.g., increased predation in the leaf litter) and physiological processes (e.g., increased metabolism diminishing energy reserves) would ensure that such a substantial phenology mismatch would result in low fitness for spring diapausing *D. carinulata* (Bean et al 2007b). To better understand evolution of the photoperiodic cue It would be useful to discover

and quantify the agent or agents of selection (MacColl 2011), such as predators that feed on prematurely diapausing beetles or elevated temperatures that increase metabolic rates in prematurely diapausing insects.

During *D. carinulata* dispersal, aggregation behavior and reproductive state are linked in a way that favors the movement of reproductive insects to the leading edge of range expansion, resulting in spatial sorting of reproductive insects. Reproductive beetles are more likely than diapause-destined beetles to fly (Bean et al 2007a) so dispersing populations are in most cases reproductive beetles that aggregate on host plants in response to a pheromone released by reproductive males (Cossé et al 2005; Bean et al 2007b). In this way spatial sorting early and late in the season would not only favor generally more dispersive individuals, as seen in other systems (Shine et al 2011) but also individuals in which shorter CDLs allow reproductive activity during shorter days. As a result, we expect spatial sorting of beetles with genetically encoded shorter day length cues, particularly in the spring and late summer. The *Diorhabda-Tamarix* system may provide an example of spatial sorting (Shine 2011), offering a rare opportunity to investigate how rapid trait evolution due to spatial genetic structure affects eco-evolutionary dynamics, using a planned range expansion (Miller et al 2020).

The case of *D. carinulata* provides another example of evolution in an introduced species with limited genetic variation due to bottlenecks imposed by the process of introduction (Hufbauer 2008; Dlugosch et al 2008a). Standing genetic variation is reduced in North American populations of *D. carinulata*, compared with populations from the ancestral range (Stahlke et al 2022), yet beetles have been successful in the new range and have undergone rapid evolution (Bean et al 2012; this study). The paradox of reduced genetic variation in invasive species has various explanations, one of which is that multiple introductions may provide the additional genetic raw material for evolution and successful invasion (Dlugosch and Parker 2008b). *Diorhabda carinulata* originated from two populations from widely separated (600 km) sites in Central Asia (Tracy and Robbins 2009). While the primary source of beetles in the LCRB is the Sevier site (Chilik beetles), a secondary source originated from central Nevada (Fukang beetles), arriving in the Virgin River Valley via tributaries such as the Muddy River/ Meadow Valley Wash system and joins the Virgin River near Stewarts Point (Figure 22, Dudley, and Bean 2012). Molecular genetic evidence indicates gene flow between the two populations in the Virgin River Valley, although the genetic background of southward moving beetles is primarily Chilik (Stahlke et al 2022). Releasing biocontrol agents from two source populations may have supported rapid range expansion in this species. This is an intriguing possibility since it would provide an example within biological control of what is now apparent from studies in invasion biology; that additional genetic variation provided by multiple introductions may drive population expansion and dispersal in introduced species (Wagner et al 2017).

The *Diorhabda-Tamarix* system and evolution in biological control agents

The number of examples of evolution in invasive plant biocontrol agents remains small (Szücs et al 2019; Wepprich and Grevstad 2020) although instructive for answering theoretical and practical questions related to the practice of biocontrol (Szücs et al 2019; Stahlke et al 2022). The *Diorhabda-Tamarix* system is particularly attractive since the introduction and expansion of

populations as well as the status of phenology and environmental cues have been the subject of investigation since the beginning of open field releases (Carruthers et al 2008; Bean et al, 2012). As described in this study, the northern tamarisk beetle has expanded range into subtropical desert areas, accompanied by a dramatic shift in CDL for diapause induction. This case of range expansion offers numerous avenues for investigation of post release evolution as well as providing a non-model organism for molecular genetic evaluation of evolution, which is considered an essential component of for advancing the field of developmental photoperiodism (Denlinger et al 2017).

Thermal Modulation of CDL

Temperature modulates CDL in two southern adapted *Diorhabda* species with higher temperatures decreasing CDL, allowing increased voltinism (Dalin et al 2010) while CDL in the northern adapted *D. carinulata* showed little thermal sensitivity (Bean et al 2007). After seven years in the field there were indications of increased thermal modulation during evolution of CDL (Bean et al 2012) making *D. carinulata* a promising study system for investigating thermally regulated plasticity of the CDL, particularly in warm climates. Evolution of thermal sensitivity of the photoperiod cue for diapause has been measured in an invasive agricultural pest, the fall webworm *Hyphantria cunea* (Gomi 1997, 2007) but generally, temperature influences on CDL evolution are not well investigated. In this regard, the *Diorhabda-Tamarix* system could prove useful for understanding the relative contributions and interactions of temperature and photoperiod as phenology cues and the evolution of those interactions in different ecological settings (Chmura et al. 2019).

Molecular Genetics of CDL Evolution

The rapid evolution of CDL and possibly other southern adapted traits in the northern tamarisk beetle is likely to have a detectable genetic signature, instructive in defining the molecular mechanisms regulating phenology and its evolution in this species. The genome of *D. carinulata* has been recently sequenced making it an attractive candidate for molecular genetic studies (Stahlke et al 2018; 2022). The recent introduction of *D. carinulata* and the maintenance of the ancestral CDL over the northern portion of the introduced range (Fig 4) are also valuable attributes for use of this experimental system. There is a rich history of inquiry into the molecular mechanisms of photoperiodism and diapause regulation (Saunders 2002, Bradshaw and Holzapfel 2001a; Emerson et al 2009) which provide a collection of genes that may be critical in the evolution of the diapause response (Ragland et a 2019). Genes associated with diapause induction and termination have been identified using Genome Wide Association (GWA) and quantitative trait loci (QTL) mapping studies (Ragland et al 2019; Kozak et al 2019). Butterfly populations collected from the wild have been investigated using GWA (Pruisscher et al 2018, 2021) have been used to pinpoint loci of large effect in diapause evolution, providing a case study using non-model organisms (Pruisscher et al 2018, 2020). While progress has been made in understanding the underlying genetics of diapause evolution, there is a call for more

integration of functional and evolutionary studies of diapause genetics (Ragland et al 2019), and work on this topic using diverse study systems made tractable through newly available molecular techniques (Denlinger et al 2017, Saunders 2020). The *Diorhabda-Tamarix* system offers a system amenable for study of the mechanisms underlying phenology as well as the evolution of diapause cues (Chmura et al 2019; Stahlke et al 2022).

Evolution of Host Plant Relations

The rapid evolution of CDL has enabled *D. carinulata* to move into regions with some of the densest *Tamarix* stands in North America while expanding voltinism to undergo as many as eight generations per season (Fig 27) setting up possible shifts in agent/target host plant relations. The impact of biological control in the southern range of tamarisk may be greater than has been recorded in the more northern range, where mortality averages about 30% and canopy biomass reduction averages about 60% (Kennard et al 2016). Two factors could play into elevating impact; increased seasonal herbivory, including multiple defoliations by *D. carinulata* that have become multivoltine, and a higher representation of the *T. chinensis* genetic background within the admixture of *T. chinensis* x *T. ramosissima,* which results from hybridization and introgression between these species in in North America (Gaskin and Kazmer 2009). It has been shown that *T. chinensis* is less tolerant of defoliation by *D. carinulata* (Williams et al 2014) and that *T. chinensis* may be more susceptible to mortality following extended herbivory (Hultine et al 2013). This could be due to less resource allocation into root reserves in *T. chinensis* (Hultine et al 2013; Williams et al 2014). The genetic diversity found in tamarisk in North America (Gaskin and Schaal 2003; Gaskin and Kazmer 2009) and the fitness impact of multiple defoliations per season will likely provide a setting for eco-evolutionary dynamics (Schoener 2011) to act within the *Tamarix-Diorhabda* system on both *Diorhabda* as well as the host plant tamarisk (Long et al 2017).

CDL evolution and *Tamarix* management

The LCRB downstream of Lake Mead has dense stands of tamarisk including extensive infestations on three National Wildlife Refuges (Fig 22). These infestations were formerly out of the range of the northern tamarisk beetle (Bean et al 2007a) but following CDL evolution *Tamarix* defoliation is common in the LCRB (Nagler et al 2014; Hultine et al 2015). Informed management will require knowledge of the projected evolutionary trajectory of the biocontrol program (Thrall et al 2011) with evolution of *D. carinulata* phenology factored into long-term trajectories of tamarisk density and impact (Gonzales et al 2020).

7. Quantitative prediction of the optimal critical photoperiod for insect diapause based on climate and latitude

Introduction

Life history traits vary over space and time as natural selection pares distributions to better match environmental constraints. Adaptation to local environment may enable faster population responses to change when traits can evolve to track novel conditions. While no population is likely to have optimal traits for each environmental fluctuation, gradients in phenotypes across space emerge as long-term fitness determines trait variation between populations. We model how a relatively labile trait, photoperiod thresholds for diapause, would vary across geographic variation in climate and environmental cues to optimize population growth rates. In a comparison with documented rapid evolution in these traits, we ask whether this model predicts the observed trait divergence over a timescale of decades.

Insects with facultative diapause, which allows for multiple generations, commonly use day length as a cue to switch between reproductive and diapause states in temperate biomes (Danilevskii 1965, Tauber et al. 1986). The switch typically occurs towards the end of summer, before conditions worsen, when a photoperiod-sensitive life stage is exposed to day lengths shorter than a threshold which is genetically determined (Bradshaw and Holzapfel 2008). Photoperiodic responses are an example of both adaptive phenotypic plasticity, with reproductive or diapause phenotypes expressed from the same critical photoperiod, and a local adaptation that varies geographically in accordance with the environment's seasonality and latitude (Simons 2011). The emergent outcome of diapause decisions—the number of generations completed in a year, or voltinism—is a key life history trait that determines insect fitness in seasonal environments (Roff 1980, Wagner et al. 1985). The evolutionary responses to a variable environment diversity in voltinism across latitudinal or temperature gradients within single species, including partial generations when the population is split between diapause and reproduction (Danilevskii 1965, Lindestad et al. 2019, Joschinski and Bonte 2019).

In cases of rapid warming or range expansions into new climates, diapause decisions may follow less informative or maladaptive cues and attempt a number of generations not matched to the seasonal window for development (Van Dyck et al. 2015, Grevstad and Coop 2015). Mismatches between attempted voltinism and the growing season length can cause high mortality in late-season "lost" generations, called developmental traps due to the maladaptive response to environmental cues (Van Dyck et al. 2015). With too few generations attempted due to early diapause, insects may have insufficient energy reserves to span the long wait for more favorable conditions, as has been observed in biocontrol agents (Bean et al. 2007a). In unpredictable seasonal environments, the number of generations that matches the annual conditions may change and choosing to reproduce has a variable value for fitness depending on the year (Kivelä et al. 2016). Using a lifecycle model and historic climate data, we compare the photoperiod response needed to maximize fitness over many years to see how annual differences in voltinism

and fitness consequences compound to estimate the optimal photoperiod responses for different locations.

We apply the model to two classical biological control agents whose critical photoperiod has diverged geographically since their introduction into North America.

Our motivation for predicting voltinism matching and its consequences comes from the field of classical biological control of invasive weeds, where nonnative specialist insect herbivores, usually from one or a few source locations in the native range, are introduced purposefully to novel conditions with potential for voltinism mismatches (Grevstad and Coop 2015). If we knew what the optimal day length threshold is for a particular insect's lifecycle when placed into a new environment, we could better predict population growth and herbivory impacts from an introduced agent with known photoperiod responses. Although climate matching has a long history in purposeful introductions, voltinism matching is rarely considered before introductions due to the difficulty of predicting the complex interactions of annual temperature variability, insect developmental phenology, photoperiod cues varying seasonally and across latitudes, and distributions of day length thresholds within the population.

With an individual-based insect lifecycle model of two classical biological control agents, we examine the voltinism expected across spatial and annual variation in both temperature and environmental cues. After we model the optimal critical photoperiod for diapause that may evolve by natural selection, we use two recent studies to validate its predictions against growth chamber experiments that measured rapid divergences in photoperiod responses across 10° latitude.

Methods

Study species

We model two widespread Chrysomelid beetles introduced as classical biological control agents for exotic weeds in the United States. They have similar facultative multivoltine lifecycles with a short-day diapause response, in which a day length cue sensed during the teneral adult stage determines whether they develop for reproduction or diapause (Wepprich and Grevstad 2021; Velarde et al. 2002, Bean et al. 2007b). Beetles either lay eggs to initiate a new generation or prepare physiologically to enter winter in a diapause state in the adult life stage. In mid-winter, independent of day lengths, diapausing adult beetles become responsive to warmer temperatures, resume development, and emerge as reproductive adults in the spring. All life stages advance after fulfilling accumulated degree-day requirements that are based on temperature-dependent development rates multiplied by the daily temperature available within species-specific thresholds (Chuine and Régnière 2017).

Galerucella calmariensis L., the black-marginated loosestrife beetle, was introduced in 1992 across the United States and Canada as a classical biological control agent for purple loosestrife (*Lythrum salicaria*), a nonnative wetland perennial introduced from Europe more than 200 years ago (Stuckey 1980, Hight et al. 1995). *Galerucella calmariensis* populations established across

North America from two sources in Germany at 50 and 54° latitude (Hight et al. 1995). Establishment at some southern latitudes failed, such as in California below 39° latitude (Pitcairn 2018).

Diorhabda carinulata Desbrochers, the northern tamarisk beetle, was released in 2001 in the western United States as a classical biological control agent for Tamarisk (*Tamarix* spp.), a nonnative shrub that establishes monocultures in riparian habitat (Lewis et al. 2003, DeLoach et al. 2003). With original stock collected in China and Kazakhstan near 44° latitude, northern populations in the United States readily established while southern populations below 38° latitude did not because they entered diapause too early in the summer (Lewis et al. 2003, Bean et al. 2007a). The beetles subsequently expanded their range southward, evolving a shorter critical photoperiod as they went (Bean et al. 2012).

Study sites

We modeled *G. calmariensis* at six sites spanning 9.4° latitude where populations have established (Fig. 29). These populations have different histories, with some relatively unaltered since the introduction of German stock in the first 1992 releases (Oregon and Washington sites) and others requiring multiple introductions across years with beetles from other states (McArthur, CA 1998-2002 and Palermo, CA 1998-2006) (Pitcairn 2018, Wepprich and Grevstad 2020).

We modeled *D. carinulata* at 12 sites spanning 11.8° latitude with a wider range of years when populations were established. Populations Wyoming, Nevada, and Utah were the result of releases made in 2001. Populations to the south of these including the Virgin and Colorado Rivers were the result of range expansion by way of natural dispersal (Nagler et al. 2014, Bean et al. unpublished). The southernmost sites have had populations established for only a few years, following rapid dispersal from Princess, NV since 2017 (Bean et al. unpublished).

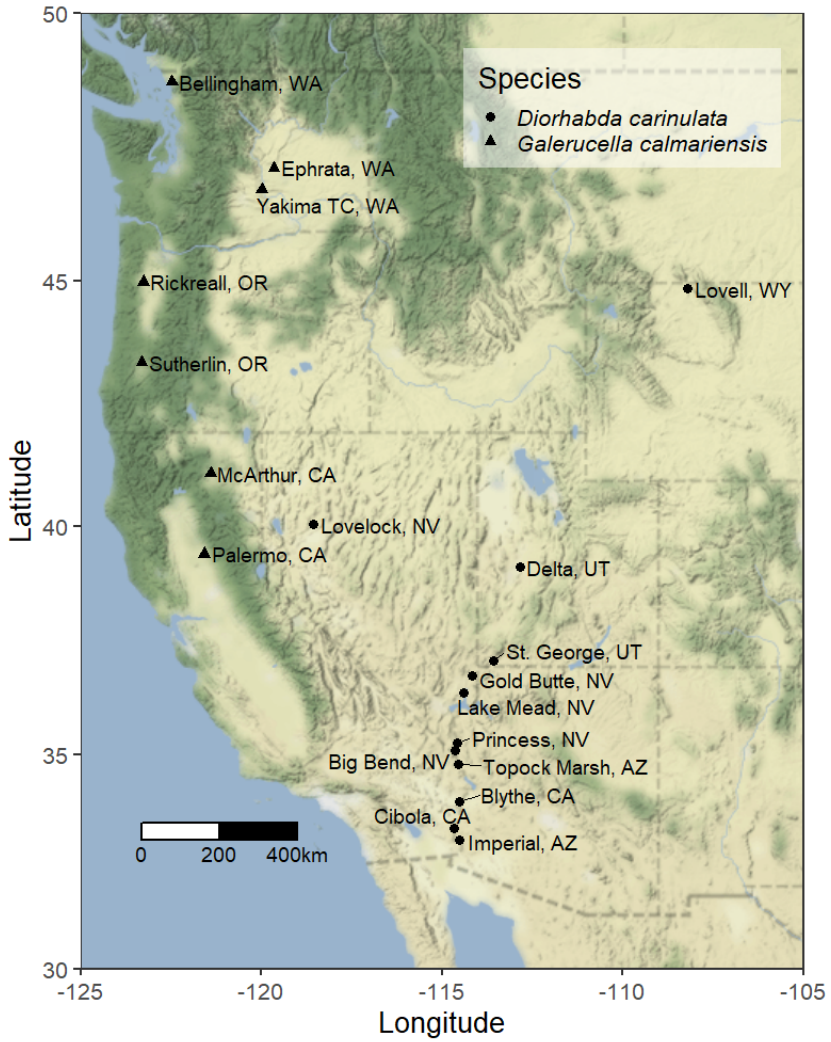

Figure 29. Locations in the western United States modeled in this study. Map tiles by Stamen Design, under CC BY 3.0. Data by OpenStreetMap, under ODbL. Plotted with the ggmap R package (Kahle and Wickham 2013).

Environmental data

Daily growing degree-days were estimated using the single-sine method from the daily temperature range and the species' developmental thresholds (Allen 1976). We used interpolations of daily minimum and maximum temperatures from weather stations with gridded climate data from Daymet (Thornton et al. 1997, 2017). The hours of daylight were calculated based on latitude, day of year, and an assumed twilight that extends day length until the sun is 1.5 degrees below the horizon (Forsythe et al. 1995). We included weather from 1992-2018 for *G. calmariensis* sites and 1999-2018 for *D. carinulata* sites to match with the time after the beetles' releases.

Individual-based model

Individual-based models provide a mathematically simple representation of insect populations with realistic biological mechanisms (Chuine and Régnière 2017). We simulate individual lifecycles from springtime adult emergence through one or more generations, dictated by facultative diapause decisions induced by day length cues. We include individual variation in development time for each life stage and the day length thresholds for diapause. In aggregate, we measure the effects of lifecycles traits and their interactions on population voltinism and demography across the observed variation in temperature and day length at each site and year.

Model parameters were informed by published studies on temperature-dependent development or field observations with values and references for each parameter in

. We reanalyzed temperature-dependent development rates from published studies to estimate a single lower development threshold using linear regression to use a common degree-day timescale for all life stages. The upper development thresholds were set at temperatures with high mortality in rearing experiments (McAvoy and Kok 2004, Herrera et al. 2005). Individuals (all females) tracked accumulated degree-days from January 1 to determine their progression between life stages. Degree-day requirements for spring emergence and initiation of oviposition by overwintered adults were assigned from a skewed normal distribution with mean and variance estimated from field studies. Females in this parental generation were all reproductive and assumed to have one egg each, as we did not have information about overwintering fecundity and the number of subsequent facultative generations would have a larger impact on demography. For filial generations, we assigned stage-specific time requirements in degree-days and day length thresholds to each simulated individual by sampling from normal distributions. We assumed that adult beetles must complete a pre-oviposition or pre-diapause stage before successfully reproducing or entering diapause, although most studies only measure pre-oviposition time requirements. We tracked the timing (day of year and accumulated degree-days) of lifecycle transitions for each simulated individual across all generations if reproduction occurred.

Table 8. Model parameters in individual-based models of beetle lifecycles. Above, parameters for each species were used in all model runs, accounting for degree-day requirements through life stages and individual variation. Below, parameters that varied in models to test for the trait values that maximize full-season population growth rates.

Parameters	***Galerucella calmariensis***	**Notes/References**	***Diorhabda carinulata***	**Notes/References**
Lifecycle parameters used in all models				
Lower developmental threshold (°C) for egg through pre-oviposition	12.2	Reanalysis of (McAvoy and Kok 2004) from egg through pre-oviposition	12.0	Reanalysis of (Herrera et al. 2005) for egg through pupa.
Upper developmental thresholds (°C)	30	Mortality at this treatment (McAvoy and Kok 2004)	40	Mortality at this treatment (Herrera et al. 2005)
Life stage degree-day requirement (mean)	Egg: 87.8 Larva: 128.2 Pupa: 126.0 Pre-ovip: 72.9 Total: 414.9	Derived from (McAvoy and Kok 2004) by mean percent time in stage x total time	Egg: 91.4 Larva: 176.7 Pupa: 174.0 Pre-ovip: 47.2 Total: 489.3	(Herrera et al. 2005), pre-oviposition from (Lewis et al. 2003) at one temperature.
Life stage degree-day requirement (variation)	SD = 5% of egg-through-larva degree-day mean	Simulated data SD 5-10% (McAvoy and Kok 2004)	SD = 5% of egg-through-adult degree-day mean	Simulated data SD 3-4% from (Herrera et al. 2005)
Overwintering adult emergence and oviposition	Skew normal (mean = 120, SD = 25, xi = 3)	Emergence and oviposition observations in Rickreall, OR (Fritzi Grevstad, pers.), oviposition length in (McAvoy and Kok 2004)	Skew normal (mean = 100, SD = 25, xi = 3)	First adult emergence in Grand Junction, CO 2012-2016 (Dan Bean, pers.), oviposition length at one temperature (Lewis et al. 2003)
Reproductive adult oviposition timing	Poisson(15) degree-days	Assumption	Poisson(15) degree-days	Assumption

Photoperiod sensitive stage	1st day of adult stage	Teneral adult (Velarde et al. 2002)	1st day of adult stage	Teneral adult (Bean et al. 2007b)
Overwintering generation fecundity	$\lambda = 1$	Assumption	$\lambda = 1$	Assumption
Lifecycle parameters varying in models to test for optimal traits				
Day length threshold for diapause (mean)	10 to 20 hours at intervals of 0.25	Mean of normal distribution, =critical day length	8 to 17 hours at intervals of 0.25	Mean of normal distribution, =critical day length
Day length threshold for diapause (variation)	0 to 1.5 hours at intervals of 0.25	Standard deviation of normal distribution	0 to 1.5 hours at intervals of 0.25	Standard deviation of normal distribution
Between-generation fecundity	$\lambda = 1.5$, 2, or 2.5	Assumption	$\lambda = 1.5$ or 2	Assumption
Diapause survival rate (penalty for early diapause)	0-15% mortality per 1000 degree-days at intervals of 5%	No data, assume range similar to *D. carinulata*	0-15% mortality per 1000 degree-days at intervals of 5%	27% mortality rate over 55 days (Lewis et al. 2003)

Seasonal changes in day length exposure (varying by latitude and day of year) and degree-day accumulation (varying by site and year) determined the timing and outcome of diapause decisions in our model, which we visualize for a *G. calmariensis* example with a photothermograph in Figure 30. Using individual variation in day length thresholds, instead of a single critical day length, results in partial generations that include both reproductive and diapausing individuals occurs in real field populations (Lindestad et al. 2019, Kerr et al. 2020). On the first day of the photosensitive stage, teneral adults are reproductive if the day length is longer than their assigned threshold (Fig. 30a). For each generation, we tracked the proportion of reproductive adults and the outcome of the offspring, which could either fit within the season's degree-days or be lost to mortality if winter came before reaching the adult diapause stage (Fig. 30b). Only diapause adults contribute to the annual population growth rate in this model, because we assume non-diapause insects would not overwinter successfully. Day length thresholds within a population may be mismatched for a site, with too low (top row) or too high (bottom row) thresholds resulting in lost generations or early diapause, respectively (Fig. 30). We included a penalty for early diapause by decreasing diapause survival by the degree-days elapsed before winter, giving high mortality if diapause occurred in spring (Bean et al. 2007a). We estimated annual population growth rate, our measure of fitness across all generations, by dividing the final number of individuals in diapause, with each multiplied by their diapause

survival rate, from the parental generation size at the simulation start (Taylor and Spalding 1988). We measure voltinism, with partial generations, with a weighted mean of the generation number for each individual at the end of the year (Kerr et al. 2020), which can include only those that *completed* their lifecycle and entered diapause or all that *attempted* a generation (successfully or not).

2500

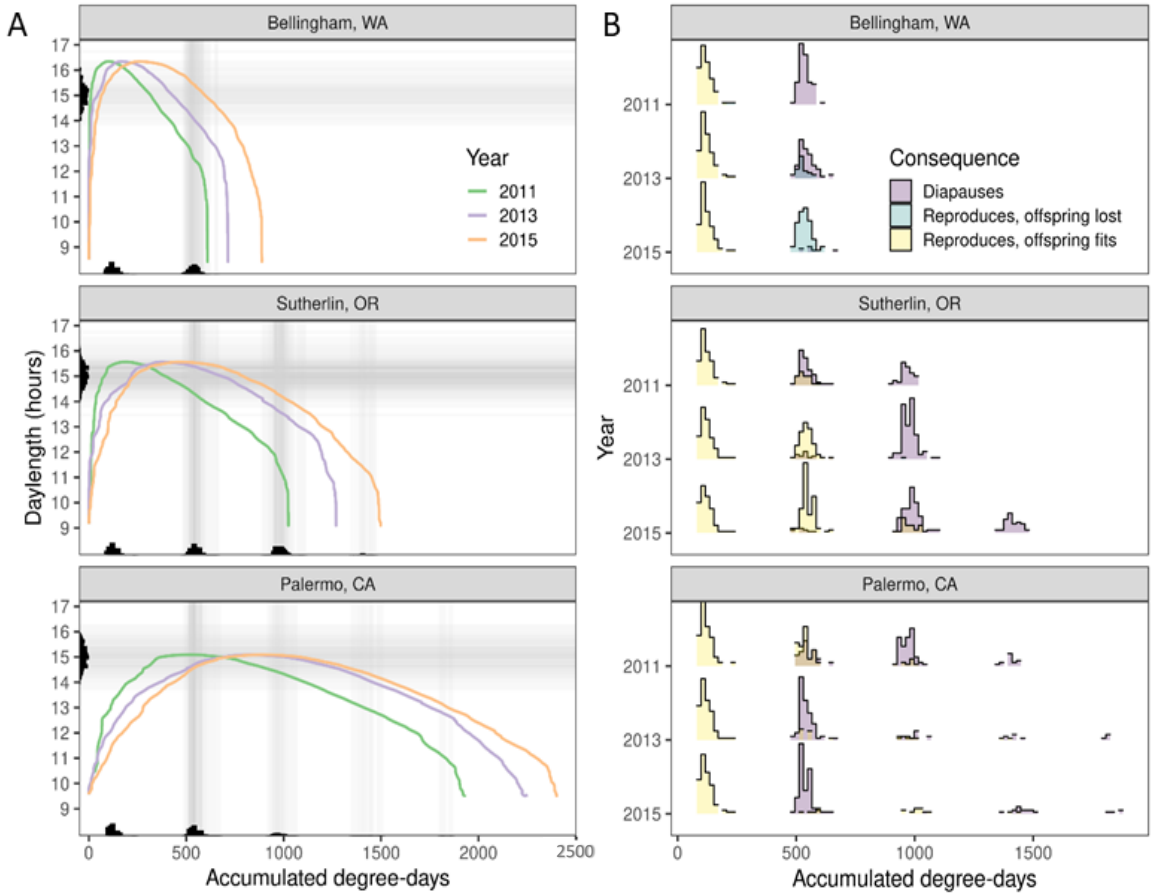

Figure 30. Photothermograph plots demonstrate voltinism in populations with individual variation in development time and critical photoperiod. (A) Plotted curves of day length as a function of accumulated degree-days. When the day length is longer than an individual's critical photoperiod (represented by histogram on y-axis) at the time when the sensitive stage emerges (represented by histograms on x-axis), that individual develops to reproduce; when shorter, it develops to diapause. (B) Newly emerged adults in each generation fall into three categories: those that reproduce successfully (offspring complete development within the season's available degree-days), those that reproduce unsuccessful (offspring cannot complete development within the remaining degree days), and those that enter diapause. Day length thresholds may be mismatched for a site's conditions, with too low (top row) or too high (bottom row) distributions resulting in lost generations or early diapause, respectively.

Optimal photoperiodic response

We systematically varied the parameters for the day length threshold distribution within the population (mean and standard deviation) and for two other lifecycle parameters that could affect

the photoperiod response—between-generation population growth rates and the penalty for earlier diapause (Table 8). Lower day length thresholds, when a greater proportion reproduces, would have a larger fitness payoff under higher population growth rates between each generation or higher fitness costs for early diapause, and vice versa. For each year of climate data for each site, we ran simulations with all possible combinations of the varying parameters. After recording the proportions of individuals from each generation entering diapause, reproducing successfully, or reproducing unsuccessfully, we calculated the annual population growth rate and voltinism.

The optimal mean critical photoperiod was considered to be the one that maximized the geometric mean of the annual population growth rates. With a geometric mean, the sequential order of the years does not matter because the simulation resets with new individuals at the beginning of each year. For each site, we compared the optimal photoperiod response across all years to the annual variation in the best day length threshold in any given year separately. The effects of three varying parameters and their interactions (standard deviation of day length threshold, between-generation growth rate, and early diapause penalty) on the estimated optimal mean day length threshold were assessed by linear regression.

Growth chamber experiments

In both species, recent studies have demonstrated divergence across populations in their critical photoperiod, or the day length exposure at which half the population enters the diapause pathway (Bean et al. 2012, Wepprich and Grevstad 2020, Bean et al. ms.). Although we lack reciprocal transplant experiments to prove that these genetic differences are local adaptations, we compare the photoperiod responses documented in growth chamber experiments to our model estimation of optimal day length thresholds for the environment at each study site.

Briefly, adults were collected from our study sites to establish laboratory colonies used for growth chamber experiments. Beetles completed at least one generation in a common environment before we assigned newly hatched eggs to growth chambers under different photoperiod treatments to complete development. For *G. calmariensis*, these treatments ranged from 14:30 to 17:00 hours of day light at constant 23°C. For *D. carinulata*, these treatments ranged from 11:05 to 15:20 hours of day light at fluctuating day/night temperatures of 35/15°C. Once adult beetles had completed their pre-oviposition or pre-diapause requirement, we scored them as reproductive or diapause by either surgical (*D. carinulata*) or behavioral (*G. calmariensis*) assessments. For our comparison with the modeled optimal photoperiod response, we limited our analysis of growth chamber experiments to the most recent year beetles were collected at each site (2018 for *G. calmariensis*, ranges from 2014 to 2019 for *D. carinulata*).

Beetles from each site and year were analyzed separately for the response of diapause proportion to photoperiod treatments. We used generalized linear models with a binomial error distribution and probit link function weighted by the number of beetles in each sample. Coefficients from these models were transformed to obtain the means and standard deviations of normal distributions of the day length thresholds used by individual beetles in different populations. All simulations, analysis, and visualization was performed in R 3.6.2 (R Core Team 2019).

Results

Based on the model output, the optimal mean critical day length that would maximize long-term annual population growth rates varies by 5.5 hours (13-18.5 range) for *G. calmariensis* sites spanning 9.4° latitude and by 5 hours (11-16 range) for *D. carinulata* sites spanning 11.8° latitude. In general, the optimal mean day length threshold increases with latitude with both exposure to longer days and shorter growing seasons requiring earlier entrance into diapause (dashed vertical lines, Fig. 31). Except for Bellingham, WA where the population would always be univoltine, annual variation in temperature can lead to different voltinism (and annual population growth rates) each year at the same optimal day length threshold (solid gray lines, Figure **2** 31). A range of photoperiod responses could lead to long-term positive population growth, especially for more southern locations that typically would have more generations per year (solid black lines, Figure 2).

The mean annual population growth rates at the optimal day length threshold are higher when the standard deviation is zero, with all individuals using the same threshold. Greater variation in the distribution of day length thresholds increases the optimal mean day length threshold at high latitudes but decreases it at low latitudes (Fig. 32). At higher latitudes, greater variation leads to more individuals with too low of day length threshold that never are cued to diapause and do not contribute to population growth (top row, Figure 32). Increased variation at more southern sites could mean the difference between positive and negative long-term population growth at lower mean day length thresholds (bottom row, Figure 32).

Increasing the between-generation population growth rate lowers the optimal mean day length threshold and increases annual population growth rates for any set of parameters that had multivoltine populations. The penalty for early diapause does not alter the optimal mean day length threshold and its impact on annual population growth rates is negligible.

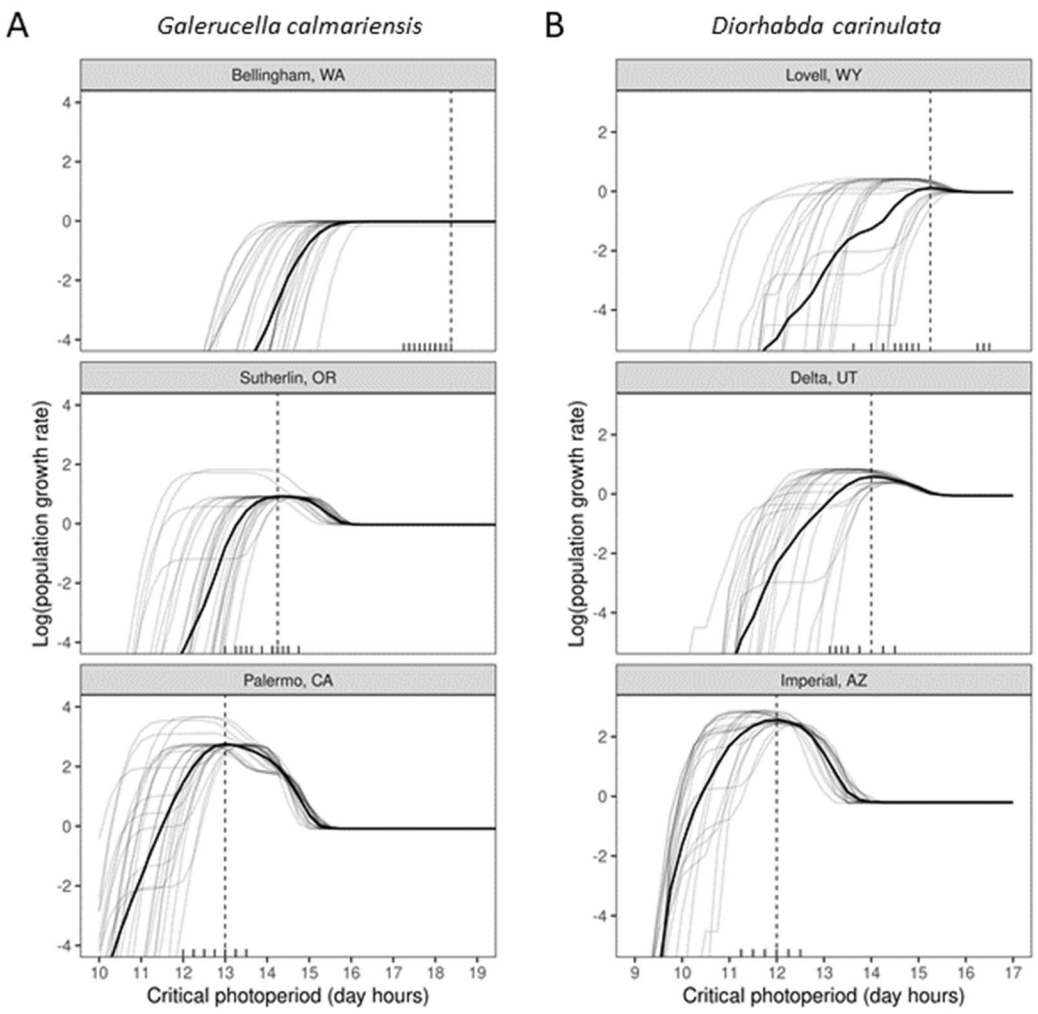

Figure 21. Annual population growth rates modeled across varying mean critical day length. The solid black line represents the geometric mean of annual population growth rates at different day length thresholds, with its optimal trait across all years shown by the dashed vertical lines for each species and site. Geometric means are derived from each year's population growth rate projected for varying day length thresholds (solid gray lines). Each year may have a different optimal critical photoperiod, shown by the tick marks above the x-axis. As modeled, the only way for log (population growth rate) to exceed zero is if the population has more than one generation. Sites for each species are arranged from northern sites (top row) with typically univoltine populations to southern sites (bottom row) with many generations attempted if the day length threshold is sufficiently low. This figure uses intermediate values of the parameters for day length threshold standard deviation, between-generation population growth rate, and penalty for early diapause.

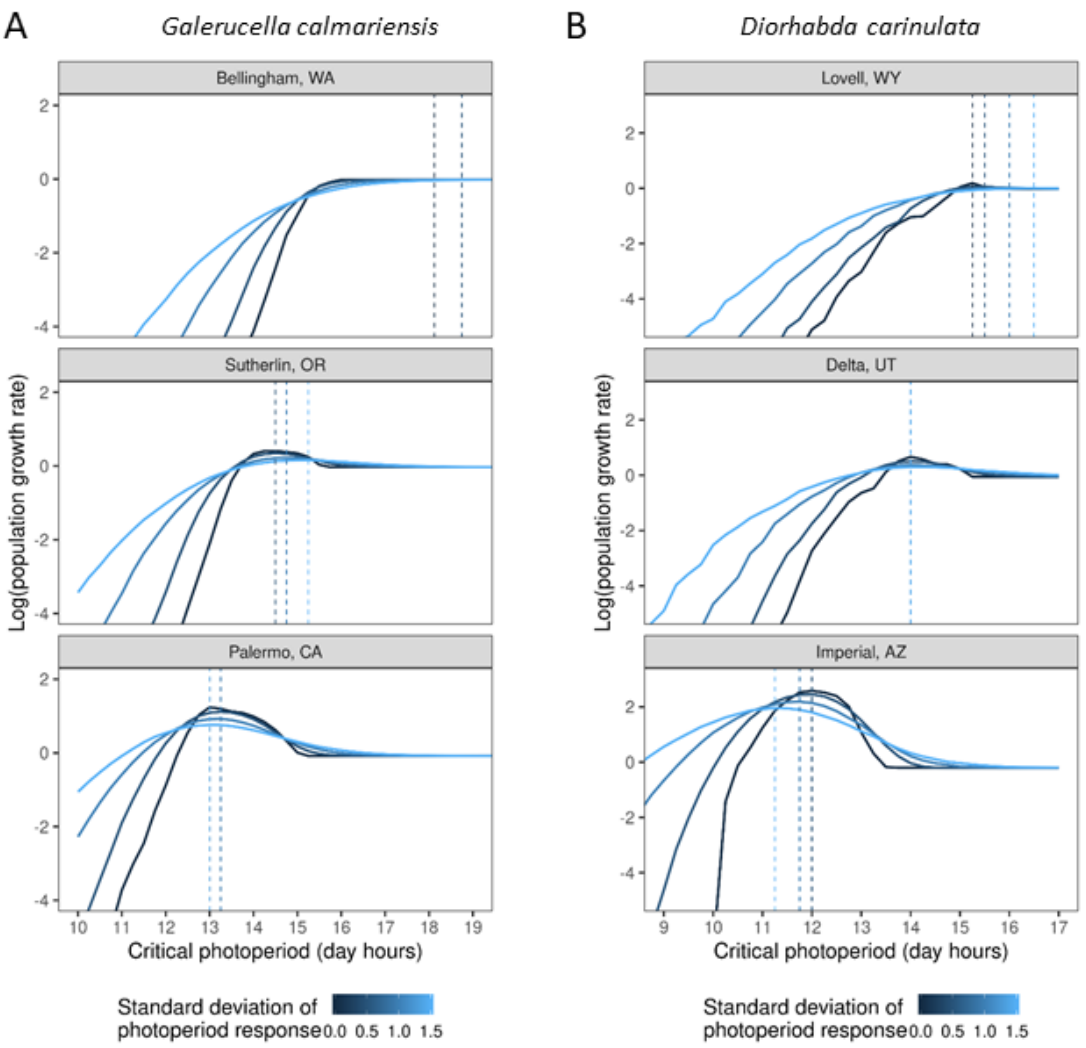

Figure 32. Optimal mean day length thresholds change with the standard deviation. The solid lines represent the geometric mean of annual population growth rates at different day length thresholds, with the optimal trait across all years for different standard deviations of day length thresholds shown by the dashed vertical lines for each species and site. Sites for each species are arranged from northern sites (top row) where greater variation leads to higher optimal critical photoperiods (fewer generations attempted) to southern sites (bottom row) where greater variation leads to lower optimal critical photoperiods (more generations attempted).

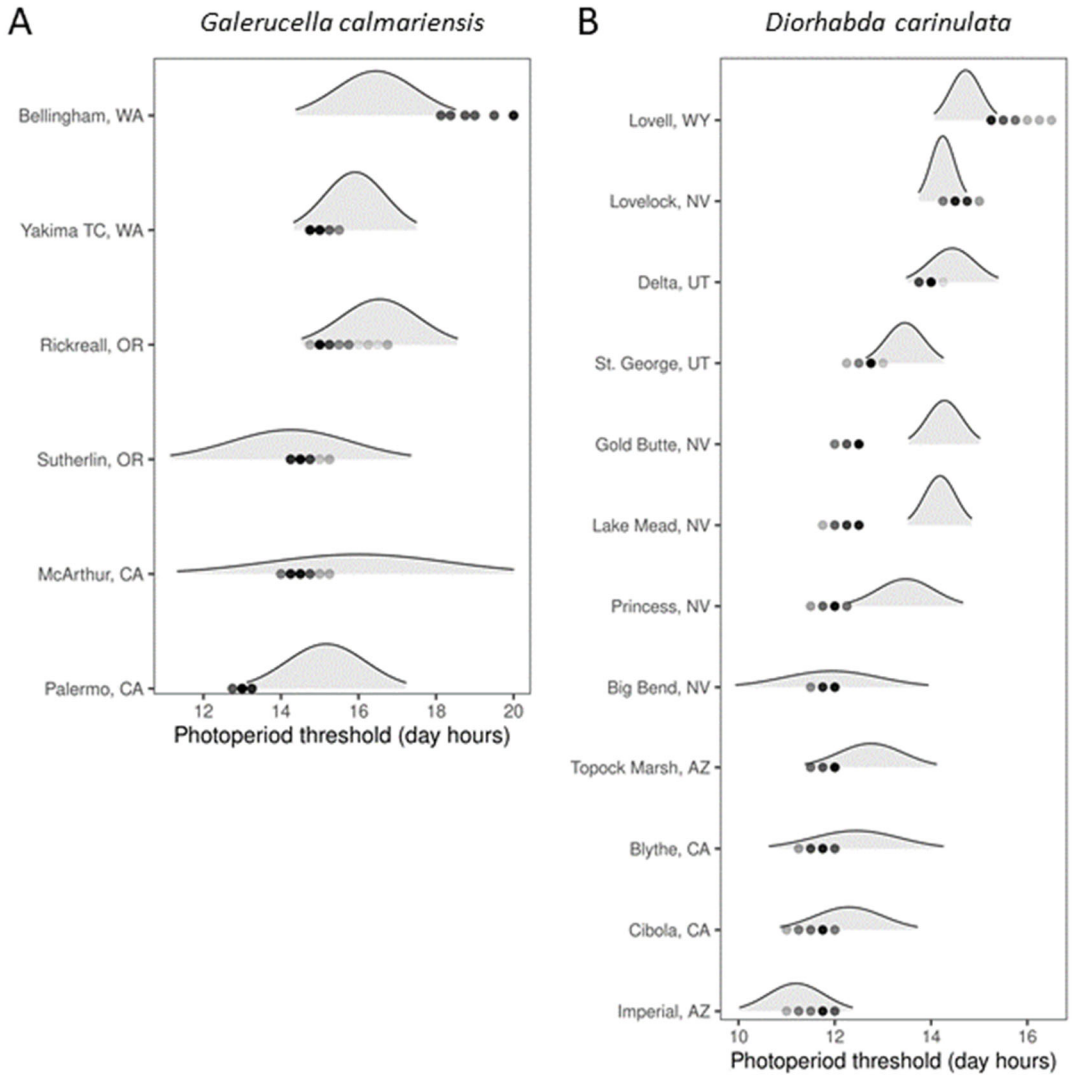

Figure 33. Comparison of modeled optimal traits to distributions of day length thresholds measured with growth chamber experiments. Dots show the modeled optimal mean day length threshold that maximizes population growth rates across all years. Each translucent dot represents one parameter set and darker dots show thresholds selected in multiple sets. Shaded distributions show the normal distributions (95% of density) of day length thresholds estimated for beetles collected from these sites with growth chamber experiments measuring photoperiod-based diapause responses. Sites are arranged from north to south for each species starting with the top row.

Both beetle species have smaller ranges in mean day length thresholds between locations in the growth chamber experiments compared to the model predicted optima (**Error! Reference source not found.** 32). The standard deviation of day length thresholds varies across populations in the growth chamber experiments. Although *D. carinulata* day length threshold distributions are broader at locations that are more southern, this relationship is not as clear in *G. calmariensis* distributions. The model generally over-predicts day length thresholds at higher latitudes and under-predicts day length thresholds at lower latitudes. Different sets of model

parameters lead to optimal threshold predictions that varied within locations but maintain similar latitudinal gradients across locations (Fig. 32). The model predicts locations where the growth chamber mean day length threshold deviates from the monotonic gradient across latitudes for *G. calmariensis* at Rickreall, OR and McArthur, CA (Fig. 32).

Discussion

We demonstrate an insect lifecycle model that predicts how optimal photoperiod responses that induce diapause vary geographically based on annual temperature variability and developmental traits. The day length thresholds that maximize long-term population growth rates show similar patterns to the recently diverged photoperiod responses for two biological control agents, supporting that their rapid evolution is local adaptation. While traits in introduced beetles would not be expected to match environmental constraints as closely as native insects, these systems show how quickly insects may adapt to novel climates (Urbanski et al. 2012, Bean et al. 2012, Levy et al. 2015). Even though photoperiod responses are the best documented cases of genetic evolution due to climate change (Bradshaw and Holzapfel 2008), it is not well established whether most phenological changes, including voltinism and diapause, in response to climate warming are adaptive in many insects (Kellermann and Heerwaarden 2019). Predicting how local adaptation varies across the landscape and interacts with environment change will be necessary to assess population performance and vulnerability (Roy et al. 2015, Tsai et al. 2020).

We show in this model how a single trait, the day length threshold for diapause, can regulate annual variation in voltinism and demography. For a defined set of years with known or forecasted temperatures, we could predict the optimal day length threshold and its changes through time or population performance in new locations. Assessments of where insects may be successful invaders, either planned as in biological control or with unwanted nonnative introductions, may benefit from considering day length thresholds and the predicted voltinism matching in the new environment in addition to environmental niche modeling (Grevstad and Coop 2015). For species of conservation concern, these models could help assess whether generations lost due to voltinism mismatches and developmental traps (Van Dyck et al. 2015) are more probable than population increases from additional generations (MacGregor et al. 2019, Kerr et al. 2020).

The simulated latitudinal gradient in the optimal day length threshold across sites (175 minutes per 5° latitude for *G. calmariensis* and 127 minutes per 5° latitude for *D. carinulata*) changes more quickly than the latitudinal gradients in critical photoperiods observed in growth chamber experiments. Although the measured photoperiod responses in these two species have diverged genetically (Bean et al. 2012, Wepprich and Grevstad 2020), they may not reach an optimal response within decades or with fluctuating selection due to annual climate variation. Typical latitudinal gradients in locally adapted populations range from 60-80 minutes per 5° latitude in classic experiments (Danilevskii 1965) or 48 minutes per 5 degrees latitude in a recent meta-analysis of temperate insects (Joschinski and Bonte 2019). Our simulation only tests for the photoperiod cues acting in isolation that would maximize fitness, with diapause decisions

unmodified by factors known to be important like temperature and host plant quality (Abarca 2019). We would expect that insects using multiple cues would have more information when selecting diapause pathways, lessening the relative importance of a single cue like photoperiod (McNamara et al. 2011). Models incorporating heritability and annual fluctuating selection could provide a closer estimate for optimal photoperiod responses than our model averaging growth rates without regard to sequence.

Our model shows that a range of potential day length thresholds could support long-term population viability at locations that fit multiple generations (30). At southern sites, where consecutive generations build up population sizes, the risks of mortality from early diapause or lost generations are overwhelmed by exponential growth. Northern sites in our model had narrower ranges of day length thresholds with positive long-term population growth. Including density-dependent growth rates may limit the benefit of multiple generations. We know that early diapause, the negative consequence of too-high day length thresholds, has prevented establishment of new biocontrol populations when introduced into southern sites (Lewis et al. 2003, Bean et al. 2007a) but it might be infrequently observed in native insects. The opposite mismatch, with too-low day length thresholds and lost generations, could arise from movement to more northern sites in biocontrol insects, as we see steep declines in mean population growth rates at thresholds where more individuals attempt generations without time to complete them (Fig. 31). While multivoltine insects have expanded their populations when adding extra generations (MacGregor et al. 2019), the locations in which expansions or voltinism mismatches occur may shift over time and fluctuate with annual temperature variability (Kerr et al. 2020).

Our individual-based model improves over previous models for this system by incorporating variation in both development time and photoperiod responses. Previous models of *G. calmariensis* voltinism mismatches assumed one critical photoperiod for all individuals and degree-day requirements for each stage that would best model the leading edge of each generation (Grevstad and Coop 2015). Individual variation in this simulation, while slower computationally for large regions, allows for a more complete accounting of partial generations and mismatches in voltinism beyond integer values. The lessons from that model still hold, that moving individuals with maladapted critical photoperiods into different regions can lead to too many or too few attempted generations depending on the specific interactions of the local temperature regime, latitude, and the insect's photoperiod-based diapause decisions.

8. Field Phenology Using Time Lapse Cameras

To be successful and effective, weed biocontrol agents need to align their life cycles with the availability of palatable host plants during the growing season. The timing of appearance of leafy foliage in the spring and the decline in host plant quality at the end of the growing season may have consequences for insects that emerge too early and/or remain reproductive late in the season (in addition to killing frosts and end of degree days). To gain insight to the seasonal "window," we set out stationary time lapse field cameras that visually recorded host plant stages and quality throughout the growing season at six purple loosestrife sites, two Japanese knotweed sites, and three tamarisk sites during 2018 and 2019.

Methods

The locations for purple loosestrife included Bellingham, WA, Yakima Training Center, WA, Camp Rilea, OR, and Palermo, CA, Fort Drum, NY and West Point, NY. The knotweed sites were located at West Point and Fort Drum, NY. The tamarisk sites included two military bases in eastern Colorado--Fort Carson (Army) and the Piñon Canyon Maneuver Site (PCMS, Army) --and a site called Horsethief in a riparian corridor managed by the Bureau of Land Management (BLM). Two cameras were used at most sites, except four cameras were used at Ft. Carson PCMS. The cameras were set up to face north, secured on sturdy metal posts, and programmed to take daily photos from spring through fall. One of two cameras set up at the Yakima Training Center was lost in a brush fire and one camera at West Point tipped over. All others contained data sufficient to determine flowering and senescence timing. After transferring the photographs to computers, they were examined carefully to determine the date of plant senescence for each site. We considered senescence date to be when 50% of foliage had yellowed with 50% green remaining green (Figs. 34 and 35).

We used our model to simulate the lifecycle of biocontrol agents at these sites for the year 2018 to determine how the life cycle aligns with plant phenology and other seasonal events (Fig. 36). In this report, we show the case for *G. calmariensis* at Yakima Training Center. We used a critical photoperiod of 15.9 hours of light (estimated from growth chamber experiments, section 4) for determining whether beetles became reproductive or went into diapause to overwinter (OW Adult). In this case, three generations were able to develop without exposing vulnerable stages to frost or plant senescence though this may not be the case in all years.

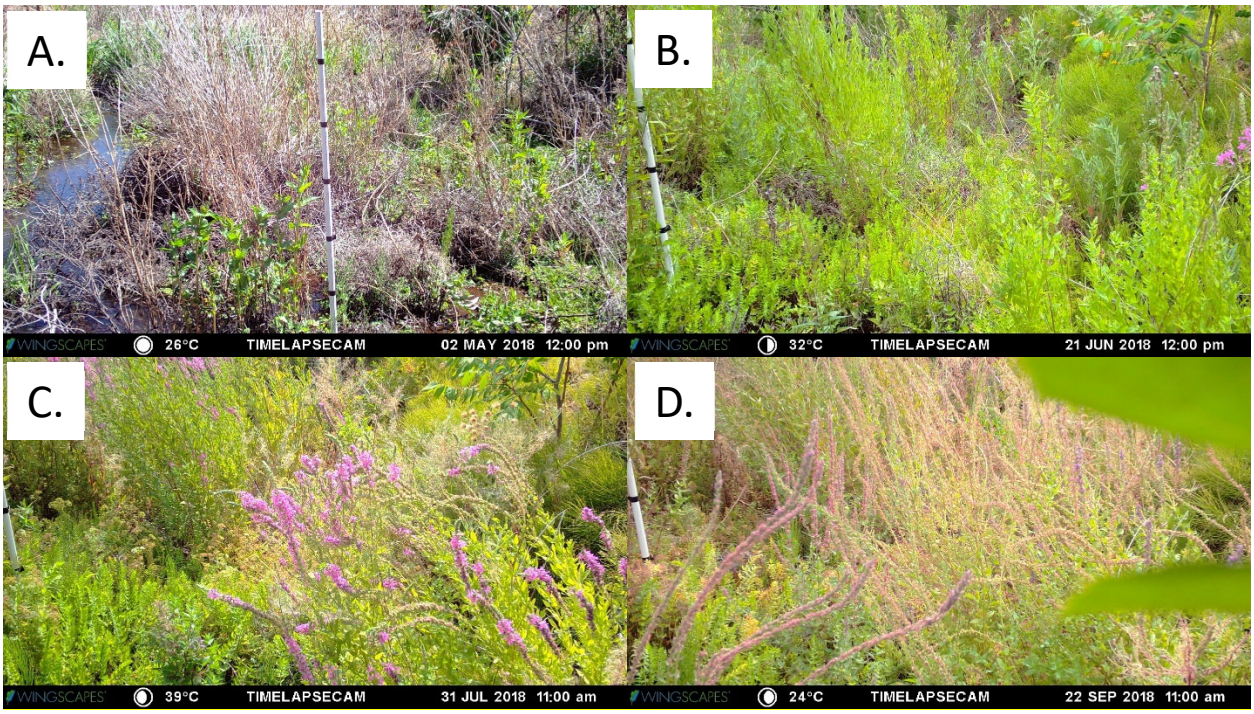

Figure 34. Photographs from time lapse camera set up to document phenology of purple loosestrife plants at the Yakima Training Center field site. Key identifiable phenology events include (A) initial growth of foliage, (B) first flowers, (c) full flower, (D) 50% senesced.

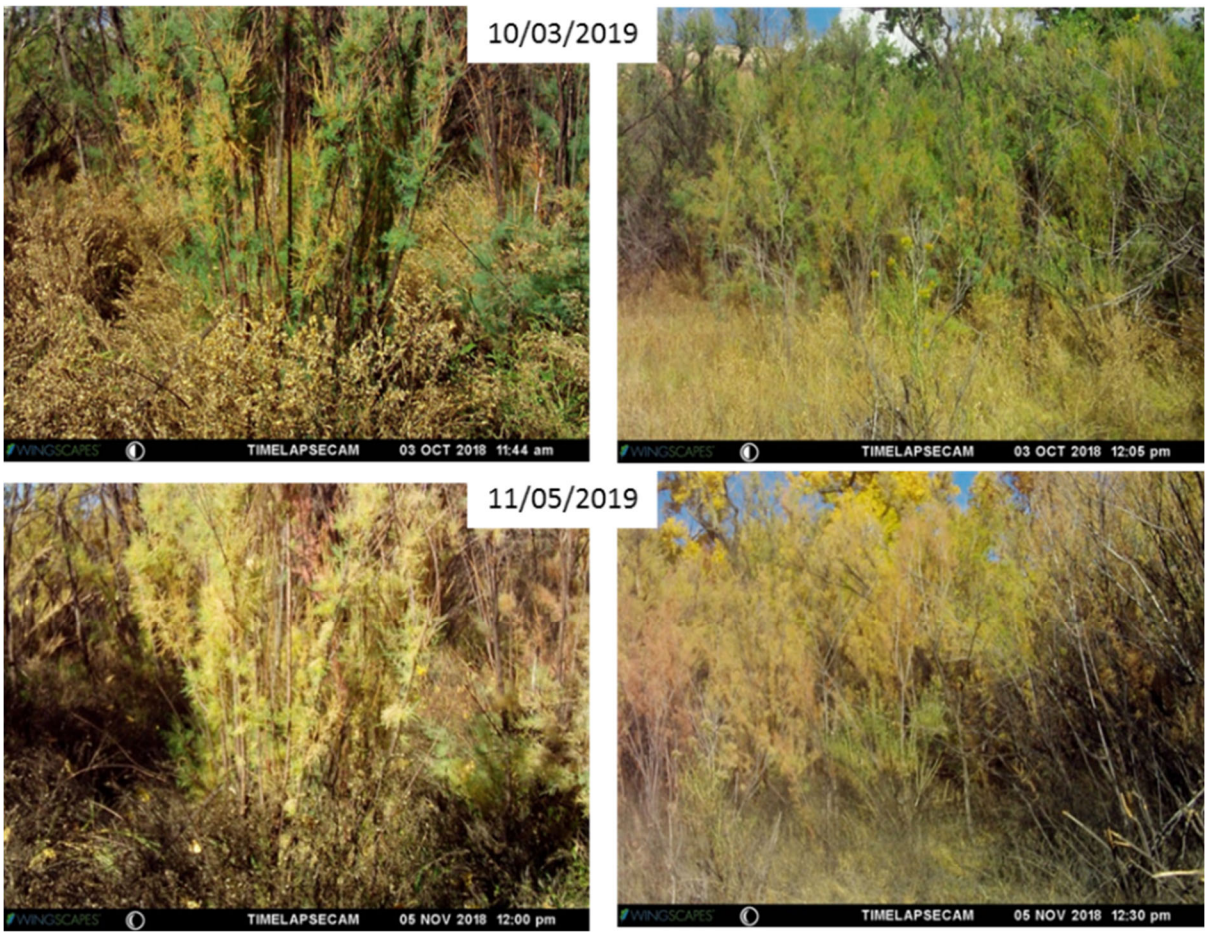

Figure 35. Time lapse photos from the Horsethief site in western Colorado showing the initial stages of senescence recorded on cameras trained on two different tamarisk stands (upper panels) and the same stands about a month later when plants were >50% senescent (lower panels).

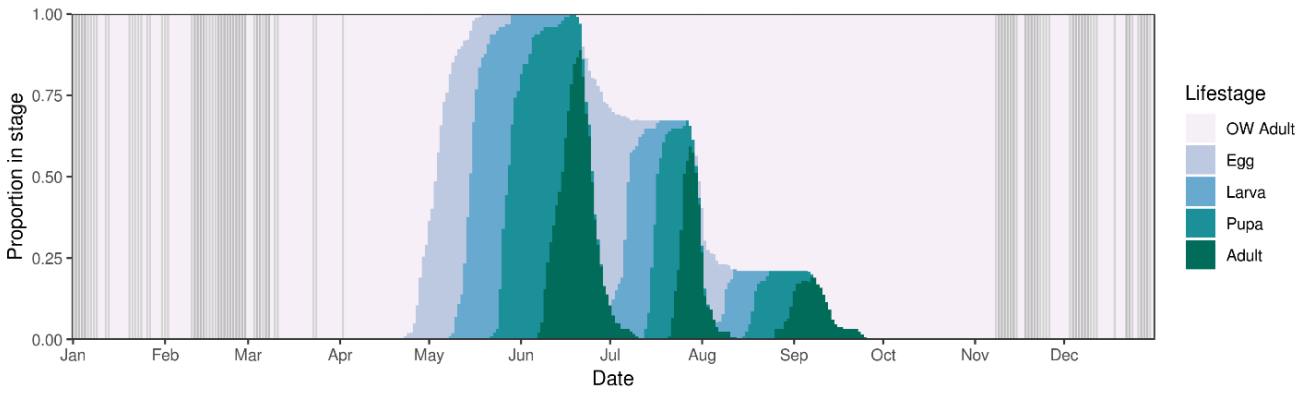

Figure 36. Lifecycle simulation from the stochastic individual-based model for *G. calmariensis* at Yakima Training Center, WA in 2018. Insects emerge from overwinter diapause and a proportion of subsequent generations return to diapause when adults based on the photoperiod. We expect that beetles had two full generations and one partial generation in the field. Vertical lines show days with light (0 °C) and hard (-2 °C) frosts.

Results

From the field photos at the Yakima field site, we can track loosestrife phenology to understand what may limit beetle voltinism (e.g., frost, degree-days, or plant senescence). In late April and early May, when the beetles became active, frost risk had passed, and loosestrife was up to 0.5 m tall for overwintering adults' oviposition. There is no noticeable summer drying in the loosestrife leaves at this site despite there being little summer precipitation. Leaf greenness decreases towards the end of flowering in September and has completed senescence by mid-October (Table 9). Fall frost in 2018 occurred more than a month after all beetles were likely in diapause and the loosestrife had already senesced (Fig. 35). Other sites appear to similarly senesce later than beetles would be active. However, the case for Palermo California is different. That site has a lot of flooding through the winter and early spring. The plants grow rapidly through spring, flower relatively early, and then senesce by early July due to dry conditions in the Central Valley, CA. As pointed out in section 4 (Discussion), the critical photoperiod cuing diapause in this population appears to be under two conflicting selective forces. It needs to be short enough to allow more than one generation, but long enough to end reproduction before the plants senesce in mid-summer.

Tamarisk reached the 50% point for senescence at the Fort Carson site on 10/16/2019. All three functional cameras recorded the same pattern even though trained on tamarisk in two different stands. At the Pinon Canyon Maneuver Site four cameras all recorded 50% senescence on 10/17/2019 while at the Horsethief site in western Colorado senescence, measured using two cameras, was recorded on 11/03/2019.

Table 9. Dates of phenological events as obtained from time lapse cameras set up at purple loosestrife and knotweed sites.

Site	Plant	Year	Camera	Start	End	First Shoots	Height 40 cm	First Flowers	Full Flower	50% Senesced	Flood Events
Palermo	Lythrum	2018	1	29-Mar	31-Dec	29-Mar	8-May	12-Jun	5-Jul	18-Jul	7-Apr, 17-Dec
Palermo	Lythrum	2019	1	1-Jan	11-Nov	30-Mar	14-May	19-Jun	15-Jul	8-Jul	17-Jan, 3-Feb, 26-Feb, 6-Mar, 26-Mar
Palermo	Lythrum	2018	2	29-Mar	31-Dec	29-Mar	27-Apr	16-Jun	26-Jun	4-Jul	7-Apr
Palermo	Lythrum	2019	2	1-Jan	22-Nov	23-Mar	24-Apr	16-Jun	3-Jul	26-Jul	14-Feb, 26-Feb
Bellingham	Lythrum	2019	1	1-Jan	3-Dec	22-Mar	22-May	NA	NA	NA	
Camp Rilea	Lythrum	2018	1	3-May	31-Dec	NA	3-May	NA	NA	25-Jun	
Camp Rilea	Lythrum	2019	1	1-Jan	3-Dec	8-Apr	30-Apr	NA	NA	25-Aug	
Fort Drum	Lythrum	2018	1	11-Aug	31-Dec	NA	NA	NA	17-Aug	10-Oct	
Fort Drum	Lythrum	2019	1	1-Jan	1-Nov	15-May	7-Jun	28-Jul	8-Sep	28-Sep	
Fort Drum	Fallopia	2018	2	12-Aug	31-Dec	NA	NA	27-Aug	12-Sep	6-Oct	
Fort Drum	Fallopia	2019	2	1-Jan	1-Nov	6-May	16-May	22-Aug	12-Sep	5-Oct	
West Point	Lythrum	2018	1	11-Aug	24-Nov	NA	NA	NA	20-Aug	5-Oct	
West Point	Fallopia	2018	2	10-Aug	31-Dec	NA	NA	26-Aug	13-Sep	20-Oct	
West Point	Fallopia	2019	2	1-Jan	1-Dec	21-Apr	24-Apr	15-Aug	NA	NA	
Yakima	Lythrum	2018	1	2-May	16-Nov	NA	2-May	20-Jun	29-Aug	10-Oct	
Yakima	Lythrum	2019	1	1-Jan	4-Dec	5-Apr	2-May	23-Jun	29-Jul	20-Oct	

9. Climate forecasting and prospectus reports for managers

Using model results and information gained from this project, we completed six written reports that were presented to Department of Defense land managers. The reports include decision support tools relating to weed biocontrol and climate change. Customized for each installation, the reports cover model results for biocontrol agents present at the base, including predictions of future phenology and voltinism (based using climate predictions from general circulation models), and recommendations for improved weed management using biological control.

All of these reports can be accessed for viewing and download from https://oregonstate.box.com/s/a9c5fk3yr7spcbtv6dzn7gxizmwsi7is and have also been uploaded into the SEMS system. They were distributed by email to our DoD collaborators at the following military installations and wildlife refuge:

- Yakima Training Center, WA
- Fort Drum, NY
- West Point, NY
- Piñon Canyon Maneuver Site, CO
- Fort Carson, CO
- Yuma Proving Ground, AZ
- Cibola and Imperial National Wildlife Refuge, AZ

For each military installation, our report included the following sections:

1. Introduction
2. Overview of biological control for weeds
3. Biological control agents and their target weeds at the installation
4. Insect photoperiodism and diapause
5. Phenology model
6. Climate variation effects on biocontrol system(s)
7. Phenology predictions
8. How will predicted future climate affect biocontrol systems?
9. Potential strategic redistribution of biological control agents (where appropriate)
10. Potential for evolutionary adaptation
11. Summary and recommendations
12. Literature cited

10. Summary of Project Tasks Completed

Tasks	Status
Model Expansion and Improvement	
Add substage development & photoperiod response (version 1)	Completed as planned
Fully integrate climate forecasting capabilities (version 2)	Completed as planned
Fully calibrate parameters for each biocontrol system	Completed as planned
Field and lab experiments to validate model predictions	
Photoperiod chamber experiments (Aphalara)	Completed as planned
Photoperiod chamber experiments (Diorhabda and Galerucella)	Completed as planned
Field phenology monitoring (phenocams)	Completed as a planned in 2018 and repeated in 2019
Reciprocal transplant experiment (Diorhabda and Galerucella)	Completed as a common garden experiment for *Galerucella* in both 2018 and 2019. *Diorhabda* experiment could not be completed due to mass migration of beetles into the study site.
Apply the model to improve biocontrol effectiveness	
Phenology/voltinism prediction map for Aphalara	Completed as planned
Targeted release and monitoring of *Aphalara* (pending permit)	Permit issued and releases initiated in spring of 2020
Strategic redistribution and monitoring of *Galerucella*	Completed, but with unclear results
Share and encourage the model for use in other systems	
Model vers. 1.0 made available online	Completed as planned
Model vers. 2.0 made available online	Completed as planned
Online model fine tuning and continued support	Completed as planned
Climate change prospectus reports to DOD managers	Completed as planned
Meeting presentations	Completed (see list)
Write up key papers and final report	Completed, with some in progress (see list)

11. List of military installations in regions with the focal weed species

We compiled a list of military bases that are located in regions where our three focal weeds (purple loosestrife, Japanese knotweed, and tamarisk) are common. Not all of these bases have these weed species currently, but all could be considered possibly at risk from these weeds due to their climate and proximity to the weed current distribution.

Tamarisk

Arizona	Davis-Monthan AFB, Tucson
	Ft Huachuca, AZ, US ARMY
	Yuma Proving Ground, AZ
California	Fort Hunter Liggett, CA
	Marine Corps Logistics Base - MCLB Barstow, Barstow, CA
	Naval Air Facility, El Centro, CA
	Edwards AFB, Edwards, CA
	Ft Carson, including the Piñon Canyon Maneuver Site, CO
Colorado	
Nevada	Naval Air Station, Fallon, NV
	Nellis AFB, Las Vegas, NV
	Creech AFB, NV
New Mexico	Holloman AFB, NM
	US Army Garrison, White Sands Missile Range, NM
	Kirtland AFB, NM
Texas	Laughlin AFB, TX

Purple loosestrife and knotweeds

Connecticut	Naval Submarine Base New London
Delaware	Dover AFB
District of Columbia	Joint Base Anacostia-Bolling
	Naval Support Activity Washington
	Pentagon – Air Force/Army
	USCG Base National Capital Region
Illinois	Naval Station Great Lakes
	Rock Island Arsenal
	Scott Air Force Base
	US Army Cadet Command 3rd Brigade
	USAREC, Chicago Battalion
Indiana	Naval Support Activity Crane

	USAREC, Indianapolis Battalion
Maine	Portsmouth Naval Shipyard
	USAREC, New England Battalion
Maryland	Aberdeen Proving Ground
	Fort Detrick
	Fort George G. Meade
	Joint Base Andrews-Naval Air Facility Washington
	Naval Air Station Patuxent River
	Naval Support Activity Annapolis – U.S. Naval Academy
	Naval Support Activity Bethesda Home of Walter Reed National Military Medical Center
	Naval Support Activity South Potomac (NSF Indian Head)
	USAREC, 1st Medical Recruiting Battalion
	USAREC, Baltimore Battalion
Massachusetts	Fort Devens
	Hanscom AFB
	Natick Soldier Systems Center (NSCC)
	Westover ARB
	USCG Base Boston
	USCG Base Cape Cod
Michigan	Hart-Dole-Inouye Federal Center
	USAG Detroit Arsenal
	USAREC, Great Lakes Battalion
Minnesota	USAREC, Minneapolis Battalion
New Hampshire	Portsmouth Naval Shipyard
New Jersey	Joint Base McGuire-Dix-Lakehurst
	Naval Weapons Station Earle
	Picatinny Arsenal
	US Army Cadet Command 2nd Brigade
	USAREC, Mid-Atlantic Battalion
New York	Fort Drum
	Fort Hamilton
	Naval Support Activity Saratoga Springs
	United States Military Academy at West Point
	USAREC, Albany Battalion
	USAREC, New York City Battalion
	USAREC, Syracuse Battalion
Ohio	Defense Supply Center Columbus
	USAREC, Cleveland Battalion
	USAREC, Columbus Battalion
	USCG Base Cleveland
	Wright-Patterson AFB
Oregon	USAREC, Portland Battalion

Pennsylvania	Carlisle Barracks
	Defense Logistics Agency at Susquehanna
	Raven Rock Mountain Complex
	Tobyhanna Army Depot
	USAREC, Harrisburg Battalion
Rhode Island	Naval Station Newport
Virginia	BSU Portsmouth
	Defense Supply Center Richmond
	DLA McNamara HQC
	Fort Belvoir
	Fort Lee
	Fort Myer (Joint Base Myer – Henderson Hall)
	Fort Pickett
	Henderson Hall (Joint Base Myer – Henderson Hall)
	Joint Base Langley-Eustis
	Joint Expeditionary Base Little Creek-Fort Story
	Marine Corps Base Quantico
	MCCS Hampton Roads
	Naval Air Station Oceana
	Naval Air Station Oceana Dam Neck Annex
	Naval Station Norfolk
	Naval Support Activity Hampton Roads Northwest Annex
	Naval Support Activity South Potomac (NSF Dahlgren)
	Naval Weapons Station Yorktown
	Newport News Shipyard
	Norfolk Naval Shipyard
	Surface Combat Systems Center Wallops Island
	USAREC, Richmond Recruiting Battalion
Washington	Fairchild AFB
	Joint Base Lewis-McChord
	Naval Air Station Whidbey Island
	Naval Base Kitsap
	Naval Station Everett
	US Army Cadet Command 8th Brigade
	USAREC, Seattle Battalion
	USCG Base Seattle
Wisconsin	Fort McCoy
	USAREC, Milwaukee Battalion

12. Literature Cited

Abarca, M. 2019. Herbivore seasonality responds to conflicting cues: Untangling the effects of host, temperature, and photoperiod. PLOS ONE 14:e0222227.

Abram, P. K., and C. E. Moffat. 2018. Rethinking biological control programs as planned invasions. Curr. Opin. Insect Sci. 27: 9–15.

Allen, J. C. 1976. A Modified Sine Wave Method for Calculating Degree Daysl. ENVIRONMENTAL ENTOMOLOGY 5:9.

APHIS (2010) USDA APHIS PPQ Moratorium for biological control of saltcedar. http://www.usbr.gov/uc/albuq/library/eaba/saltcedar/pdfs/2010/BeetleMemoUSDA.pdf

Barker, B.S., L. Coop, T. Wepprich, F. Grevstad, and G. Cook. 2020. DDRP: real-time phenology and climatic suitability modeling of invasive insects. PLoS ONE 15: e0244005. https://doi.org/10.1371/journal.pone.0244005

Bartelt, R. J., A. A. Cossé, B. W. Zilkowski, R. N. Wiedenmann, and S. Raghu. 2008. Early summer pheromone biology of Galerucella calmariensis and relationship to dispersal and colonization. Biol. Control. 46: 409–416.

Bateman HL, Paxton EH, Longland WS (2013) Tamarix as wildlife habitat. in: Sher A, Quigley M (Eds), Tamarix: A Case Study of Ecological Change in the American West. Oxford Univ Press 168-188

Bateman, H.L., T.L. Dudley, D.W. Bean, S.M. Ostoja, K.R. Hultine, and M.J. Kuehn. 2010. A river system to watch: documenting the effects of saltcedar (*Tamarix* spp.) biocontrol in the Virgin River valley. Ecological Restoration **28**: 405-410

Bates, D., M. Mächler, B. Bolker, and S. Walker. 2015. Fitting linear mixed-effects models using lme4. J. Stat. Softw. 67: 1–48.

Bean, D. W., P. Dalin, and T. L. Dudley. 2012. Evolution of critical day length for diapause induction enables range expansion of *Diorhabda carinulata*, a biological control agent against tamarisk (*Tamarix* spp.). Evolutionary Applications 5:511-523.

Bean, D. W., T. L. Dudley, and J. C. Keller. 2007. Seasonal timing of diapause induction limits the effective range of *Diorhabda elongata deserticola* (Coleoptera: Chrysomelidae) as a biological control agent for tamarisk (*Tamarix* spp.). Environmental Entomology 36:15-25.

Bean, D. W., T. Wang, R. J. Bartelt, and B. W. Zilkowski. 2007b. Diapause in the Leaf Beetle *Diorhabda elongata* (Coleoptera: Chrysomelidae), a Biological Control Agent for Tamarisk (*Tamarix* spp.). Environmental Entomology 36:531–540.

Beck, S. D. 1983. Insect Thermoperiodism. Annu. Rev. Entomol. 28: 91–108.

Beck, S. D. and J. W. Apple. 1961. Effects of temperature and photoperiod on voltinism of geographic populations of the European corn borer, *Pyrausta nubilalis*. Journal of Economic Entomology 54:550-558.

Beck, S.D. 1980. Insect photoperiodism, 2nd ed. Academic Press, New York, NY.

Beerling, D.J. and H.A. Dawah. 1993. Abundance and diversity of invertebrates associated with *Fallopia japonica* (Houtt. Ronse Decraene) and *Impatiens glandulifera* (Royle): two alien plant species in the British Isles. The Entomologist 112: 127-139.

Bell, G. 2010. Fluctuating selection: the perpetual renewal of adaptation in variable environments. Philos. Trans. R. Soc. B Biol. Sci. 365: 87–97.

Blossey, B. 1995. Coexistence of two leaf-beetles in the same fundamental niche, distribution, adult phenology and oviposition. Oikos. 74: 225–234.

Bolker, B. M. 2008. Ecological models and data in R. Princeton University Press.

Bolker, B. M. 2015. Linear and generalized linear mixed models, pp. 309–333. In Fox, G.A., Negrete-Yankelevich, S., Sosa, V.J. (eds.), Ecol. Stat. Oxford University Press.
Bradshaw WE. 1976. Geography of photoperiodic response in a diapausing mosquito. Nature 262:384–86.
Bradshaw, W.E. and C.M. Holzapfel. 2001. Genetic shift in photoperiodic response correlated with global warming. Proceedings of the National Academy of Sciences 98:14509-14511.
Bradshaw, W.E., and C.M. Holzapfel. 2001. Phenotypic evolution and the genetic architecture underlying photoperiodic time measurement. J. Insect Physiol. 47: 809-820
Bradshaw, W. E., and C. M. Holzapfel. 2006. Evolutionary response to rapid climate change. Science. 312: 1477–1478.
Bradshaw, W. E., and C. M. Holzapfel. 2007. Evolution of animal photoperiodism. Annu. Rev. Ecol. Evol. Syst. 38: 1–25.
Bradshaw, W. E., and C. M. Holzapfel. 2008. Genetic response to rapid climate change: it's seasonal timing that matters. Molecular Ecology 17:157–166.
Campbell, A., Frazer, B.D., Gilbert, N., Gutierrez, A.P. and Mackauer, M. 1974. Temperature requirements of some aphids and their parasites. The Journal of Applied Ecology 11: 431–8. doi:10.2307/2402197.
Carroll, S.P., A.P. Hendry, D.N. Reznick, and C.W. Fox. 2007. Evolution on ecological time scales. Functional Ecology **21**: 387-393.
Carruthers, R. I., C. J. DeLoach, J. C. Herr, G. L. Anderson, A. E. Knutson, K. Opender, G. Cuperus, and N. Elliott. 2008. Saltcedar areawide pest management in the western USA, pp. 271-299. In: O. Koul , G.W. Cuperus and N. Elliot eds., Areawide Pest Management Theory and Implementation. CAB International, Wallingford, U.K.
Chmura, H.E., H. M. Kharouba, J. Ashander, S. M. Ehlman, E. B. Rivest, and L. H.
Chuine, I. 2010. Why does phenology drive species distribution? Philosophical Transactions of the Royal Society B **365**: 3149-3160
Chuine, I., and J. Régnière. 2017. Process-Based Models of Phenology for Plants and Animals. Annual Review of Ecology, Evolution, and Systematics 48:159–182.
Coetzee, J. A., M. J. Byrne, and P. M. Hill. 2007. Predicting the distribution of *Eccritotarsus catarinensis*, a natural enemy released on water hyacinth in South Africa. Entomologica Experimentalis et Applicata 125:237-247.
Cornes, R.C., G. van der Schrier, E.J. van den Besselaar, and P.D. Jones. 2018. An ensemble version of the E-OBS temperature and precipitation data sets. Journal of Geophysical Research: Atmospheres 123:9391-9409.
Corrigan, J., D. R. Gillespie, R. De Clerck-Floate, and P. G. Mason. 2013. Lythrum salicaria L., purple loosestrife (Lythraceae). Biol. Control Programme Can. 2001–2012. 363.
Cossé, A.A., R.J. Bartelt, B.W. Zilkowski, D.W. Bean, and R.J. Petroski. 2005. The aggregation pheromone of *Diorhabda elongata,* a biological control agent of saltcedar (*Tamarix* spp.): identification of two behaviorally active components. Journal of Chemical Ecology **31**:657-670.
Dalin, P., D.W. Bean, T.L. Dudley, V.A. Carney, D. Eberts, K.T. Gardner, E. Hebertson, E.N. Jones, D.J. Kazmer, G.J. Michels, S.A. O'Meara, and D.C. Thompson. 2010. Seasonal adaptations to day length in ecotypes of *Diorhabda* spp. (Coleoptera: Chrysomelidae) inform selection of agents against saltcedars (*Tamarix* spp) Environmental Entomology **39**: 1666-1675.
Daly, C., H. Halbleib, J. Smith, W. Gibson, M. Doggett, G. Taylor, J. Curtis, and P. Pasteris. 2008. Physiographically sensitive mapping of climatological temperature and precipitation across the conterminous United States. International Journal of Climatology 28:2031–2064.

Daly, C., J. I. Smith, and K. V. Olson. 2015. Mapping atmospheric moisture climatologies across the conterminous United States. PLoS ONE 10:e0141140.
Danilevskii, A. S. 1961. Photoperiodism and seasonal development of insects. (English version published in 1965) Oliver and Boyd, London, United Kingdom.
Danilevskii, A.S. 1965. Photoperiodism and seasonal development of insects. Oliver and Boyd, London, UK.
Danks, H.V. 1987. Insect dormancy: an ecological perspective. Biological Survey of Canada, Ottawa, Canada.
DeLoach, C. J., P. A. Lewis, J. C. Herr, R. I. Carruthers, J. L. Tracy, and J. Johnson. 2003. Host specificity of the leaf beetle, Diorhabda elongata deserticola (Coleoptera: Chrysomelidae) from Asia, a biological control agent for saltcedars (Tamarix: Tamaricaceae) in the Western United States. Biological Control 27:117–147.
DeLoach, C.J., R. Carruthers, T. Dudley, D. Eberts, D. Kazmer, A. Knutson, D. Bean, J. Knight, P. Lewis, J. Tracy, J. Herr, G. Abbot, S. Prestwich, G. Adams, I. Mityaev, R. Jashenko, B. Li, R. Sobhian, A. Kirk, T. Robbins, and E. Delfosse. 2004. First results for control of saltcedar (*Tamarix* spp.) in the open field in the western United States. In J. Cullen ed.: Eleventh International Symposium on Biological Control of Weeds, Canberra, Australia
Denlinger, D. L., D. A. Hahn, C. Merlin, C. M. Holzapfel, and W. E. Bradshaw. 2017. Keeping time without a spine: what can the insect clock teach us about seasonal adaptation? Philos. Trans. R. Soc. B Biol. Sci. 372: 20160257.
Dlugosch, K.M. and I.M. Parker. 2008a. Invading populations of an ornamental shrub show rapid life history evolution despite genetic bottlenecks. Ecology Letters 11: 701-709.
Dlugosch, K.M. and I.M. Parker. 2008b. Founding events in species invasions: genetic variation, adaptive evolution and the role of multiple introductions. Molecular Ecology **17**: 431-449.
DoD Natural Resources Program, Strategic Plan for Bird Conservation and Management on Department of Defense Lands. 2014.
Dudley, T., and J. DeLoach. 2004. Saltcedar (*Tamarix* spp.), endangered species, and biological weed control – can they mix? Weed Technology **18**: 1542-1551.
Dudley, T.L., and D.W. Bean. 2012. Tamarisk biocontrol, endangered species risk and resolution of conflict through riparian restoration. BioControl **57**: 331-347
Emerson, K.J., Bradshaw, W.E., and C.M. Holzapfel. 2009. Complications of complexity: integrating environmental, genetic and hormonal control of insect diapause. Trends in Genetics **25**: 217-225.
Forrest, J.R.K. 2016 Complex responses of insect phenology to climate change. Current Opinion in Insect Sci. 17: 49-54
Forsythe, W. C., E. J. Rykiel, R. S. Stahl, H. Wu, and R. M. Schoolfield. 1995. A model comparison for daylength as a function of latitude and day of year. Ecological Modelling 80:87-95.
Frankham, R. 2005. Resolving the genetic paradox in invasive species. Heredity **94**: 385
Friedman, J.M., G.T. Auble, P.B. Shafroth, M.L. Scott, M.F. Merigliano, M.D. Preehling, and E.K. Griffin. 2005. Dominance of non-native riparian trees in western USA. Biological Invasions **7**: 747-751.
Gaskin, J.F., and B.A. Schaal. 2003. Molecular phylogenetic investigation of U.S. invasive *Tamarix*. Systematic Botany **28**: 86-95.
Gaskin, J.F., Kazmer, D.J., 2009. Introgression between invasive saltcedars (Tamarix chinensis and T. ramosissima) in the USA. Biol. Invas., 11, 1121-1130.
Gomi, T. 1997. Geographic variation in critical photoperiod for diapause induction and its temperature dependence in *Hyphantria cunea* Drury (Lepidoptera: Arctiidae). Oecologia, **111**: 160-165.

Gomi, T. 2007. Seasonal adaptations of the fall webworm Hyphantria cunea (Drury) (Lepidoptera: Arctiidae) following its invasion of Japan. Ecological Research **22**: 855-861.

Gomi, T., M. Muraji and M. Takeda 2004. Mitochondrial DNA analysis of the introduced fall webworm, showing its shift in life cycle in Japan. Entomological Science **7**: 183-188.

Gomi, T., M. Nagasaka, T. Fukuda, and H. Hagihara. 2007. Shifting of the life cycle and life-history traits of the fall webworm in relation to climate change. Entomologia Experimentalis et Applicata **125**: 179-184.

González, E., Shafroth, P.B., Lee, S.R., Ostoja, S.M., and M. Brooks 2020 Combined effects of biological control of an invasive shrub and fluvial processes on riparian vegetation dynamics. Biol Invasions. 22:2339–235. https://doi.org/10.1007/s10530-020-02259-9

Grapputo, A., S. Boman, L. Lindström, A. Lyytinen, and J. Mappes. 2005. The voyage of an invasive species across continents: genetic diversity of North American and European Colorado potato beetle populations. Molecular Ecology **14**: 4027-4219.

Grevstad, F. S. 1999. Experimental invasions using biological control introductions: the influence of release size on the chance of population establishment. Biol. Invasions. 1: 313–323.

Grevstad, F. S., and L. B. Coop. 2015. The consequences of photoperiodism for organisms in new climates. Ecological Applications 25:1506–1517.

Grevstad, F.S., J.E. Andreas, R.S. Bourchier, R. Shaw, R.L. Winston, and C.B. Randall. 2018. Biology and Biological Control of Knotweeds. USDA Forest Service, Forest Health Assessment and Applied Sciences Team, Morgantown, WV. FHTET-2017-03. 75 pp.

Grevstad, F.S., R.H. Shaw, R. Bourchier, P. Sanguankeo, G. Cortat, and R. Reardon. 2013. Efficacy and host specificity compared between two populations of the psyllid *Aphalara itadori*, candidates for biological control of invasive knotweeds in North America. Biological Control 65: 53-62.

Grevstad, F.S., T. Wepprich, B. Barker, L.B. Coop, R. Shaw, and R. S. Bourchier. 2022. Combining photoperiod and thermal responses to predict phenology mismatch for introduced insects. Ecological Applications e2557.

Hairston, N.G., S.P. Ellner, M.A. Gerber, T. Yoshida, and J.A. Fox. 2005. Rapid evolution and the convergence of ecological and evolutionary time. Ecology Letters 8: 1114-1127.

Harms, N.A., J.T. Cronin, R. Diaz, and R.L. Winston. 2020. A review of the causes and consequences of geographic variability in weed biological control successes. Biological Control 151: 104398. https://doi.org/10.1016/j.biocontrol.2020.104398

Hendry, A.P., and M.T. Kinnison. 1999. The Pace of Modern Life: Measuring Rates of Contemporary Microevolution. Evolution 53: 1637-1653

Hendry, A.P., M.T. Kinnison, M. Heino, T. Day, T.B. Smith, G. Fitt, C.T. Bergstrom, J. Oakeshott, P.S. Jørgensen, M.P. Zalucki, G. Gilchrist, S. Southerton, A. Sih, S. Strauss, R.F. Denison, and S.P Carroll. 2011. Evolutionary principles and their practical application. Evolutionary Applications 4: 159-183

Henrich, V.C. and D.L. Denlinger (1982) A maternal effect that eliminates pupal diapause in progeny of the flesh fly *Sarcophaga bullata*. J. Insect Physiol. 28: 881-884

Herrera, A. M., D. D. Dahlsten, N. Tomic-Carruthers, and R. I. Carruthers. 2005. Estimating Temperature-Dependent Developmental Rates of *Diorhabda elongata* (Coleoptera: Chrysomelidae), a Biological Control Agent of Saltcedar (*Tamarix* spp.). Environmental Entomology 34:775–784.

Hight, S. D., B. Blossey, J. Laing, and R. Declerck-Floate. 1995. Establishment of insect biological control agents from Europe against *Lythrum salicaria* in North America. Environmental Entomology 24:967–977.

Hinz, H. L., M. Schwarzländer, A. Gassmann, and R. S. Bourchier. 2014. Successes we may not have had: A retrospective analysis of selected weed biological control agents in the United States. Invasive Plant Sci. Manag. 7: 565–579.

Hudgeons, J.L., A.E. Knutson, K.M. Heinz, C.J. DeLoach, T.L. Dudley, R.R. Pattison, and J.R. Kiniry. 2007. Defoliation by introduced *Diorhabda elongata* leaf beetles (Coleoptera: Chrysomelidae) reduces carbohydrate reserves and regrowth of Tamarix (Tamaricaceae). Biological Control **43**: 213-221.
Hufbauer, R.A. 2008. Biological invasions: paradox lost and paradise gained. Current Biology **18**: R246-R247.
Hufbauer, R.A., and G.K. Roderick. 2005. Microevolution in biological control: Mechanisms, patterns and processes. Biological Control **35**: 227-239
Hultine KR, Bean DW, Dudley TL, Gehring C. 2015. Species introductions and their cascading impact on biotic interactions in desert riparian ecosystems. Integr. Comp. Biol. 55:587–601
Hultine KR, Dudley TL, Leavitt SW (2013) Herbivory-induced mortality increases with radial growth in an invasive riparian phreatophyte. Ann Bot 111:1197–1206
Izzo, V. M., J. Armstrong, D. Hawthorne, and Y. Chen. 2014. Time of the season: the effect of host photoperiodism on diapause induction in an insect herbivore, *Leptinotarsa decemlineata*. Ecol. Entomol. 39: 75–82.
Johnson, G.T. 2007. Case studies: Invasive species: Fairchild AFB. In: Conserving Biodiversity on Military Lands: A Guide for Natural Resources Managers. Nature Serve. http://www.dodbiodiversity.org/case_studies/ch_7_2.html
Jones, I.M., S.M. Smith, and R.S. Bourchier. 2020. Establishment of the biological control agent *Aphalara itadori* is limited by native predators and foliage age. Journal of Applied Entomology 144: 710-718.
Joschinski, J., and D. Bonte. 2020. Diapause is not selected as a bet-hedging strategy in insects: a meta-analysis of reaction norm shapes. bioRxiv. 752881.
Kahle, D., and H. Wickham. 2013. ggmap: Spatial Visualization with ggplot2. The R Journal 5:144–161.
Kawecki, T. J., and D. Ebert. 2004. Conceptual issues in local adaptation. Ecol. Lett. 7: 1225–1241.
Kellermann, V., and B. van Heerwaarden. 2019. Terrestrial insects and climate change: adaptive responses in key traits. Physiological Entomology 44:99–115.
Kennard D, Louden N, Gemoets D, Ortega S, González E, Bean DW, Cunningham P, Johnson T, Rosen K, Stahlke A (2016) *Tamarix* dieback and vegetation patterns following release of the northern tamarisk beetle (*Diorhabda carinulata*) in western Colorado. Biol Control 101:114–122
Kerr, N. Z., T. Wepprich, F. S. Grevstad, E. B. Dopman, F. S. Chew, and E. E. Crone. 2020. Developmental trap or demographic bonanza? Opposing consequences of earlier phenology in a changing climate for a multivoltine butterfly. Global Change Biology 26:2014–2027.
Kivelä, S. M., P. Välimäki, and K. Gotthard. 2013. Seasonality maintains alternative life-history phenotypes. Evolution. 67: 3145–3160.
Kivelä, S. M., P. Välimäki, and K. Gotthard. 2016. Evolution of alternative insect life histories in stochastic seasonal environments. Ecology and Evolution 6:5596–5613.
Knutson, A. E., J. L. Tracy, C. Ritzi, P. J. Moran, T. Royer, and C. J. DeLoach. 2019. Establishment, hybridization, dispersal, impact, and decline of *Diorhabda* spp. (Coleoptera: Chrysomelidae) released for biological control of Tamarisk in Texas and New Mexico. Environmental Entomology 48: 1297-1316.
Koštál, V. 2006. Eco-physiological phases of insect diapause. Journal of Insect Physiology 52:113-127.
Kozak, G.M., Wadsworth, C.B., Kahne, S.E., Bogdanowicz, S.M, Harrison, R.G., Coates, B.S. and E.B. Dopman (2019) Genomic Basis of Circannual Rhythm in the European Corn Borer Moth. Current Biology 29, 3501–3509
Lankau, R., P.S. Jørgensen, D.J. Harris, and A. Sih. 2011. Incorporating evolutionary principles into environmental management and policy. Evolutionary Applications **4**: 315-325
Lenth, R. 2020. emmeans: Estimated marginal means, aka least-squares means.

Levy, R. C., G. M. Kozak, C. B. Wadsworth, B. S. Coates, and E. B. Dopman. 2015. Explaining the sawtooth: latitudinal periodicity in a circadian gene correlates with shifts in generation number. Journal of Evolutionary Biology 28:40–53.

Lewis, P. A., C. J. DeLoach, A. E. Knutson, J. L. Tracy, and T. O. Robbins. 2003. Biology of Diorhabda elongata deserticola (Coleoptera: Chrysomelidae), an Asian leaf beetle for biological control of saltcedars (Tamarix spp.) in the United States. Biological Control 27:101–116.

Li, B., X. Kong, and L. Meng. 2000. An observation on the life cycle of *Diorhabda elongata deserticola* Chen: a potential biocontrol agent of saltcedar. Chinese Journal of Biological Control **16**: 48–49.

Lindestad, O., C. W. Wheat, S. Nylin, and K. Gotthard. 2019. Local adaptation of photoperiodic plasticity maintains life cycle variation within latitudes in a butterfly. Ecology 100:e02550.

Long, R.W., Bush, S.E., Grady, K.C., Smith, D.S., Potts, D.L., D'Antonio, C.M., Dudley, T.L., Fehlberg, S.D., Gaskin, J.F., Glenn, E.P. and Hultine, K.R., 2017. Can local adaptation explain varying patterns of herbivory tolerance in a recently introduced woody plant in North America? Conservation Physiology 5(1).

MacColl, A.D.C. (2011) The ecological causes of evolution. Trends in Ecology and Evolution 26: 514-522.

MacGregor, C. J., C. Thomas, D. B. Roy, M. Beaumont, B. James, T. Brereton, J. R. Bridle, C. Dytham, R. Fox, K. Gotthard, and others. 2019. Climate-induced phenology shifts linked to range expansions in species with multiple reproductive cycles per year. Nature Communications.

Maerz, J.C., B. Blossey, and V. Nuzzo. 2005. Green frogs show reduced foraging success in habitats invaded by Japanese knotweed. Biodiversity and Conservation 14: 2901-2911.

Manguin, S., R. White, B. Blossey, and S. D. Hight. 1993. Genetics, taxonomy, and ecology of certain species of *Galerucella* (Coleoptera: Chrysomelidae). Ann. Entomol. Soc. Am. 86: 397–410.

Marlin, D., E.R. Smit and M.J. Byrne. 2019. A successful biocontrol agent in the USA, *Diorhabda carinulata* (Coleoptera: Chrysomelidae) on Tamarix spp.(Tamaricaceae), rejected in South Africa due to insufficient host specificity. Biological Control 136: 104002.

Marsico, T.D., J.W. Burt, E.K. Espeland, G.W. Gilchrist, M.A. Jamieson, L. Lindström, G.K. Roderick, S. Swope, M. Szücs, and N.D. Tsutsui. 2010. Underutilized resources for studying the evolution of invasive species during their introduction, establishment, and lag phases. Evolutionary Applications **3**: 203-219

Masaki, S. 1961. Geographic variation of diapause in insects. Bull. Fac. Agric. Hirosaki Univ. 7: 66–98.

Masaki, S. 1999. Seasonal adaptations of insects as revealed by latitudinal diapause clines. Entomological Science 2:539–549.

Mausel, D.L., R.G. Van Driesche, and J.S. Elkinton. 2011. Comparative cold tolerance and climate matching of coastal and inland *Laricobius nigrinus* (Coleoptera: Derodontidae), a biological control agent of hemlock woolly adelgid. Biological Control 58: 96-102.

McAvoy, T. J., and L. T. Kok. 2004. Temperature dependent development and survival of two sympatric species, *Galerucella calmariensis* and *G. pusilla*, on purple loosestrife. BioControl 49:467–480.

McClay, A. S., and R. B. Hughes. 1995. Effects of temperature on developmental rate, distribution, and establishment of *Calophasia lunula* (Lepidoptera, Noctuidae), a biocontrol agent for toadflax (*Linaria* spp.). Biological Control 5:368-377.

McEvoy, P. B., K. M. Higgs, E. M. Coombs, E. Karaçetin, and L. Ann Starcevich. 2012. Evolving while invading: rapid adaptive evolution in juvenile development time for a biological control organism colonizing a high-elevation environment. Evol. Appl. 5: 524–536.

McNamara, J. M., Z. Barta, M. Klaassen, and S. Bauer. 2011. Cues and the optimal timing of activities under environmental changes: Cues and the optimal timing of activities. Ecology Letters 14:1183–1190.

Meinhardt, K. A. and C. A. Gehring. 2013. Tamarix and soil ecology, pp. 225–239. In: Sher, A. and M. Quigley (eds.) *Tamarix*: a Case Study of Ecological Change in the American West. Oxford University Press, New York.

Menne, M.J., I. Durre, R.S. Vose, B.E. Gleason, and T.G. Houston. 2012. An overview of the Global Historical Climatology Network-Daily Database. Journal of Atmospheric and Oceanic Technology, 29, 897-910, doi:10.1175/JTECH-D-11-00103.1. http://dx.doi.org/10.1175/JTECH-D-11-00103.1

Menzel, R. 1979. Spectral Sensitivity and Color Vision in Invertebrates, pp. 503–580. In Autrum, H., Bennett, M.F., Diehn, B., Hamdorf, K., Heisenberg, M., Järvilehto, M., Kunze, P., Menzel, R., Miller, W.H., Snyder, A.W., Stavenga, D.G., Yoshida, M., Autrum, H. (eds.), Comp. Physiol. Evol. Vis. Invertebr. Invertebr. Photoreceptors, Handbook of Sensory Physiology. Springer, Berlin, Heidelberg.

Merilä, J., and A. P. Hendry. 2014. Climate change, adaptation, and phenotypic plasticity: the problem and the evidence. Evol. Appl. 7: 1–14.

Michels, G. Jr., E. Parks, K. Davis, and B. Denman. 2013. Biological Control of Weeds on Federal Installations in Colorado and Wyoming. Consolidated Report. Texas A&M AgriLife Research 2301 Experiment Station Road, Bushland, Texas 79012.

Miller, T. E. X., A. L. Angert, C. D. Brown, J. A. Lee-Yaw, M. Lewis, F. Lutscher, N. G. Marculis, B. A. Melbourne, A. K. Shaw, M. Szücs, O. Tabares, T. Usui, C. Weiss-Lehman, and J. L. Williams. 2020. Eco-evolutionary dynamics of range expansion. Ecology 101(10):e03139. 10.1002/ecy.3139

Myint, Y. Y., K. Nakahira, M. Takagi, N. Furuya, and R. H. Shaw. 2012. Using life-history parameters and a degree-day model to predict climate suitability in England for the Japanese knotweed psyllid *Aphalara itadori* Shinji (Hemiptera: Psyllidae). Biological Control 63:129-134.

Nagler, P. L., S. Pearlstein, E. P. Glenn, T. B. Brown, H. L. Bateman, D. W. Bean, and K. R. Hultine. 2014. Rapid dispersal of saltcedar (*Tamarix* spp.) biocontrol beetles (*Diorhabda carinulata*) on a desert river detected by phenocams, MODIS imagery and ground observations. Remote Sensing of Environment 140:206–219.

Nei, M., T. Maruyama and R. Chakraborty. 1975. The bottleneck effect and genetic variability in populations. Evolution **29**: 1-10

Nelson, R.J., D.L. Denlinger, and D.E. Somers. 2010. Photoperiodism: The Biological Calendar. Oxford University Press.

Paxton E.H., M.K. Sogge, S.L. Durst, T.C. Theimer, and J. R. Hatten. 2007. The ecology of the southwestern willow flycatcher in Central Arizona-a 10-year synthesis report. USGS Open-File Report 2007-1381.

Pemberton, R.W. 2000. Predictable risk to native plants in weed biological control. Oecologia **125**: 489-494.

Phillips, B.L., G.P. Brown and R. Shine. 2010. Life-history evolution in range-shifting populations. Ecology **96**: 1617-1627

Pimentel, D., R. Zuniga and D. Morrison. 2005. Update on the environmental and economic costs associated with alien-invasive species in the United States. Ecological Economics 52: 273–288.

Pitcairn, M. J. 2018. Weed biological control in California, USA: review of the past and prospects for the future. BioControl 63:349–359.

Ponti, R., and M. Sannolo. 2022 The importance of including phenology when modelling species ecological niche. Ecography e06143, doi: 10.1111/ecog.06143

Pruisscher, P., Nylin, S., Gotthard, K., and C.W. Wheat. 2018. Genetic variation underlying local adaptation of diapause induction along a cline in a butterfly. Molecular Ecology 27: 3613-3626

Pruisscher, P., Nylin, S., Wheat, C.W., and K. Gotthard. 2020. A region of the sex chromosome associated with population differences in diapause induction contains highly divergent alleles at clock genes. Evolution 75: 490-500

R Core Team. 2018. R: A Language and Environment for Statistical Computing. R Foundation for Statistical Computing, Vienna, Austria.
R Core Team. 2019. R: A language and environment for statistical computing. R Foundation for Statistical Computing, Vienna, Austria. URL https://www.R-project.org/
Ragland, G.J, Armbruster, P.A. and M.E. Meuti 2019 Evolutionary and functional genetics of insect diapause: a call for greater integration. Current Opinion in Insect Science 36:74–81.
Reznick, D.N. and C.K. Ghalambor. 2001. The population ecology of contemporary adaptations: what empirical studies reveal about the conditions that promote adaptive evolution. Genetica **112-113**: 183-198
Reznik, S. Ya., M. Yu. Dolgovskaya, A. N. Ovchinnikov, and N. A. Belyakova. 2015. Weak photoperiodic response facilitates the biological invasion of the harlequin ladybird *Harmonia axyridis* (Pallas) (Coleoptera: Coccinellidae). J. Appl. Entomol. 139: 241–249.
Riley, E., S. Clark, and T. Seeno. 2003. Catalog of the leaf beetles of America north of Mexico. Special publication no. 1. Coleopterists Society.
Roderick, G. K., R. Hufbauer, and M. Navajas. 2012. Evolution and biological control. Evol. Appl. 5: 419–423.
Roderick, G.K. and M. Navajas. 2003. Genes in new environments: genetics and evolution in biological control. Nature Review Genetics **4**: 889-899
Roff, D. 1980. Optimizing development time in a seasonal environment: The "ups and downs" of clinal variation. Oecologia. 45: 202–208.
Roy, D. B., T. H. Oliver, M. S. Botham, B. Beckmann, T. Brereton, R. L. H. Dennis, C. Harrower, A. B. Phillimore, and J. A. Thomas. 2015. Similarities in butterfly emergence dates among populations suggest local adaptation to climate. Global Change Biology 21:3313–3322.
Saikkonen, K., K. Taulavuori, T. Hyvönen, P. E. Gundel, C. E. Hamilton, I. Vänninen, A. Nissinen, and M. Helander. 2012. Climate change-driven species' range shifts filtered by photoperiodism. Nat. Clim. Change. 2: 239–242.
Saunders, D.S. 2002. Insect clocks, 3rd ed. Elsevier Science, Amsterdam, The Netherlands.
Schoener, T.W. 2011. The newest synthesis: understanding the interplay of evolutionary and ecological dynamics. Science 331: 426-429.
Schwarzländer, M., H.L. Hinz, R.L. Winston, and M.D. Day. 2018. Biological control of weeds: an analysis of introductions, rates of establishment and estimates of success, worldwide. BioControl 63: 319-331.
Shafroth, P. B., J. R. Cleverly, T. L. Dudley, J. P. Taylor, C. van Riper, E. P. Weeks, and J. N. Stuart. 2005. Control of Tamarix in the western United States: Implications for water salvage, wildlife use, and riparian restoration. Environmental Management 35: 231–246.
Shaw, R.H., S. Bryner, and R. Tanner. 2009. The life history and host range of the Japanese knotweed psyllid, *Aphalara itadori* Shinji: Potentially the first classical biological weed control agent for the European Union. Biological Control 49:105–113.
Simons, A. M. 2011. Modes of response to environmental change and the elusive empirical evidence for bet hedging. Proceedings of the Royal Society B: Biological Sciences 278:1601–1609.
Stahlke AR, Ozsoy AZ, Bean DW, Hohenlohe PA. 2019. Mitochondrial genome sequences of *Diorhabda carinata* and *Diorhabda carinulata*, two beetle species introduced to North America for biological control. Microbiology Resource Announcements 8:e00690-19. https://doi.org/10.1128/MRA.00690-19.
Stahlke, A.R., Bitume, E.V., Özsoy, A.Z., Bean, D.W., Veillet, A., Clark, M.I., Clark, E.I., Moran, P., Hufbauer, R.A. and Hohenlohe, P.A., 2022. Hybridization and range expansion in tamarisk beetles

(Diorhabda spp.) introduced to North America for classical biological control. Evolutionary Applications 15:60-77.
Stuckey, R. L. 1980. Distributional History of *Lythrum salicaria* (Purple Loosestrife) in North America. Bartonia:3–20.
Suckling, David Maxwell, and René François Henri Sforza. 2014. What magnitude are observed non-target impacts from weed biocontrol?" PloS one 9: e84847.
Sutherst, R. W., G. F. Maywald, and D. J. Driticos. 2007. CLIMEX version 3: User's Guide. Hearne Scientific Software, Melbourne, Australia.
Szűcs M, U Schaffner, WJ Price and M Schwarzländer. 2012. Post-introduction evolution in the biological control agent *Longitarsus jacobaeae* (Coleoptera: Chrysomelidae). Evolutionary Applications 5: 858-868
Szücs, M., E. Vercken, E.V. Bitume, R.A. Hufbauer (2019) The implications of rapid
Takeda, M., and S. Masaki. 1979. Asymmetric perception of twilight affecting diapause induction by the fall webworm, *Hyphantria cunea*. Entomol. Exp. Appl. 25: 317–327.
Tauber, C. A., and M. J. Tauber. 1981. Insect Seasonal Cycles: Genetics and Evolution. Annu. Rev. Ecol. Syst. 1: 281–308.
Tauber, M.J., C.A. Tauber, and S. Masaki. 1986. Seasonal Adaptations of Insects. Oxford University Press, New York.
Taylor, F., and J. B. Spalding. 1988. Fitness Functions for Alternative Developmental Pathways in the Timing of Diapause Induction. The American Naturalist 131:678–699.
Thomas, C.D., E.J. Bodsworth, J.R. Wilson, A.D. Simmons, Z.G. Davies, M. Musche, and L. Conradt. 2001. Ecological and evolutionary processes at expanding range margins. Nature **411**: 577-581
Thornton, P. E., M. M. Thornton, B. W. Mayer, Y. Wei, R. Devarakonda, R. S. Vose, and R. B. Cook. 2017. Daymet: Daily surface weather data on a 1-km grid for North America, version 3. ORNL Distributed Active Archive Center.
Thornton, P. E., S. W. Running, and M. A. White. 1997. Generating surfaces of daily meteorological variables over large regions of complex terrain. Journal of Hydrology 190:214–251.
Thornton, P. E., S. W. Running, and M. A. White. 1997. Generating surfaces of daily meteorological variables over large regions of complex terrain. J. Hydrol. 190: 214–251.
Thornton, P.E., M.M. Thornton, B.W. Mayer, Y. Wei, R. Devarakonda, R.S. Vose, and R.B. Cook. 2018. Daymet: Daily Surface Weather Data on a 1-km Grid for North America, Version 3. ORNL DAAC, Oak Ridge, Tennessee, USA. https://doi.org/10.3334/ORNLDAAC/1328.
Thornton, P.E., M.M. Thornton, B.W. Mayer, Y. Wei, R. Devarakonda, R.S. Vose, and R.B. Cook. 2016. Daymet: Daily Surface Weather Data on a 1-km Grid for North America, Version 3. ORNL DAAC, Oak Ridge, Tennessee, USA. https://doi.org/10.3334/ORNLDAAC/1328
Thrall, P.H., J.G. Oakeshott, G. Fitt, S. Southerton, J.J. Burdon, A. Sheppard, R.J. Russell, M. Zalucki, M. Heino, and R.F. Denison. 2011. Evolution in agriculture: the application of evolutionary approaches to the management of biotic interactions in agro-ecosystems. Evolutionary Applications **4**: 200-215.
Tobin, P. C., S. Nagarkatti, G. Loeb, and M. C. Saunders. 2008. Historical and projected interactions between climate change and insect voltinism in a multivoltine species. Glob. Change Biol. 14: 951–957.
Tracy J.T., and T.O. Robbins. 2009. Taxonomic revision and biogeography of the *Tamarix*-feeding *Diorhabda elongata* (Brullé, 1832) species group (Coleoptera: Chrysomelidae: Galerucinae: Galerucini) and analysis of their potential in biological control of Tamarisk. Zootaxa 2101: 1-152

Tsai, H.-Y., D. R. Rubenstein, Y.-M. Fan, T.-N. Yuan, B.-F. Chen, Y. Tang, I.-C. Chen, and S.-F. Shen. 2020. Locally-adapted reproductive photoperiodism determines population vulnerability to climate change in burying beetles. Nature Communications 11:1398.

Turelli, M. and N.H. Barton. 2006. Will population bottlenecks and multilocus epistasis increase additive genetic variance? Evolution **60**: 1763-1776.

Uller, T. 2008. Developmental plasticity and the evolution of parental effects. Trends Ecol. Evol. 23: 432–438.

Urbanski, J., M. Mogi, D. O'Donnell, M. DeCotiis, T. Toma, and P. Armbruster. 2012. Rapid adaptive evolution of photoperiodic response during invasion and range expansion across a climatic gradient. The American Naturalist 179:490–500. DOI: 10.1086/664709

Urgenson, L.S., S.H. Reichard, and C.B. Halpern. 2009. Community and ecosystem consequences of giant knotweed (*Polygonum sachalinense*) invasion into riparian forests of western Washington, USA. Biological Conservation 142:1536-41.

US District Court, Nevada (2017) Case No. 2: 13-cv-01785-RFB-GWH

Van Dyck, H., D. Bonte, R. Puls, K. Gotthard, and D. Maes. 2015. The lost generation hypothesis: could climate change drive ectotherms into a developmental trap? Oikos 124: 54-61.

van Klinken, R. D., and O.R. Edwards. 2002. Is host specificity of weed biological control agents likely to evolve rapidly following establishment? Ecology Letters **5**: 590-596

Velarde, R. A., R. N. Wiedenmann, and D. J. Voegtlin. 2002. Influence of photoperiod on the overwintering induction of *Galerucella calmariensis* L. BioControl 47:587–601.

Venables, W. N., and B. D. Ripley. 2002. Modern applied statistics with S, Fourth. ed. Springer, New York.

Vuković, N., V. Šegota, A. Alegro, N. Koletić, A. Rimac, and S. Dekanić. 2019. "Flying under the radar"-how misleading distributional data led to wrong appreciation of knotweeds invasion (*Reynoutria* spp.) in Croatia. BioInvasions Record 8(1).

Wagner, N.K., Ochochki, B.M., Crawford, K.M., Compagnoni, A. and Miller, T.E.X. 2017. Genetic mixture of multiple source populations accelerates invasive range expansion. Journal of Animal Ecology 86: 21-34.

Wagner, T. L., H.-I. Wu, R. M. Feldman, P. J. H. Sharpe, and R. N. Coulson. 1985. Multiple-cohort Approach for Simulating Development of Insect Populations under Variable Temperatures. Annals of the Entomological Society of America 78:691–704.

Wepprich, T. and Grevstad, F.S., 2021. Divergence in photoperiod responses of a classical biological control agent, *Galerucella calmariensis* (Coleoptera: Chrysomelidae), across a climatic and latitudinal gradient. Environmental Entomology 50: 306-316.

Wepprich, T., Grevstad, F.S., Barker, B., Coop, L.B., Shaw, R., and Bourchier, R.S. 2021. Data and code for "Combining photoperiod and thermal responses to predict phenological mismatch for introduced insects" [Data set]. Zenodo. https://doi.org/10.5281/zenodo.5542617

Westbrook, C. and K. Ramos. 2005. Under siege: invasive species on military bases. National Wildlife Federation. Available online: http://www.dmg.gov/documents/RPT_Under_Siege_Invasive_Species-_on_Military_Bases_NWF_101405.pdf

Wilcove, D. S., Rothstein, D., Dubow, J., Phillips, A., & Losos, E. 1998. Quantifying threats to imperiled species in the United States. BioScience 48: 607-615.

Williams WI, Friedman JM, Gaskin JF, Norton AP (2014) Hybridization of an invasive shrub affects tolerance and resistance to defoliation by a biological control agent. Evol Appl 7:381–393

Wright, M. G., and G. M. Bennett. 2018. Evolution of biological control agents following introduction to new environments. BioControl. 63: 105–116.

Yang. 2019. The mechanisms of phenology: the patterns and processes of phenological shifts. Ecological Monographs 89(1):e01337. 10.1002/ecm.1337
Zalom, F.G. and P.B. Goodell. 1983. Degree days: the Calculation and Use of Heat Units in Pest Management. University of California, Division of Agriculture and Natural Resources.
Zalucki, M. P., and R. D. van Klinken. 2006. Predicting population dynamics of weed biological control agents: science or gazing into crystal balls? Aust. J. Entomol. 45: 331–344.

13. Websites and Software Manuals

Websites for model versions:

1. Web interface to DDRP spatial phenology models for the three weed biocontrol agents. This is the main model tool developed by our project with model details described in Grevstad et al. 2022.
https://uspest.org/dd/dodmaps

2. Link to site-specific degree-day calculator for tamarisk beetle.
https://uspest.org/dd/model_app?spp=dca&sta=CLRW3&tab=intro

2. Link to site-specific degree-day calculator for purple loosestrife beetle.
https://uspest.org/dd/model_app?spp=gca&sta=CLRW3&tab=intro

3. Link to site-specific degree-day calculator for Japanese knotweed psyllid.
https://uspest.org/dd/model_app?spp=jkp&sta=CLRW3&tab=intro

4. Link to online version of the individual-based model.
https://tyson-wepprich.shinyapps.io/Biocontrol_Voltinism_Simulation/

5. Link to subscription sign-up page to receive email "push" model predictions for the above phenology models
https://uspest.org/cgi-bin/account

Software manuals and open-access code:

1. Coop, L., Grevstad, and B. S. Barker. 2022. User Guide for uspest.org/dd/dodmaps. For online models of three weed biocontrol agent species with photoperiod-cued diapause induction. Available at: https://uspest.org/CAPS/DDRP_DODMAPS_user_guide.pdf

2. Wepprich, T., F.S. Grevstad, B. Barker, L. Coop, R. Shaw, and R. Bourchier. 2021. Data and code for "Combining photoperiod and thermal responses to predict phenological mismatch for introduced insects" For model version published in Ecological Applications (Grevstad et al. 2022). Available at: https://zenodo.org/record/5542618#.YrOLYuzMKUk

3. Grevstad, F.S., T. Wepprich, B. Barker, L.B. Coop, R. Shaw, and R. S. Bourchier. 2022. Combining photoperiod and thermal responses to predict phenology mismatch for introduced insects. ***Ecological Applications*** e2557

4. Coop, L., and B. S. Barker. 2020. Computing infrastructure requirements and user guide for hosting DDRP models. Prepared for APHIS PPQ and other collaborators. Available at: https://uspest.org/CAPS/ and at https://github.com/bbarker505/ddrp_v2

5. Barker, B. S., L. Coop, T. Wepprich, G. Cook, and D. Upper. 2020. Degree-Day, establishment Risk, and Phenological event mapping (DDRP) system, version 2. OSU Oregon IPM Center Web Available at: https://uspest.org/CAPS/ and at https://github.com/bbarker505/ddrp_v2

14. Publications Resulting from this Project

Published

Grevstad, F.S., T. Wepprich, B. Barker, L.B. Coop, R. Shaw, and R. S. Bourchier. 2022. Combining photoperiod and thermal responses to predict phenology mismatch for introduced insects. ***Ecological Applications*** e2557.

Wepprich, T. and Grevstad, F.S., 2021. Divergence in photoperiod responses of a classical biological control agent, *Galerucella calmariensis* (Coleoptera: Chrysomelidae), across a climatic and latitudinal gradient. ***Environmental Entomology*** 50: 306-316.

Coop, L. and B. S. Barker. 2020. Advances in understanding species ecology of crop insect pests and applications to IPM: Phenological and life cycle modeling of insect pests. In: Kogan, M, E. Heinrichs (eds.) Integrated Management of Insect Pests: Current and Future Developments. Burleigh Dodds Publishing, Cambridge, England. Pp 44-98.

Barker, B. S., L. Coop, T. Wepprich. F., Grevstad, G. Cook. 2020. DDRP: Real-time phenology and climatic suitability modeling of invasive insects. ***PLoS ONE*** 15(12): e0244005. https://doi.org/10.1371/journal.pone.0244005

Kerr, N., T. Wepprich, F. Grevstad, E. Dopman, F. Chew, and E. Crone. 2020. Developmental trap or demographic bonanza? Opposing consequences of earlier phenology in a changing climate for a multivoltine butterfly." ***Global Change Biology*** 26: 2014-2027

Manuscripts in Preparation

Bean, D.W., T. Wepprich, T.L. Dudley, F.S. Grevstad, L. B. Coop, A. Stahlke, B. Barker, and P. Dalin. Southward range expansion of a biocontrol agent, *Diorhabda carinulata,* for an invasive riparian shrub *Tamarix* in North America, is linked to the rapid evolution of photoperiodically-cued diapause. In preparation for Ecological Monographs.

Wepprich, T., D.W. Bean, F. Grevstad, L. Coop, and B. Barker. Quantitative prediction of the optimal critical photoperiod for insect diapause based on climate and latitude. In preparation for American Naturalist.

Grevstad, F.S. and Wepprich, T. Photoperiodism determines voltinism and host impact of weed biocontrol insects moved to a new climate: a common garden experiment using the loosestrife leaf beetle *Galerucella calmariensis.*

15. Presentations

* = invited presentation

Barker, B. S., L. B Coop, and T. Crimmins. 2022. DDRP: a modeling tool to guide decision making for pest surveillance and management. Poster presentation at the 10th International IPM Summit, Mar. 2, 2022. Denver, CO. Online at: https://ipmsymposium.org/2022/Documents/Posters/P53.pdf

Barker, B., L. Coop. 2022. DDRP: phenology and climate suitability modeling to predict when and where invasive and IPM pests can arise. Oregon State Agency IPM Coordinating Committee Semiannual Meeting. Feb. 2, 2022, online event. 13 attendees.

Coop, L., C. Hedstrom, D. Upper. 2022. A new "push" email delivery system for pest and crop models. 81st Annual Pacific Northwest Insect Management Conference. Jan. 10, 2022, online event. 95 attendees.

Barker, B. S. 2021. Modeling pest distributions, phenology, and population dynamics to safeguard US agricultural lands. Seminar for the Dept. of Crop and Soil Science, Oregon State University, Oct. 25, 2021. Corvallis, OR.

Grevstad, F.S., T. Wepprich, D. Bean, and L. Coop. 2020. Incorporating photoperiodism in insect phenology models with application to biological control of weeds. SERDP and ESTP Annual Symposium. November 2020 (virtual oral presentation)

*Barker, B. S., L. Coop, and T. Wepprich. 2021. Modeling phenology and climate suitability of invasive insects in real-time to improve surveillance and management. Oral presentation at the Entomological Society of America Conference (given remotely), Oct. 13, 2021. Denver, CO.

*Barker, B. S. 2020. Modeling real-time climate suitability and phenology of invasive pests to safeguard U.S. agricultural resources. Seminar for the Dept. of Biological Sciences, Northern Arizona State University (given over Zoom), Oct. 23, 2020. Flagstaff, AZ.

Barker, B. S., L. Coop, T. Wepprich, and F. Grevstad. 2020. DDRP: a new platform to model phenology and risk of establishment. Oral presentation at the Pacific Northwest Insect Management Conference, Jan. 6, 2020. Portland, OR.

Wepprich, T, Grevstad, F, Coop, L. 2019. Validating models of phenology, diapause, and voltinism in the field. Entomological Society of America annual meeting, St. Louis, MO. November 17-20, 2019.

Wepprich, T. 2019. Presentation on SERDP project to environmental staff at Yakima Training Center, Yakima, WA. October 27, 2019.

Wepprich, T. 2019. Presentation on knotweed biocontrol to Luckiamute Watershed Council, Monmouth, OR. May 2, 2019.

Grevstad, F.S., T. Wepprich, D. Bean, and L. Coop. 2019. Incorporating photoperiodism in insect phenology models with application to biological control of weeds. A poster presented at the SERDP and ESTP Annual Symposium. December 2019, Washington D.C.

Barker, B. S. 2019. Modelling climate suitability and phenology to safeguard U.S. agricultural and natural resources from invasive pests. Lightning talk at the Cascadia R Conference, Jun. 8, 2019. Bellevue, WA. Available at: Available at: https://cascadiarconf.com/img/presentations_2019/BBarker_RCascadia_talk.pdf5.

Coop, L. B., B. S. Barker, T. Wepprich, and F. Grevstad. 2019. DDRP: Modeling degree-days, risk of establishment, and phenological event maps. Poster presentation at the Pacific Branch of the Entomological Society of America Conference, Apr. 2, 2019. San Diego, CA. Available at: http://uspest.org/ipm/Coop_etal_DDRP_platform_ESA_Pacific_March_2019.pdf7.

Grevstad, F.S., T. Wepprich, D. Bean, and L. Coop. 2018. Incorporating photoperiodism in insect phenology models with application to biological control of weeds. A poster presented at the SERDP and ESTP Annual Symposium. November 27-29, 2018, Washington D.C.

*Grevstad, FS, T. Wepprich, L. Coop and D. Bean. 2018. A model for understanding phenological mismatch and adaptation in introduced insects that are cued by photoperiod. Annual Meeting of the Entomological Society of America, November 11-14, 2018, Vancouver, B.C.

*Bean, D., T. Wepprich, F. Grevstad, T. Dudley and L. Coop. 2018. Rapid evolution of photoperiod cues across a latitudinal gradient allows expansion from two generations per season to six in the biocontrol agent *Diorhabda carinulata.* Annual Meeting of the Entomological Society of America, November 11-14, 2018, Vancouver, B.C.

Wepprich, T, Grevstad, F, Coop, L. 2018. Locally-adapted diapause decisions of biological control agents affect insect voltinism and host plant damage. Annual Meeting of the Entomological Society of America, November 11-14, 2018, Vancouver, B.C.

Bean, D. T. Dudley, F. Grevstad and L. Coop. 2018. How Two Generations Became Six: Evolving Photoperiod Cues and Shifting Temperature Regimes Alter the Life History and Phenology of *Diorhabda carinulata*, a Biocontrol Agent for *Tamarix spp*. presented at the annual Riparian Restoration Conference, sponsored by the Tamarisk Coalition and the Water Center at Colorado Mesa University, Grand Junction, CO, February 6, 2018

*Bean, D., Dudley, T. Grevstad, F. and Coop, L. 2017. Rapidly evolving responses to photoperiod cues allow phenology shifts and southward range expansion in *Diorhabda carinulata*, a biocontrol agent for *Tamarix* An invited presentation for the symposium Tamarisk: from organism to landscape at the 14th Biennial Conference of Science and Management for the Colorado Plateau and Southwest Region, Flagstaff, AZ, Sept. 13, 2017

Appendix 1

User Guide for uspest.org/dd/dodmaps (a version of DDRP)

Len Coop, coopl@science.oregonstate.edu
Fritzi Grevstad, Fritzi.Grevstad@oregonstate.edu
Brittany Barker, Brittany.Barker@oregonstate.edu
Depts. of Horticulture and Botany & Plant Pathology and the Oregon IPM Center (OIPMC), Oregon State University

Last updated on 10/25/2022

Introduction

DDRP (Degree-Days, Risk mapping, and Phenological event mapping) is a population modeling platform that integrates mapping of phenology and climatic suitability in real-time to provide guidance on both where and when invasive insect species could potentially invade the 48-state conterminous United States (Barker et al. 2020). The DoDMaps version of DDRP includes photoperiod response, allowing the model to achieve a greater degree of realism and accuracy for species that respond to daylength for activities including initiation and termination of diapause.

This platform is in development by OSU and collaborators in collaboration with US DoD and with USDA APHIS PPQ, and it is currently being used to model three weed biocontrol agents (for US DoD), 16 high-priority invasive insects (for APHIS CAPS program), and with one plant pathogenic disease (boxwood blight) (with funding provided by APHIS PPQ/Farm Bill). DDRP may also be used to monitor and manage populations of IPM pests and could also be readily extended to model other temperature-dependent organisms such as non-insect invertebrates and plants. The platform uses a process-based modeling approach in which degree-days, photoperiod, and (for the non-DoDMaps version of DDRP) temperature stress, are calculated daily and accumulate over time to model phenology, photoperiod response, and climatic suitability, respectively. We refer users to Barker et al. (2020) for a more thorough description of DDRP and its products, the process of model parameterization, and its potential applications. Knowledge of the R programming language, and experience with systems administration and spatial weather database management, are recommended for using DDRP.

Program features

Some of the major features of DDRP currently include:

1) Degree-day parameters including durations and lower and upper developmental thresholds for four separate life stages (these are the egg, the larva or nymph, the pupa or pre-oviposition, and the adult), plus a separately parameterized overwintering stage.
2) The ability to spread the population using cohorts. Typically seven cohorts are specified but any number can be used. While cohorts offer the ability to spread the population in a Gaussian or other distribution, there is currently no distributed-delay function, meaning that the spread does not increase over multiple generations.
3) Phenological event maps (PEMs, also known as pest event maps), which depict estimated calendar dates of seasonal activities or population events. PEM parameters are specified as degree-days within each of the four (plus overwintering) stages. For example, DDRP can be parameterized to make first

egg-hatch PEMs by setting a degree-day value near the completion of the egg stage, or at the beginning of the larval stage. If the former is used, then a second PEM, say for mid-larval development, could be parameterized using a value such as one-half of the degree-day total for larval development.

4) Climatic suitability maps (not DoDMaps), which show two levels of climatic suitability (moderate and severe stress exclusions). These are intended to indicate risk likelihood of short vs. long-term establishment but could also indicate migration zones, and uncertainties such as in species parameterization, model structure, and in the sources of climate data.
5) Potential vs. Attempted Voltinism & Mismatch maps (DoDMaps only). These maps show:

Potential Voltinism – number of generations assuming to photoperiod response
Attempted Voltinism – number of generations with photoperiod response
Mismatch – the difference in number of generations between potential and attempted voltinism maps.

Description and requirements

DDRP is an R program/script ("DDRP_v2.R," currently *ca.* 2,400 lines) that processes daily minimum (Tmin) and maximum (Tmax) data to produce predictions of phenology and climatic suitability in raster and image file formats. The use of precipitation or types of moisture data is pending further development of DDRP. The program requires an auxiliary R script ("DDRP_v2_funcs.R," currently *ca.* 2,100 lines) that contains 21 functions needed for modeling.

Operating system and hardware

DDRP can be run in a UNIX/Linux environment (we recommend Scientific Linux or CentOS, but other distributions should work as well) and in Microsoft Windows. We have run the program on a Windows 10 PC with eight cores, but have not yet attempted to run it on a Windows server. The computer/server should have multicore functionality because many DDRP processes are run in parallel to increase speed and efficiency. The program may crash if there are insufficient cores available to complete an operation, particularly for memory intensive processes such as the daily time step ("DailyLoop" function) and certain post-processing operations. For running DDRP on a server, we recommend an HP (or equivalent) rack mount server such as DL380, dual processors (8 or more cores per processor), ≥128GB memory, ≥4TB SAS RAID (5 or 50 or similar configuration) hard (or solid state) drives. Connectivity to the server via HTTPS, SSH, SCP is required.

Software

The latest version of R should be installed with the following libraries: "doParallel", "dplyr", "foreach", "ggplot2", "ggthemes", "lubridate", "mapdata", "mgsub", "optparse", "parallel", "purrr", "RColorBrewer", "rgdal", "raster", "readr", "R.utils", "sp", "stringr", "tidyr", "tictoc", "tools," and "toOrdinal". Additionally, the Geospatial Data Abstraction Library (GDAL) software must be installed. The "sp" library in R automatically links to GDAL and depends on it for reading and writing raster and vector geospatial data formats.

Input files

Species parameter file

Each species modeled by DDRP requires a parameter file, which may be stored in a subdirectory under the DDRP code directory (e.g. /home/DDRP/spp_params/ALB.params). Each parameter file has comment lines beginning with "#" and parameter lines such as:

larvaeLDT <- 10 # IPPC modeling

Here, the lower developmental threshold for larvae (larvaeLDT) is set to 10°C. A description of each species parameter and an example parameter file are provided in Appendix 1 and 2 of this document, respectively.

Temperature (Tmin and Tmax) data

Real-time temperature data (PRISM)

For real-time modeling, we have been using daily Tmin and Tmax data at a 4 km spatial resolution from the PRISM (Parameter-elevation Relationships on Independent Slopes Model) database (available at http://www.prism.oregonstate.edu). Tmax and Tmin data are read from a local directory directly into the DDRP platform. We use a 50 line BASH script that controls a 230 line R script to download these data on a daily basis. The PRISM data should not be modified (i.e., retain the cartographic projection, file name, and other conventions of each PRISM file). Users of PRISM data should become familiar with their file naming conventions including the increasing data quality (and lag time) of their data types classified as "early", "provisional", and "stable". We also place forecast data (next section) in the PRISM-containing directories. Past year data directories can be purged of forecast data and "early" and "provisional" PRISM data, leaving only "stable" PRISM data if storage is limited. DDRP can be readily modified to ingest 800 m PRISM data (available for a price), or 2.5 km DAYMET data for past years (DAYMET is not available in real-time during the current year). Users may also wish to consider using downscaled global climate model (GCM) data such as MACAv2-METDATA, available from the University of Idaho.

Forecast temperature data

For forecast models, we currently use NMME (North American Multi-Model Ensemble) daily temporal-downscaled 7-month forecast data, followed by 10-year recent average PRISM data as the primary forecast regime. The 10-year recent average data can be readily calculated either monthly or yearly using R. Other options include using 30-year (1981–2010) NORMALS (e.g., available from the PRISM group and DAYMET), NDFD 7-day forecasts, and CFSv2 (NCEP Coupled Forecast System model version) forecasts that, like NMME, extend to 7 months. We use a Perl+GRASS GIS program to temporally downscale monthly NMME forecast data (Tmax, Tmin and Precip) to a daily resolution each month but a similar program could also be written in R. Both 10-year average PRISM data and NMME forecasts can be freely obtained from the OSU OIPMC/USPEST.ORG server if users need a product that does not require Perl+GRASS GIS (to run our code) or require reprogramming from Perl+GRASS GIS to R. Contact us if this is your preference.

Temperature data organization, naming, and quality

We keep temperature data for each year in its own folder. For example, all data for 2020 are located in /data/PRISM/2020/. PRISM file names are not changed from the naming conventions used by the PRISM group, but we rename other file types (e.g., 10-year averages and NMME) to mimic the PRISM naming conventions. A full explanation for naming of PRISM files is available from the PRISM website. Below is a description of each part of a file name using the example file "PRISM_tmin_early_4kmD2_20200222_bil.bil."

File name part	Description
PRISM_	Data source (this is ignored by DDRP so it may be edited if desired)
tmin_	Data type (tmin is daily minimum temperature in °C at a nominal 2 m from ground)
early_	PRISM data type (see below), others include "NMME_", "10yr1019", etc.

4kmD2_	Spatial resolution and data version; we use PRISM 4K data
20200222_	Date that the data represents; in this case Feb 22, 2020
bil.bil	File format (bil = band interleaved by line; a common raster data format)

DDRP chooses the highest quality file available for each date ("stable" > "provisional" > "early" > nmme > 10yr1019 or 30yrAVG). We compute 10-year average PRISM data and include the years represented in the file name: 10yr1019 is an average of data from 2010 to 2019. We repeat this computation every two months so that the final year includes an increasing amount of final, "stable" PRISM data. At the time of writing this document, the final year would be 2019 since the entire year has passed and data are therefore available for all dates. If the date falls in the future, users may specify if they prefer to use a 10-year average or NMME predictions. For example, available Tmin files for Feb 22, 2020 in order of quality may include:

PRISM_tmin_early_4kmD2_20200222_bil.bil
PRISM_tmin_provisional_4kmD2_20200222_bil.bil
PRISM_tmin_stable_4kmD2_20200222_bil.bil
PRISM_tmin_nmme_4kmD1_20200222_bil.bil
PRISM_tmin_10yr1019_4kmD1_20200222_bil.bil

To calibrate the climatic suitability model in accordance with CLIMEX outputs (see Barker et al. 2020), we use PRISM data for 1961–1990 to match the time-schedule of CLIMEX's climate data (CliMond CM10). These PRISM 30-year NORMALS have been scaled from a monthly to a daily temporal resolution because DDRP requires daily data, and PRISM lacks daily data for years prior to 1980. Currently these files are located in /data/PRISM/1990_daily_30yr/ and have file names such as:

PRISM_tmin_30yr6190_4kmM2_19750222.bil.bil

Input options

There are 17 command-line input options that must be specified to run DDRP, as summarized below.

Option	Description
spp	Species to model
forecast_data	Forecast data to use (PRISM 10yrAVG, NMME, etc.)
start_year	Year
start_doy	Start day of year
end_doy	End day of year
keep_leap	Should leap day be kept? (0 = no, 1 = yes)
region_param	Region [CONUS, EAST, WEST, or state (2-letter abbr.)]
exclusions_stressunits	Turn on/off climatic suitability modeling (0 = off, 1 = on)
pems	Turn on/off pest event maps (0 = off, 1 = on)
mapA	Make PEMs for adult stage (0 = no, 1 = yes)
mapE	Make PEMs for egg stage (0 = no, 1 = yes)
mapL	Make PEMs for larval stage (0 = no, 1 = yes)
mapP	Make PEMs for pupal stage (0 = no, 1 = yes)
out_dir	Output directory name
out_option	Sampling frequency (1 = 30 days, 2 = 14 days, 3 = 10 days, 4 = seven days, 5 = two days, 6 = one day)

ncohort	Number of cohorts to approximate end of overwintering stage
odd_gen_map	Create summary maps for odd generations only (0 = no, 1 = yes)

The start_doy and end_doy must range between 1 and 365 (or 366 for a leap year). The keep_leap parameter specifies whether leap day (Feb 29) should be included in the model if start_year is a leap year. Regardless of which out_option is specified, DDRP will sample the last day (end_doy), and the current date if the model is produced for the current year *and* the current date falls within the range of modeled days (i.e. between start_doy and end_doy). For example, let's say a DDRP model were run today (Oct 28, 2020) for each day of the year in 2020 (days 1 to 366), and a sampling frequency of 1 (every 30 days) was specified. DDRP would generate 14 maps: 12 for the every-30 day sampling period (i.e. 12 months), one for Oct 28, and one for the last day of the year (Dec 31).

Running DDRP

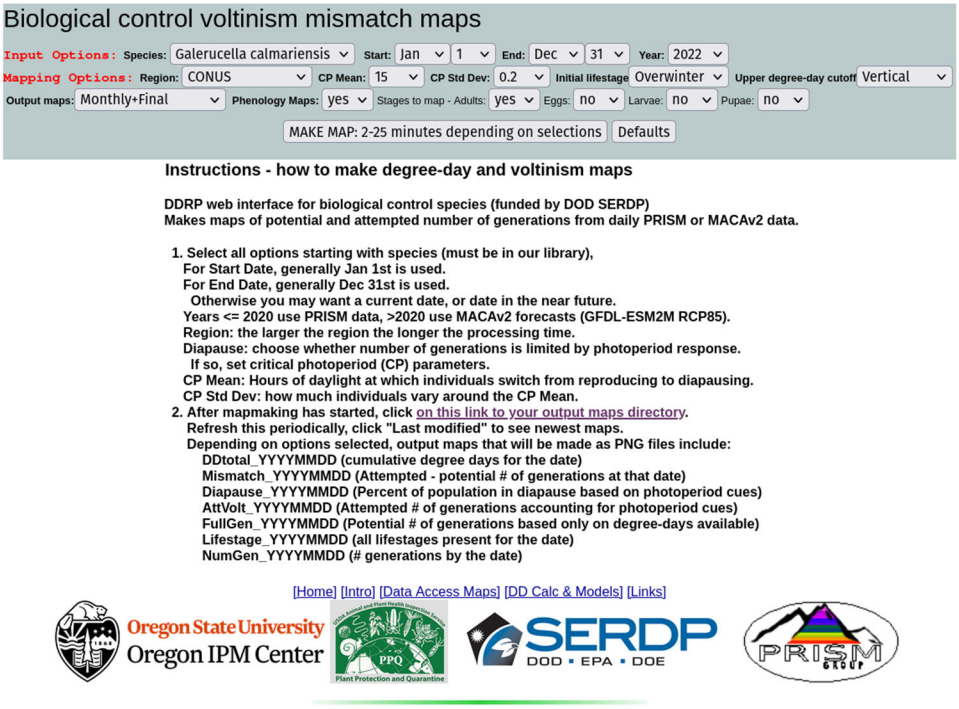

Fig. 1. Home page for web interface to DoDMaps.

A. Web Interface Guidelines – DoDMaps version at https://uspest.org/dd/dodmaps

The version of DDRP developed for the DoD SERDP project (Grevstad et al. 2022) has a web interface allowing users to run the three available weed biocontrol agent models, using a variety of options. Here we list the options with more extensive explanations than what is shown in the opening home page (Fig. 1) for the model:

Input Options (refer to Fig. 1):

1. Species. The three species parameterized for this project include:

Galerucella calmariensis – or purple loosestrife leaf beetle, is a major biocontrol agent of purple loosestrife, introduced from Germany in 1992

Diorhabda carinulata – or Tamarisk leaf beetle, is a major biocontrol agent of Tamarisk, introduced from Central Asia in 2001

Aphalara itadori – or knotweed psyllid, is a major biocontrol agent of invasive knotweed species, introduced in 2020 from Japan.

No other species requiring photoperiod response parameters have yet been analyzed to be included in DDRP as of Oct. 2022. Species not requiring photoperiod response parameters (not DoDMaps) are listed below in the section "Species with parameterized models".

2. Start and end dates. These are dates to begin and end the daily time-step in running the model. Typically model runs start Jan. 1 and end Dec. 31 of a given year. Shorter spans of time would not allow processing of phenological event maps, as an entire year is needed to determine dates of events. For year, if selecting current year, consider that observed data is available through yesterday, while future data is either the NMME 7-month climate forecast, or following that interval, if needed, recent 10-year average data. If selecting a future year, we have made MACA-V2 (GFDL-ESM2M RCP85) data available to allow examination of potential climate change on insect phenology and voltinism.

Output Options (refer to Fig. 1):

3. Region. We generally use PRISM data that is available only for CONUS (coterminous US), so we can program options for virtually any sub-region of CONUS. The smaller the region, the faster the processing. As other global climate data become available, we should be able to extend the platform to cover such regions.
4. Diapause parameters. CP is the mean critical photoperiod triggering diapause. Currently the model assumes short-day response, so for example, if the CP is 14 then diapause will be triggered when the daylength is less than 14 hr. CP Std Dev is the standard deviation around the CP to vary the response across cohorts.
5. Initial lifestage. This option allows the model to begin at a lifestage other than the overwintering stage, which may help model realism in case the operator chooses to start the model later in the year than the recommended default of Jan. 1.
6. Upper degree-day cutoff. Normally a horizontal cutoff is recommended. If you have a model that was developed using a vertical cutoff, this option may be needed.
7. Output map frequency. The greater the frequency of output maps, the slower the processing. We recommend monthly output maps. If you only need the set of maps made after the daily time step loop is completed, you should select bimonthly+final. The most frequent output map choice is weekly+final.
8. Phenology maps. This should normally be "yes". Setting to "no" may speed up processing.
9. Stages to map. These "yes" or "no" options should be set to "yes" for stages for which phenological event maps are of interest. You can review the metadata to see what particular stages are set up for phenological event maps. For example the "pupal stage" may be set up for mapping at the end of the stage, making it equivalent to a map of "first adult emergence", which should be indicated by the label for that map.
10. Make map. This initiates the model and sets up a folder for output. You may click on the link to the output maps soon after initiating the model, which links to a directory page to all recent model runs. Click the the "last modified" option at the top of your browser once or twice so that the most recent folder will appear at the top. If the time and date are current, then this folder should be where your maps are placed. Click on this link where you should initially only see a "logs_metadata" folder, which has model metadata in the file "metadata.txt", and model runtime data in the files "Model_rlogging.txt" and

“rmessages.txt”. After 2-25 minutes (depending on selections and server load), most maps should be completed and start appearing in the folder when you refresh your main folder page. See the “Output Files” section below for a description of output map types.

Running DDRP from the command line (non-DoDMaps versions)

The “DDRP_v2.R” script must be edited to specify the locations of the “DDRP_v2_funcs.R” file, the species model parameter file (“params_dir”), the temperature data (“base_dir”), and the output directory (“output_dir”).

On a Linux OS, the “DDRP_v2.R” script can be made into an executable file by using the chmod command (“chmod +x DDRP_v2.R”). We run DDRP from the command line that is either called from a web (CGI) wrapper, or from within an automated scheduling program (cron) on our server. Below is an example command that would run a DDRP model (phenology and climatic suitability model) for ALB for the entire year of 2020.

./DDRP_v2.R --spp ALB --forecast_data PRISM --start_year 2020 --start_doy 1 --end_doy 366 --keep_leap 1 --region_param CONUS --exclusions_stressunits 1 --pems 1 --mapA 1 --mapE 1 --mapL 0 --mapP 0 --out_dir ALB_cohorts --out_option 1 --ncohort 7 --odd_gen_map 0

On a Windows OS, it may be easiest to run DDRP via a Windows batch (BAT) file that has the command line argument (note that the location of Rscript needs to be specified).

"C:\Program Files\R\R-4.0.2\bin\Rscript.exe" C:\Users\barkebri\Documents\DDRP\DDRP_v2.R --spp ALB --forecast_data PRISM --start_year 2020 --start_doy 1 --end_doy 366 --keep_leap 1 --region_param CONUS --exclusions_stressunits 1 --pems 1 --mapA 1 --mapE 1 --mapL 0 --mapP 0 --out_dir ALB_2020_new --out_option 1 --ncohort 7 --odd_gen_map 0

Running DDRP within RStudio is an ideal option for troubleshooting issues, optimizing settings for a particular server/computer (e.g., specifying a different number of cores for parallel processing), and customizing code. In this case, the input options are specified within the “DDRP_v2.R” script (see the first 200 lines of code under “# Read in commands”).

Output files

Model outputs are generated in raster and image file formats (GeoTIFF and PNG files, respectively) at a user-specified sampling frequency (--out_option). The exception are PEMs, which are produced only on the last sampled day. Additionally, outputs are generated for the current day if it occurs within the specified time period, and for the last day of the time period. Rasters for each output file type have multiple layers (known as a raster stack/brick), with each layer representing the output for a sampled date. For example, if there are 14 sampled dates then the raster stack will have 14 layers. The GeoTIFF files can be readily ingested by most GIS programs including ArcGIS. The summary map (PNG) files are complete with color tables, legends, etc. and provide an example of how results may be conveyed.

<u>Output file types</u>

The types of model outputs generated by DDRP are only summarized here; we refer users to Barker et al. (2020) for a more thorough description of the methods involved in the modeling process. Phenology

model outputs are generated by analyzing results across all cohorts, except for life stage by generation (StageCount), which is currently based on results for the middle cohort only due to computational complications (most of the population will belong to a middle cohort, e.g., cohort 4 if there seven cohorts). Additionally, outputs for degree-day accumulation (DDtotal) and (for the non DODMAPS version) all climatic suitability model products (Cold_Stress_Units, Heat_Stress_Units, Cold_Stress_Excl, Heat_Stress_Excl, All_Stress_Excl) are generated only for a single cohort (cohort) because they will be representative for all cohorts.
All output file names will contain a prefix followed by the sampled date. The table below summarizes attributes of each output file type.

File name prefix(es)	Description	Value range
DDtotal	Accumulated degree-days	0 to max number of accumulated degree-days
Egg, Larvae, Pupae, Adult, OWstage	Relative size of population represented by each life stage including the overwintering stage (OWegg, OWlarvae, OWpupae, OWadult)	0 to 100
StageCount	Life stage by generation (middle cohort only). Life stage value (eggs = 1, larvae = 2, pupae = 3, adults = 4) for each generation are separated by a decimal (e.g. 1.0 and 1.2 is eggs of the overwintered and first generation, respectively)	0.1, 0.2, 0.3, 0.4, 1.1, etc.
NumGen	Relative size of population in each generation	0 to 100
Avg_PEM	Average calendar day of phenological event across cohorts	0 to 366
Earliest_PEM	Earliest calendar day of phenological event across cohorts	0 to 366
Cold_Stress_Units	Cold stress unit accumulation (not DoDMaps)	0 to max number of units
Heat_Stress_Units	Heat stress unit accumulation (not DoDMaps)	0 to max number of units
Cold_Stress_Excl	Cold stress exclusion (not DoDMaps)	0, −1, −2
Heat_Stress_Excl	Heat stress exclusion (not DoDMaps)	0, −1, −2
All_Stress_Excl	All stress exclusion (not DoDMaps)	0, −1, −2
AttVolt	Attempted no. of generations (typically for 1 year) (DoDMaps only)	0 to max generations
FullVolt	Potential no. of generations (no photoresponse) (DoDMaps only)	0 to max generations
Mismatch	Difference potential minus attempted no. of generations (DoDMaps only)	Negative max gens. To positive max. gens.
Diapause	Percent in diapause (typically assessed Dec. 31) (DoDMaps only)	0 to 100

For PEMs, output files will be named according to the stage and generation. For example, if PEMs for Asian longhorned beetle (ALB) are produced for adults for overwintering (PEMa0) and up to two additional (PEMa1 and PEMa2) generations, then the output files would include:

ALB_Avg_PEMa0_20201231.tif
ALB_Avg_PEMa1_20201231.png

ALB_Avg_PEMa2_20201231.tif
ALB_Earliest_PEMa0_20201231.tif
ALB_Earliest_PEMa1_20201231.png
ALB_Earliest_PEMa2_20201231.tif

Additionally, DDRP (not DoDMaps) integrates phenology and climatic suitability model outputs (with the exception of total accumulated degree-days) to create two additional files associated with each sampled date. The first file includes severe climate stress exclusions only, whereas the second file includes both severe and moderate stress exclusions. Thus, outputs for the average date of the overwintering adult event (first row of above example) would now include two additional files:

ALB_Avg_PEMa0_20201231.tif
ALB_Avg_PEMa0_Excl1_20201231.tif
ALB_Avg_PEMa0_Excl2_20201231.tif

Output file organization

The main output directory (out_dir) will contain select output PNG files that were generated for the last sampled day of the specified time period (e.g., Dec. 31, 2020 if the entire year was modeled). Files for life stage by generation (StageCount), however, will be for the current day (of the model run). StageCount maps are the nearest equivalent to the "Degree-day lookup table maps" that are in current production by collaborators including the APHIS PPQ SAFARIS group "Weekly Degree Day Phenology Maps" (website at https://safaris.cipm.info/safarispestmodel/StartupServlet?fieldops), and the USA National Phenology Network (NPN) group "Pheno Forecast" maps (example at https://www.usanpn.org/data/forecasts/EAB). All files in the main output directory will have names that begin with the species abbreviation.

The "Misc_files" subdirectory will contain all other model output files, including raster bricks. Additional PNG files in this folder are considered to be less important than those in the main output directory, at least not for pest monitoring purposes.

The "Logs_metadata" subdirectory will contain three text files:

1. metadata.txt: metadata including model run date and time, species parameter information, and command-line input options.
2. model_rlogging.txt: reports model run progress and certain errors and warnings (e.g., inappropriate input options).
3. rmessages.txt: may contain error messages from R resulting from an unsuccessful model run.

Model run times

The following four factors are the major determinants of model run times:

1) The number of cores available on the server or PC. For example, a model for ALB for CONUS with seven cohorts took 27 minutes on a Linux server with 36 cores, whereas it took ~3× longer to run on a Windows 10 PC with 8 cores (76 minutes).
2) The generation time of the species being modeled. Species such as ALB that are primarily univoltine (one generation per year) will run faster than multivoltine species. For example, a model run for tomato leafminer (TABS) that applied the same command-line input options as a run for ALB for 2020 took 2× longer to run (53 vs. 27 minutes) because TABS could potentially complete up to 14 generations for that year.

3) The number of cohorts. Increasing the number of cohorts will positively correlate with model run times because the daily time step is run for each cohort, and additional computational resources are needed for processing daily time step results. Typically we apply seven cohorts to approximate a normal distribution of emergence times.
4) Region size. Model runs for CONUS will take the longest, while runs for small states will complete relatively quickly.

Species with parameterized models

We have configured DDRP to output files to OSU OIPMC's server at USPEST.ORG: https://uspest.org/CAPS/xxx... where "xxx..." represents the abbreviation of any species for which DDRP phenology and climatic suitability models have been developed:

1. ALB_cohorts - Asian longhorned beetle, *Anoplophora glabripennis*
2. ASRB_cohorts – Asiatic rice borer, *Chilo suppressalis*
3. CGN_cohorts – Honeydew moth, *Cryptoblabes gnidiella*
4. EAB_cohorts – Emerald ash borer, *Agrilus planipennis* (IPM species)
5. FCM_cohorts - False codling moth, *Thaumatotibia leucotreta*
6. JPSB_cohorts - Japanese pine sawyer beetle, *Monochamus alternatus*
7. LBAM_cohorts - Light brown apple moth, *Epiphyas postvittana*
8. OAB_cohorts - Oak ambrosia beetle, *Platypus quercivorus*
9. OWBW_cohorts - Old world bollworm, *Helicoverpa armigera*
10. PTLM_cohorts - Pine tree lappet moth, *Dendrolimus pini*
11. SLI_cohorts – Common or cotton cutworm, *Spodoptera litura*
12. STB_cohorts – Small tomato borer, *Neoleucinodes elegantalis*
13. SLYM_cohorts – Silver Y moth, *Autographa gamma*
14. SUNP_cohorts – Sunn pest, *Eurygaster integriceps*
15. TABS_cohorts – Tomato leafminer, *Tuta absoluta*
16. ECW_cohorts – Egyptian cottonworm, *Spodoptera littoralis*

References

Barker, B.S., Coop, L., Wepprich, T., Grevstad, F., and Cook, G. 2020. DDRP: real-time phenology and climatic suitability modeling of invasive insects. bioRxiv. https://doi.org/10.1101/2020.05.18.102681

Grevstad, F., T. Wepprich, B. Barker, L. Coop, R. Shaw, R. Bouchier. 2022. Combining photoperiod and thermal responses to predict phenological mismatch for introduced insects. Ecological Applications. https://doi.org/10.1002/eap.2557

Appendix 1. Description of parameters in a species parameter file. The "owstage" parameter may be overwintering (OW) egg, larvae, pupae, or adult (OE, OL, OP, or OA) and the "stgorder" parameter is the owstage stage plus the four remaining stages (E = egg, L = larvae, P = pupae, and A = adult).

Parameter	Description
fullname	Full name of species
pestof	Host plants
stgorder	Stage order beginning with the OW stage
owstage	Overwintering (OW) stage

Thresholds	
eggLDT	egg lower developmental threshold
eggUDT	egg upper developmental threshold
larvaeLDT	larvae lower developmental threshold
larvaeUDT	larvae upper developmental threshold
pupaeLDT	pupae lower developmental threshold
pupaeUDT	pupae upper developmental threshold
adultLDT	adult lower developmental threshold
adultUDT	adult upper developmental threshold
Degree-day req.	
eggDD	duration of egg stage in DDs
larvaeDD	duration of larvae stage in DDs
pupaeDD	duration of pupae stage in DDs
adultDD	duration of adult stage in DDs
eggEventDD	DDs into egg stage when event occurs
larvaeEventDD	DDs into larval stage when event occurs
pupaeEventDD	DDs into pupal stage when event occurs
adultEventDD	DDs into adult stage when event occurs
OWstageDD	DDs until OW stage emerges (only used if ncohort = 1)
calctype	Degree-day calculation method
Phenological event maps	
PEMnumgens	Create PEMs for up this many generations (max is 4)
eggEventDD	DDs of egg stage event
eggEventLabel	Label for egg PEM
larvaeEventDD	DDs of larval stage event
larvaeEventLabel	Label for larval PEM
pupaeEventDD	DDs of pupal stage event
pupaeEventLabel	Label for pupal stage event
adultEventDD	DDs of adult stage event
adultEventLabel	Label for adult stage PEM
OWEventP	Prop. of OW stage completed when OW event occurs (0 - 1)
OWEventLabel	Label for OW stage PEM
Climatic suitability (not used in DoDMaps)	
coldstress_threshold	cold stress threshold
coldstress_units_max1	cold degree day limit when most individuals die
coldstress_units_max2	cold degree day limit when all individuals die
heatstress_threshold	heat stress threshold
heatstress_units_max1	heat stress degree day limit when most individuals die
heatstress_units_max2	heat stress degree day limit when all individuals die
Diapause parameters (DoDMaps vers. only)	
do_photo	Use photoresponse: 0 means “NO”; 1 means “YES”

photo_sens	Sensitive stage: 5=adult; 4=pupae; 3=larvae; 2=egg
crit_photo_mean	Daylenth that the insect is responding to (hrs daylight)
crit_photo_sd	St. dev. For variation in response to daylength
Cohorts	
distro_mean	average DDs to emergence
distro_var	variation in DDs to emergence
xdist1	minimum DDs to emergence
xdist2	maximum DDs to emergence
distro_shape	shape of the distribution

Appendix 2. Species parameter files for the three DoDMaps biocontrol species.

```
# these are OSU IPPC/PPQ CPHST DDRP_B1 params and values for
#  GCA, Galerucella calmariensis, loosestrife beetle model in Degs Celsius (C)
# Last updated in Aug 2020 for DDRP v2 (cohorts)
# southern biotype
  fullname   <- "Galerucella calmariensis"
  pestof     <- "biological control of purple loosestrife"
  stgorder   <- c("OA","E","L","P","A") # stgorder changed to 1, 2, 3, 4, 5 in DDRP v2;
# Tyson's model has "TA" stage
  owstage    <- "OA"   # OW pupae in the soil; no true diapause
  eggLDT     <- 12.2
  eggUDT     <- 30     # Unknown, only tested in lab up to 30
  larvaeLDT  <- 12.2   # same as egg stage
  larvaeUDT  <- 30     # nominal upper dev. threshold
  pupaeLDT   <- 12.2   # same as egg stage
  pupaeUDT   <- 30
  adultLDT   <- 12.2
  adultUDT   <- 30
  eggDD      <- 87.8
  larvaeDD   <- 128.2
  pupDD      <- 126.0
  OWadultDD  <- 100
  adultDD    <- 72.9    # time to complete pre-oviposition period
  calctype   <-"triangle" # similar to sine method upon which model was built

 # Pest Event Maps (PEMs) must be turned on as a runtime param for these to get used:
  PEMnumgens       <- 2     # create PEMS for up to this many generations (max is 4)
  eggEventDD       <- 87    # PEMs for egg stage is end of stage
  eggEventLabel    <- "egg hatch" # Label for PEM egg stage
  larvaeEventDD    <- 100   # PEMs for late larvae stage
  larvaeEventLabel <- "larval development" # Label for PEM larvae stage
  pupaeEventDD     <- 125   # PEMs for end pupal stage
  pupaeEventLabel  <- "adult emergence" # Label for PEM pupal stage
  adultEventDD     <- 72    # PEMs for adult stage (1st ovip.) is ca. 22 DDs into stage
```

```
 adultEventLabel  <- "egg laying" # Label for PEM adult stage
 OWEventP         <- 0.7   # PEMs is (70%) into stage
 OWEventLabel     <- "Adult emerges (pre-oviposition)" # Label for PEM OWlarvae

# OW stage emergence parameters (DDRP v2 only)
 distro_mean    <- 100
 distro_var     <- 2000
 xdist1         <- 75
 xdist2         <- 200
 length_out     <- 1000
 distro_shape   <- "normal"

# Diapause parameters
# TODO: single CP option
do_photo        <- 1   # 0 means don't
photo_sens      <- 5   # adult stage sensitive
crit_photo_mean  <- 15
crit_photo_sd    <- 0.25


# these are OSU IPPC/PPQ CPHST DDRP_B1 params and values for
# APH, Aphalara itadori, knotweed psyllid model in Degs Celsius (C)
# Last updated in August 2020 for DDRP v2 (cohorts)
# southern biotype
 fullname   <- "Aphalara itadori"
 pestof     <- "biological control of Japanese and Giant knotweed"
 stgorder   <- c("OA","E","L","P", "A") # stgorder changed to 1, 2, 3, 4, 5 in DDRP v2;
 # P for APH represents late larval stage when photosensitive
 owstage    <- "OA"    # OW pupae in the soil; no true diapause
 eggLDT     <- 6.9
 eggUDT     <- 30      # Unknown, only tested in lab up to 30
 larvaeLDT  <- 6.9     # same as egg stage
 larvaeUDT  <- 30      # nominal upper dev. threshold
 pupaeLDT   <- 6.9     # same as egg stage
 pupaeUDT   <- 30
 adultLDT   <- 6.9
 adultUDT   <- 30
 eggDD      <- 147
 larvaeDD   <- 269     # Nymph 1-4 instars
 pupDD      <- 132     # Nymph 5th instar
 OWadultDD  <- 306
 adultDD    <- 70      # time to complete pre-oviposition period
 calctype   <-"triangle" # similar to sine method upon which model was built

 # Pest Event Maps (PEMs) must be turned on as a runtime param for these to get used:
 PEMnumgens       <- 2     # create PEMS for up to this many generations (max is 4)
 eggEventDD       <- 145   # PEMs for egg stage is end of stage
```

```
  eggEventLabel    <- "egg hatch" # Label for PEM egg stage
  larvaeEventDD    <- 265   # PEMs for late larvae stage
  larvaeEventLabel <- "late larvae photosensitive" # Label for PEM larvae stage
  pupaeEventDD     <- 130   # PEMs for end pupal stage
  pupaeEventLabel  <- "adult emergence" # Label for PEM pupal stage
  adultEventDD     <- 69    # PEMs for adult stage (1st ovip.)
  adultEventLabel  <- "egg laying" # Label for PEM adult stage
  OWEventP         <- 0.7   # PEMs is (70%) into stage
  OWEventLabel     <- "Adult emerges (pre-oviposition)"

# OW stage emergence parameters (DDRP v2 only)
  distro_mean   <- 220
  distro_var    <- 2500
  xdist1        <- 150
  xdist2        <- 300
  length_out    <- 1000
  distro_shape  <- "normal"
#
# Diapause parameters
# TODO: single CP option
do_photo          <- 1   # 0 means don't
photo_sens        <- 4   # late larvae (pupa here for convenience) stage sensitive
crit_photo_mean   <- 15
crit_photo_sd     <- 0.25


# these are OSU IPPC/PPQ CPHST DDRP_B1 params and values for
# DCA, Diorhabda carinulata, tamarisk beetle model in Degs Celsius (C)
# Last updated in Aug 2020 for DDRP v2 (cohorts)
# southern biotype
  fullname   <- "Diorhabda carinulata"
  pestof     <- "biological control of saltcedar/tamarisk"
  stgorder   <- c("OA","E","L","P", "A") # stgorder changed to 1, 2, 3, 4, 5 in DDRP v2;
# Tyson's model has "TA" stage
  owstage    <- "OA"   # OW pupae in the soil; no true diapause
  eggLDT     <- 12
  eggUDT     <- 40     # Unknown, only tested in lab up to 30
  larvaeLDT  <- 12   # same as egg stage
  larvaeUDT  <- 40   # nominal upper dev. threshold
  pupaeLDT   <- 12   # same as egg stage
  pupaeUDT   <- 40
  adultLDT   <- 12
  adultUDT   <- 40
  eggDD      <- 91.4
  larvaeDD   <- 176.7
  pupDD      <- 174
  OWadultDD  <- 275
```

```
 adultDD    <- 47.2  # time to complete pre-oviposition period
 calctype   <-"triangle" # similar to sine method upon which model was built

# Pest Event Maps (PEMs) must be turned on as a runtime param for these to get used:
 PEMnumgens       <- 2      # create PEMS for up to this many generations (max is 4)
 eggEventDD       <- 90     # PEMs for egg stage is end of stage
 eggEventLabel    <- "egg hatch" # Label for PEM egg stage
 larvaeEventDD    <- 150    # PEMs for late larvae stage
 larvaeEventLabel <- "peak larval development" # Label for PEM larvae stage
 pupaeEventDD     <- 173    # PEMs for end pupal stage
 pupaeEventLabel  <- "adult emergence" # Label for PEM pupal stage
 adultEventDD     <- 45     # PEMs for adult stage (1st ovip.) is ca. 22 DDs into stage
 adultEventLabel  <- "egg laying" # Label for PEM adult stage
 OWEventP         <- 0.7    # PEMs is (70%) into stage
 OWEventLabel     <- "Adult emerges (pre-oviposition)" # Label for PEM OWlarvae

# OW stage emergence parameters (DDRP v2 only)
 distro_mean  <- 200
 distro_var   <- 1000
 xdist1       <- 120
 xdist2       <- 350
 length_out   <- 1000
 distro_shape <- "normal"

# Diapause parameters
# TODO: single CP option
do_photo         <- 1     # 0 means don't
photo_sens       <- 5     # adult stage sensitive
crit_photo_mean  <- 14.32 # intercept of model of %diapause vs daylength
crit_photo_sd    <- 0.25  # slope of model of %diapause vs daylength
```